MONTHLY NOTICES

OF THE

ROYAL ASTRONOMICAL SOCIETY

Vol. 115 No. 4 1955

Published and Sold by the
ROYAL ASTRONOMICAL SOCIETY
BURLINGTON HOUSE
LONDON, W.1

Price Thirteen Shillings and Sixpence

NOTICE TO AUTHORS

1. *Communications.*—Papers must be communicated to the Society by a Fellow. They should be accompanied by a summary at the *beginning* of the paper conveying briefly the content of the paper, and drawing attention to important new information and to the main conclusions. The summary should be intelligible in itself, without reference to the paper, to a reader with some knowledge of the subject; it should not normally exceed 200 words in length. **Authors are requested to submit MSS. in duplicate. These should be typed using double spacing and leaving a margin of not less than one inch on the left-hand side. Corrections to the MSS. should be made in the text and not in the margin.** Unless a paper reaches the Secretaries more than seven days before a Council meeting it will not normally be considered at that meeting. By Council decision, MSS. of accepted papers are retained by the Society for one year after publication; unless their return is then requested by the author, they are destroyed.

2. *Presentation.*—Authors are allowed considerable latitude, but they are requested to follow the general style and arrangement of *Monthly Notices*. References to literature should be given in the standard form, including a date, for printing either as footnotes or in a numbered list at the end of the paper. Each reference should give the **name and initials** of the author cited, irrespective of the occurrence of the name in the text (some latitude being permissible, however, in the case of an author referring to his own work). The following examples indicate the style of reference appropriate for a paper and a book, respectively :—

A. Corlin, *Zs. f. Astrophys.*, **18**, 239, 1938.
H. Jeffreys, *Theory of Probability*, 2nd edn., section 5.45, p. 258, Oxford, 1948.

3. *Notation.*—For technical astronomical terms, authors should conform closely to the recommendations of Commission 3 of the International Astronomical Union (*Trans. I.A.U.*, Vol. VI, p. 345, 1938). Council has decided to adopt the I.A.U. 3-letter abbreviations for constellations where contraction is desirable (Vol. IV, p. 221, 1932). In general matters, authors should follow the recommendations in *Symbols, Signs and Abbreviations* (London : Royal Society, 1951) except where these conflict with I.A.U. practice.

4. *Diagrams.*—**These should be designed to appear upright on the page, drawn about twice the size required in print and prepared for direct photographic reproduction except for the lettering, which should be inserted in pencil. Legends should be given in the manuscript indicating where in the text the figure should appear.** Blocks are retained by the Society for 10 years; unless the author requires them before the end of this period they are then destroyed.

5. *Tables.*—**These should be arranged so that they can be printed upright on the page.**

6. *Proofs.*—Costs of alteration exceeding 5 per cent of composition must be borne by the author. Fellows are warned that such costs have risen sharply in recent years, and it is in their own and the Society's interests to seek the maximum conciseness and simplification of symbols and equations consistent with clarity.

7. *Revised Manuscripts.*—When papers are submitted in revised form it is especially requested that they be accompanied by the original MSS.

Reading of Papers at Meetings

8. When submitting papers authors are requested to indicate whether they will be willing and able to read the paper at the next or some subsequent meeting, and approximately how long they would like to be allotted for speaking.

9. Postcards giving the programme of each meeting are issued some days before the meeting concerned. Fellows wishing to receive such cards whether for Ordinary Meetings or for the Geophysical Discussions or both should notify the Assistant Secretary.

MONTHLY NOTICES

OF THE

ROYAL ASTRONOMICAL SOCIETY

Vol. 115 No. 4

MEETING OF 1955 MAY 13

Professor Sir Harold Jeffreys, President, in the Chair

The election by the Council of the following Fellows was duly confirmed :—

Vivian Mary Bradley, B.Sc., Department of Astronomy, University of Manchester (proposed by Z. Kopal) ;

Gilbert Fielder, B.Sc., Department of Astronomy, University of Manchester (proposed by Z. Kopal) ;

Vera Hewison, B.Sc., Department of Astronomy, University of Manchester (proposed by Z. Kopal) ;

George Edwin Stone Kendall, Ph. C., F.N.A.O., M.P.S., 23 High Street, Ascot, Berkshire (proposed by R. L. Waterfield) ;

Peter Yorke Millns, B. Sc., Department of Astronomy, University of Manchester (proposed by Z. Kopal) ; and

Gordon Ernest Taylor, Celestia, London Road, Horsebridge, near Hailsham, Sussex (proposed by D. H. Sadler).

The election by the Council of the following Junior Members was duly confirmed :—

Robert Owen Bishop, University Observatory, Oxford (proposed by H. H. Plaskett) ; and

Francis Wykes, 1 Brookmead, Hildenborough, Kent (proposed by P. Moore)

One hundred and eighteen presents were announced as having been received since the last Meeting, including :—

Sir Richard Phillips, *Wonders of the Telescope* (presented by Sir Eric Miller);

Roger Boscovitch, *Nova methodus adhibendi phasium observationes* (presented by Sir Eric Miller) ;

J. Cassini, *Tables astronomiques du Soleil, de la Lune, des Planètes, etc.* (presented by Sir Eric Miller) ; and

International Astronomical Union, *Symposium No. 1.—Co-ordination of galactic research* (presented by the Cambridge University Press).

THE SYMMETRY OF THE CORONA OF 1954 JUNE 30

T. Gold

(Communicated by the Astronomer Royal)

(Received 1955 March 2)

The corona seen during the total eclipse of 1954 June 30 was extraordinary for its regularity. The time of the eclipse was as nearly the sunspot minimum as can be determined, and no spot was seen at the Solar Observatory at Herstmonceux for 8 days preceding or 12 days following the eclipse. The corona did not possess any streamers extending out in odd directions as is normally the case, but was of a high degree of symmetry. In the equatorial direction there was the furthest extension, a little more to the east than to the west. In higher latitudes there were polar plumes fairly regularly spaced. There was a sharply defined position of changeover on the Sun's limb in each quadrant between the striated polar plume zone and the smooth zone associated with the equatorial extension.

The Royal Greenwich Observatory expedition to Syd Koster island, Sweden, (T. Gold, A. Hunter, E. W. Bastin, D. W. Sciama) had intended to photograph the eclipse star field with a telescope of 21 ft focal length, for the purpose of a measurement of the Einstein deflection of light. Thin cloud prevented this, but a good picture of the corona was obtained, marred by cloud only in the north-west quadrant. The negative contains a very large range of density and this renders it unsuitable for direct reproduction in print. The print shown was obtained from the negative by a process involving the subtraction of intensity by an amount which was a suitable function of radius only. The real isophotes are much more nearly circular than appears in the reproduction; but the reproduction serves to show some of the coronal pattern. On the negative the following measurements were carried out.

1. *The direction of the equatorial extension.*—A line was drawn through the equatorial extension splitting it as symmetrically as possible into the northern and southern parts. On the east side this required drawing it through the furthest extension that could be seen on the plate (about 4 solar radii from the limb) while on the west side the extension was clearly and quite symmetrically bifurcated, and the line had to be drawn through the middle of that. This line, defined solely by the outer corona, passed accurately through the centre of the Sun. Its direction seemed indeterminate by not more than $\pm \frac{1}{2}$ degree. The angle that this line made with the normal to the projection of the Sun's axis was 0·8 degrees.

2. *The changeover between the polar and the equatorial type of corona.*—The lines separating the striated polar regions from the smooth equatorial ones can be seen right in to the Sun's limb. The heliographic latitudes of these changeover points on the four quadrants of the limb are very similar and do not appear to be uncertain to more than about one degree. They are:

N.E. 60°
N.W. $59\frac{1}{2}$°
S.W. 60°
S.E. $63\frac{1}{2}$°

T. Gold, *The symmetry of the corona of 1954 June 30*

The symmetry of shape of the corona was considerably more marked between north and south than between east and west, both so far as the inner features are concerned, and also the furthest equatorial extensions. This symmetry is known to be absent at other phases of the sunspot cycle, when disturbances on the surface of the Sun appear to influence or even to determine the coronal appearance. The corona at sunspot minimum would therefore appear to have the special interest that it reveals the shape that the system settles down to when not subjected to the erratic disturbances marking periods that are richer in sunspots.

The implication of this high degree of symmetry would seem to be that the equatorial regions of the corona, even out to a distance of 4 radii, are very much under the control of the Sun. The relaxation time in which the corona settles down to this symmetrical condition is not likely to be more than a few months, judging from the evidence of previous near-minimum eclipses which still showed great disturbances. The mechanism which transfers this precise information about the rotation of the Sun out to that distance is not clear, but it seems likely that any explanation will require an outward flow of material in the equatorial region. Any suggested pattern of flow involving an inward flow in the equatorial zone would greatly augment the difficulties, for it would then be necessary to find a mechanism capable of pulling the incoming material into a shape determined by the Sun, while it is still at such a great distance.

The polar plumes, on the other hand, do not require an outward flow for their explanation. Most patchy distributions of material at some distance from the Sun would be drawn into such shapes by falling under the combined effect of gravitation and a magnetic field, whose lines of force would thereby be made visible. If, as seems very likely, the polar plumes are indicators of magnetic lines of force, then another consideration is of interest. The shapes of the plumes form an ordered sequence (as would be expected from lines of force resulting from electric currents in the Sun) and the boundary of the plume zone, namely an edge of the equatorial extension, is clearly an adjacent shape in that sequence. If the plumes are the lines of force, then the outlines of the equatorial extension, at any rate the parts within the range where the plumes can be seen, must also be lines of force. In searching for the physical difference that underlies the clear distinction in the appearance of the two zones we are again led to a hydrodynamical explanation, not only because of the difficulty of invoking another physical effect, but also because any streaming has to occur along lines of force in a system such as this, where ohmic dissipation plays no essential part, and a changeover in the direction of flow must therefore be on a surface defined by lines of force.

The greatest departure from the shape of a dipole field that can be seen in any of these outlines is in the edge of the equatorial extension and the nearby plumes. While there would be no need to suppose the currents in the Sun to be just those that make an external dipole-like field, the departure in shape is in the sense of making the loops of the lines of force stretch out very much further than a solar dipole field would. This is very unlikely to result from currents in the Sun (where sets of nearby opposing current rings would be required) but would result from the outward convection of the field due to an outward flow in the equatorial zone.

Estimates of the surface field of the Sun and of the conductivity of the corona at different ranges from the Sun will enable an estimate to be made of the strength

of the magnetic forces that the coronal material has to bear to uphold this deformation of the field; and with a knowledge of the densities this would specify the order of magnitude of the streaming velocities.

I should like to acknowledge the skilled work of Dr Hunter, and the valuable assistance of the volunteer members of the expedition, Dr E. W. Bastin and Dr D. W. Sciama.

Royal Greenwich Observatory,
Herstmonceux :
1955 *February.*

INTERFEROMETRIC MEASUREMENTS OF THE GREEN CORONA LINE DURING THE TOTAL SOLAR ECLIPSE OF 1954 JUNE 30

A. H. Jarrett and H. von Klüber

(Received 1955 March 15)

Summary

A detailed description is given of a successful attempt to observe interference fringes with a Fabry–Perot interferometer from the 5303 A corona line during a total eclipse.

Low-absorption coatings for the interferometer and a narrow pass-band interference filter (equivalent width of ~25 A of the continuous spectrum, peak transmission 25 per cent) have been employed.

In spite of thin cloud during totality, which was estimated to have reduced the available intensity by a factor of 2, it proved possible to measure fringe half-widths for various position angles and distances from the solar limb.

The measurements seem to indicate a decrease of the line widths with increasing distance from the Sun. Interpreted in terms of kinetic temperatures, $T = 2{\cdot}2 \times 10^6$ to 5×10^6 deg. K, with most values near $2{\cdot}5 \times 10^6$, for regions situated 1·05 to 1·3 radii from the solar centre.

The paper concludes with suggestions for improvements to the equipment for a future occasion.

The possibility of getting interference fringes of the green corona line with a Fabry–Perot interferometer during an eclipse, by using the well-known method that Buisson, Fabry and Bourget (**1**) applied at one time to the Orion nebula, was considered and tried as long ago as 1918 (**2**), but so far has always failed for one reason or another. W. P. Wright, and later H. D. Curtis (**2**), developed and tried specially constructed instruments for this purpose, at no less than four eclipses. At two of these eclipses (1926 and 1929) one of us had an opportunity of becoming acquainted with these experiments. Later J. A. Carroll (**3**) made three further attempts on these lines. His last attempt, in 1947, was frustrated by damage to the interferometer plates in a serious aeroplane accident. A. A. Kaliniak (**4**), with a method differing in principle from the one considered here, using a slit spectrograph combined with a Fabry–Perot interferometer, obtained interference fringes with the green coronal line at the eclipse of 1941, but only with a low resolving power of about 5000. In recent years we have learnt more about the width and intensity of the green line, while considerable technical progress has been made in preparing narrow-band light filters and efficient coatings for interferometer plates. In a short report, P. J. Treanor (**5**) recently pointed out the conditions under which it should be possible, with modern optical equipment, to get interference fringes of the desired type during an eclipse. This report, together with the fact that one of us (**6, 7, 8**) is acquainted with the technique of producing low-absorption interferometer coatings, were important reasons why we were led to make another attempt on this problem.

The aim and purpose of this present experiment was not, as the application of an interferometer may suggest, to achieve very high resolving power for investigation of the green line. This, if desired, could be done better with optical arrangements such as those used successfully for this purpose by Lyot and his collaborators (**9, 10, 11, 12**) without an eclipse. Because of the large width of the green line a resolving power of ~50 000 (~0·1 A) for most purposes would be quite sufficient. Since the line is rather broad, even less powerful instruments than those used by the authors just mentioned can give quite good results, as was shown by Waldmeier (**13, 14, 15**).

Were it possible, however, to photograph the corona during an eclipse with a Fabry–Perot interferometer (as was done in (**1**) for the Orion nebula), and in this way to obtain superimposed over the whole image of the corona a set of interference fringes of the green line, with one exposure only, the result might provide valuable information on the behaviour of the width of the green line in different parts of the corona, and should perhaps also give information with regard to Doppler shifts.

As the 1954 eclipse took place almost exactly at a very low minimum of solar activity, the intensity of the green line was expected to be very low, and the successful outcome of our experiment was, therefore, considered to be rather doubtful. To avoid as far as possible the loss of money and time which would arise from a failure, no elaborate equipment was used and the experiment was arranged rather as a first trial with future eclipses in mind. Although very thorough preliminary tests at Cambridge were essential, the optical arrangement as actually used during the eclipse was very simple.

In view of the history of this type of eclipse work one of our aims in this paper has been to describe rather completely our experimental experience, as we think it should be useful to others wishing to pursue further work of this kind.

Optical arrangement.—The optical requirements of the apparatus fall under two headings: (*a*) speed, (*b*) fringe contrast. We first deal with (*a*).

In view of the known intensity distribution between the maxima and minima given by a Fabry–Perot interferometer, and considering the fact that the width of the green line is of the order of 1 A, the range of the interferometer should be of the order of 3 to 4 A. If the range were smaller, which would be desirable since it would give greater resolving power, there would be much danger of losing contrast at the "feet" of the intensity distribution of the line (as was, for instance, experienced (**16**) in a similar problem recently by H. Brück and D. A. Jackson). After some tests we decided to use a range about 4 A, which fixes the spacer in air at 0·35 mm, giving the order of interference about 1320. The correctness of this choice was subsequently confirmed, as is shown by Fig. 9. Then if a resolving power of ~50 000 is required, one would need a reflectivity of ~92 per cent. From this figure, using the valuable measurements of Kuhn and Wilson (**17**), one can find immediately that the transmission of one of the etalons, using silver coatings of the highest quality, would be 0·045. If instead one takes multi-coated etalons, as we did, the transmission may be increased by a factor 1·5 or even 2, and for the present purpose this increase is not merely appreciable, it may be decisive.

We have furthermore to deal with an emission line superposed on a continuous spectrum, so that a very effective narrow-band light filter is needed to achieve the necessary contrast between interference fringes and the background caused

by this continuum. The method of diluting the continuum by a dispersion arrangement (prism or grating) did not seem entirely satisfactory, for reasons mentioned below. We decided therefore that we must use either a filter of the type developed by Lyot (**18, 19**) or a narrow-band interference filter of the Fabry–Perot type, as described for instance in (**21, 22, 23**). A Lyot filter using only quartz and calcite would transmit ~40 per cent. Narrow-band interference filters, if made with silver layers, transmit 20 to 30 per cent, and if made entirely with dielectric surfaces can transmit as much as 75 per cent. Interferometer and filter together would therefore pass not more than ~4 per cent of the incoming radiation of the corona. Near sunspot maximum the green line radiates ~1 per cent of the visible light of the corona (**24**). Experience by one of us at the 1952 eclipse in Khartoum showed that in good seeing a white light photograph of the corona on a plate of medium sensitivity will extend to about 0·5 solar radii from the limb, with an exposure of 20 seconds at *f*/120. Taking all these facts together a camera working at *f*/2 or *f*/3 seemed necessary to photograph the corona in 5303 A as envisaged, with an exposure time of 20 to 60 sec, an estimate which proved subsequently to be right. On account of the nearness of the eclipse to an exceptionally deep sunspot minimum, the intensity of the green line was expected to be unusually low, although no reliable information on its intensity was available. But with this knowledge in mind we did our best to achieve high speed and high contrast between continuum and fringe intensity.

It may have been supposed that some gain of light would result from the well-known formula $T^2/(1-R^2)$, giving the peak intensity of an emission line when observed with a Fabry–Perot interferometer. In our case, using multi-coated flats with $R \sim 0{\cdot}87$, $T \sim 10$ per cent (the actual values for the eclipse observations), this would lead to a peak intensity of not less than 60 per cent, whilst the continuous background from the continuous light which has passed the filter should have from $T^2/(1-R^2)$ a theoretical intensity of only ~4 per cent. But this makes the common error of supposing that all light of the line is concentrated within the instrumental line width of the interferometer, which is not the case here (resolving widths ~0·1 A, actual line widths ~1 A), so that a certain decrease of the contrast will take place. An example of a similar case can be found in (**25**). In the present instance the interferometer will work more or less like an ordinary spectrograph, giving a peak of somewhat higher intensity for the emission line, but in the absence of a filter it has the disadvantage that the continuum is diluted only by the very small amount of the range of the interferometer, here ~4 A. Furthermore this background is not uniform but depends on the intensity distribution of the continuous light of the corona.

Apart from the necessary aperture ratio of ~1 : 2 we wished to avoid too small a corona image, say of less than 1 cm diameter. In the simplest arrangement this would call for a camera with aperture not less than 30 cm and of 60 cm focal length. But then the dimensions of the narrow-band filter and the interferometer would become far too big. We decided therefore to use an optical arrangement with intermediate imaging, as sketched in Fig. 1. L_1, a normal astrographic lens of 30 cm aperture and 340 cm focal length, images the corona in the plane G_1. The focus of the lens L_2 (aperture = 7·5 cm, f_2 = 27 cm) lies in G_1. At the same time L_2 images the objective L_1 on the plane J. The interferometer is at J immediately preceded by an appropriate interference filter F. At J the cross-section of the beam is only 2·4 cm, so that the interferometer plates and the filter

need be only comparatively small. After J the light is collected by the lens L_3, a Zeiss Sonnar (aperture = 2·5 cm, $f_3 = 5$ cm) of excellent quality. This forms simultaneously images of the corona and of the interference fringes on the film P. The size of the image at G_1 is reduced by $f_3 : f_2 = 1 : 5{\cdot}4$, so that the solar diameter at P is about 6 mm. The effective aperture ratio of the whole system is $\sim 1 : 2$; some small losses will of course occur by reflections, at L_2, F, J and L_3. This arrangement has the advantage that by changing f_2 and/or f_3 one can alter the image scales of the corona and/or the fringes independently. For adjustment purposes and to obtain test fringes conveniently immediately before and after the eclipse, the light of a mercury lamp could be reflected by way of the mirrors Mi_1 and Mi_2 (Mi_2 being removed for the actual eclipse observation) on to the interferometer. The mercury lamp was imaged so that the interferometer was illuminated by the comparison light in very nearly the same way as by the corona during the eclipse. When using a Lyot or an interference filter in such a set-up it is important to remember that by re-imaging with the two supplementary lenses L_2 and L_3, reducing the image scale between G_1 and P by a factor 5·4, all angles beyond L_2 (in the sense of deviation of rays from the optical axis) are increased by the same factor.

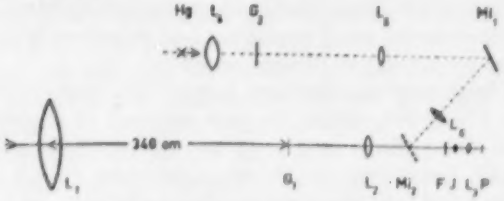

FIG. 1.—*General sketch of optical arrangement.*
Full line : optical path. Broken line : path for mercury comparison light.

Narrow-band filter.—For the investigation of a rather faint emission line superimposed on a continuous spectrum with a Fabry–Perot interferometer it is imperative to use a filter with the band width as narrow as possible, because contrast, and therefore the visibility of the fringes, in such a case depends entirely on the filter. Before modern narrow-band filters were available the obvious thing to do was to dilute the background by dispersion with a prism or grating, as was actually done in (**2**) and (**3**). But unless one is able to use very high dispersion, which could be obtained only with difficulty, one can easily see that the dispersion method will give worse results than for instance a narrow-band light filter of ~ 20 A half width, which to-day can be produced in various ways without too much difficulty. The dispersion method uses essentially a slitless spectrograph, and each half crescent of the corona can be regarded as a very wide and not uniformly illuminated slit. A good approximation to the contrast to be expected between emission line and continuous spectrum can be obtained easily by a graphic integration, taking into account the radial decrease of the light of the corona and the dispersion available. A dispersion of 20 A per mm can be obtained under reasonable conditions with two large glass prisms, but this would give lower contrast, even near the limb of the Sun, than light filters of 20 A half width. Furthermore, since in the final image the continuous spectrum gives a uniform background while the intensity of the emission line decreases rapidly with increasing distance from the Sun, the conditions for contrast are becoming

more and more unfavourable as we proceed outwards from the limb. For geometrical reasons the situation will be still worse near the lower and upper limb of the spectrum.

In preliminary experiments at Cambridge attempts were made to use an ordinary Lyot filter already existing at the Observatories. This consisted of eight quartz plates and was designed to transmit a band width of ~ 2 A at Hα. It does not seem necessary to have quite such a narrow band for the present work, and by shifting the maxima of the different steps in the well-known manner (**18**) it was quite possible to get a band width of ~ 15 A centred on $\lambda 5303$ A with only three quartz plates, using an additional interference filter with a rather wide band and high transmission to remove the unwanted maxima. But since only polaroids were available for polarizers, the transmission of this filter was found to be far too low. Another difficulty was caused by the rather large field required by our double imaging system, which demands a wide-angle type of Lyot filter, as described in (**18**), and one using only calcite instead of polaroids. This turned out to be far too expensive for the present experiment. But it is still our belief that probably the best filter for this purpose would be a wide-angle Lyot filter, constructed entirely of quartz and calcite. A system with only four quartz plates should do quite well. It would probably be possible without much difficulty to convert an Hα filter of this type so as to transmit at $\lambda 5303$ under reasonable temperature conditions.

We then tried interference filters of the type described in (**12**) and elsewhere. Several firms kindly prepared samples of such filters for us which were all tested and measured very thoroughly with respect to peak wave-lengths and transmission in many different parts of the filter, using the large solar spectrograph ($f = 900$ cm) of the Cambridge Observatories. Amongst the filters, those of Baird Associates Inc., Cambridge, Mass. and of Bausch and Lomb (**26**), both of dielectric type, showed a remarkably high peak transmission of 60 to 70 per cent, and in parallel light when only a very small area of the whole filter was used, half widths of 30 to 40 A. But there were two difficulties: (1) either the wave-length for peak transmission was not quite correct and could not in this special case be sufficiently adjusted by inclining the filter; or (2) the wave-lengths of peak transmission of different parts of the filter were widely different, a defect (sometimes known as the wedging effect) from which most interference filters suffer. After some trials, however, Hilger and Watts Ltd produced a special interference filter with semi-transparent silver coatings, the size being 25 mm square. Using only a very small area of a few mm^2 in parallel light and at normal incidence, the transmission curve of Fig. 2 was found, with a very small asymmetry on its short-wave side. The peak transmission was ~ 25 per cent, the half width as little as 15 A, the transmission dropping down in a relatively short distance from the peak to well below 1 per cent. Integrating the whole transmitted light, as indicated by Fig. 2, and allowing some correction for the low-intensity wings of the curve, the total transmission could be estimated to have an equivalent width of ~ 25 A of the continuous spectrum. A second and broader transmission maximum was found at $\lambda 4045$ A. But this excellent performance was again partly spoilt, as with the other filters, because the peak wave-lengths for different parts of the filter were found to vary as indicated in Fig. 3. This figure shows that use of the filter with its full aperture in a telecentric beam would smear out the actual half widths over a range of ~ 60 A. This scattering of the peak wave-lengths does

not increase the total background intensity allowed through the interferometer, but cuts down the transmission for the λ 5303 line and hence must have caused some loss of contrast because each point of the image at P is formed by rays which have passed through a considerable area of the filter. The way in which the

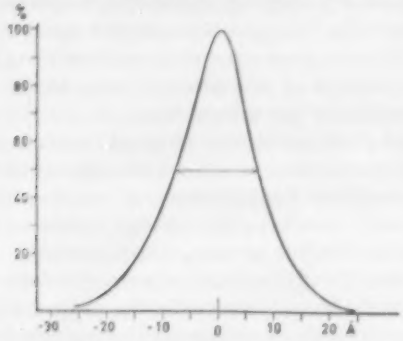

FIG. 2.—*Relative transmission of a small area of the Hilger interference filter for λ 5303 Å. Absolute peak transmission about 25 per cent.*

FIG. 3.—*Difference of peak transmission for different parts of the interference filter of Fig. 2, in angstrom units, for normal incidence.*

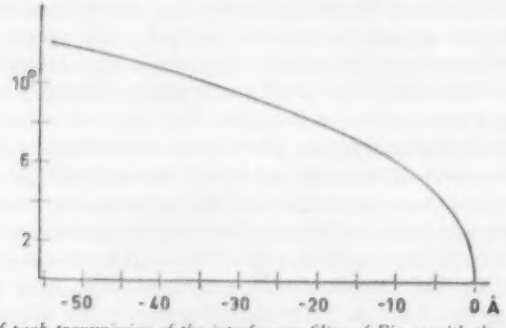

FIG. 4.—*Shift of peak transmission of the interference filter of Fig. 2 with the angle of incidence.*

peak transmission depended upon the inclination of the transmitted light relative to the normal to the filter is shown in Fig. 4. A careful test, taking into consideration the measurements illustrated in Figs. 3 and 4, led to the conclusion that a very

slight inclination of the filter would give the best result during the eclipse observation. This inclination could be set very reliably before the eclipse by using reflected light from one surface of the filter. To cut out the secondary transmission maximum near λ 4045 A the filter was combined with an OY 6 Chance glass filter, whose transmission curve as found by actual measurement in Cambridge is given in Fig. 5.

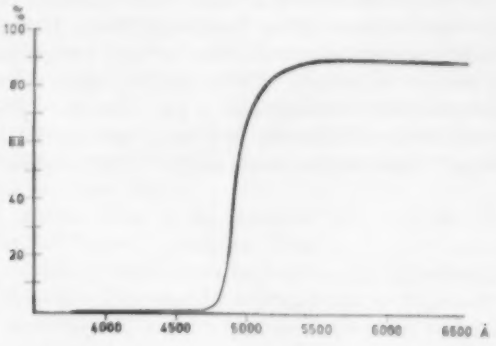

FIG. 5.—*Absorption curve of the auxiliary glass filter which was to be combined with the interference filter of Fig. 2.*

Photographic emulsion.—It seemed desirable to provide an effective cut-off also on the long-wave side of λ 5303 A. If the interference filter transmits some very small fraction of the light over a long wave-length range, the background on the photograph can accumulate so as to diminish the contrast of the fringes appreciably. As no suitable glass or gelatine filter seems available for this purpose the colour sensitivity of the photographic emulsion used was adjusted so as to give a sensitivity as near as possible to λ 5303 and then a sharp fall to the red. On the other hand, the emulsion had to have just sufficient sensitivity to record the green mercury line λ 5461 A of the comparison fringes. We are much indebted to the Research Laboratories of Kodak Ltd at Harrow for producing for this work several samples of such emulsions, sufficient both for tests with the large Cambridge spectrograph and for the actual eclipse observations. In a case like this the choice of the right emulsion is most important. Eventually an emulsion was selected similar to the Kodak IIa–J, a plate (**27**) of fairly high speed, moderately high contrast and of a graininess which seemed to give a good compromise between speed and photographic resolution. The resolving power of the actual emulsion was tested by very high enlargement and by microphotometric records of very sharp interference fringes for this purpose. A medium yellow dye was added to the emulsion to reduce halation. This had been proved most effective in earlier experiments, for instance in the photometric work of the 1952 eclipse, carried out by one of us. Such a dye, of course, may slightly affect the spectral sensitivity. Fig. 6 shows the relative colour sensitivity of the emulsion from high-dispersion spectrograms taken with the Cambridge equipment. For several reasons it was impossible to get the peak sensitivity quite at the right wave-length, but the speed proved nevertheless to be sufficiently high for our work.

Interferometer.—Some early tests were made with a single-plate quartz interferometer with a thickness of 0·5 mm, giving a range of 1·8 A, but this proved insufficient for the present purpose. Subsequently a conventional Fabry–Perot interferometer was selected; actually the one which had been used for certain tests in 1952 (7). The plates were of crystalline quartz, figured to $\lambda/40$ by Hilger, and coated by one of us with four quarter-wave layers of zinc sulphide and three layers of cryolite deposited alternately. This coating had been deposited in 1953 April and the plates had after that been in use for some considerable time for high-resolution spectroscopy in the Cambridge Solar Laboratory. As they were found to be still in quite good condition in 1954 March we decided to use the same coating also for the eclipse. When freshly coated their reflectivity was about 94 per cent and their transmission 5 per cent for wave-length 5461 A. For separators steel balls of diameter 0·35 mm, produced by Miniature Ball Bearing Co., Bienne, Switzerland, were used. They worked excellently and

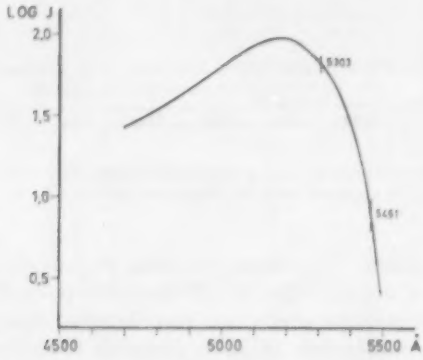

FIG. 6.—*Spectral sensitivity of the special Kodak emulsion.*

once the interferometer was properly adjusted it could be kept in this adjustment for days. For test exposures it was only necessary to remove the interference filter F (Fig. 1) and to insert the already adjusted auxiliary mirror Mi_2. For comparison the light source was a water-cooled mercury isotope lamp produced by the Research Laboratories of the General Electric Company, Wembley. From interferometric measurements with a resolving power of over 1 000 000 it was known (7) that the line width of λ 5461 from this lamp does not exceed 0·005 A. No correction for the mercury line width or for hyperfine structure was therefore necessary.

The final camera was a standard Zeiss Contax II with the Sonnar $f/2$ lens already mentioned. Although the plate adaptor of this camera with its ground glass screen proved very convenient for adjustment purposes, film was used at the eclipse, partly because it allowed a much more rapid succession of exposures than could be made when changing plate-holders, and partly because the focus for the Contax miniature plate-holders was found to be not as stable as with the film.

In a long series of test exposures made before the expedition left Cambridge the fringe definition was found to be excellent, the instrumental line width being $\frac{1}{27}$ of the range ($\sim$0·15 A). The resolving power was only slightly below the

theoretical value. The range at λ 5303 was determined with the solar spectrograph using so-called channelled spectra, and found to be 4·04 A (**28, 29, 30, 31**). Such spectra can be produced easily by a continuous light source with the interferometer in front of the large Cambridge solar spectrograph. Furthermore, before leaving Cambridge the whole optical arrangement was tested thoroughly in the laboratory with all parts exactly in the position in which they were used afterwards during the eclipse, using a kind of "artificial corona" as well as the full Moon. For the laboratory test the large coelostat system ($f = 1800$ cm) of the Cambridge solar spectrograph was used as a collimator. An "artificial corona" of correct size was set in the focal plane of the 1800 cm lens. The outgoing telecentric beam was then reflected from the auxiliary mirror back on to the optical arrangement of Fig. 1. This artificial corona could give continuous light and superimposed, when required, the green mercury emission line also. These tests were found most valuable as a check on vignetting, false light in the apparatus, and on exposure time.

Contrast.—A general idea as to exposure time was obtained by tests at Cambridge on the full Moon. However, in an experiment of this kind it is also most important to estimate the contrast to be expected between the fringe and the continuous background. Here lay the largest unknown factor in the experiment, for not all the necessary data were known sufficiently accurately. A rough estimate could, nevertheless, be made in the following way. The intensity ratio of the λ 5303 line to the continuous spectrum of the corona was measured carefully by Grotrian (**24**) on slit spectrograms taken at the 1929 eclipse (maximum of solar activity in 1928·4). He obtained a ratio about 27 : 1. We assume the ratio to be of the order 20 : 1, which agrees sufficiently well both with Grotrian's work, with the measurements of Lyot, and with estimates from other eclipses (**32, 33**). Our interference filter had an effective band width of ~ 25 A, and taking the range of the interferometer to be 4 A there is a decrease in contrast by a factor $\frac{25}{4} \sim 6$. As we have seen that the wave-length of peak transmission of the interference filter is not quite constant over its surface there is an additional decrease of contrast which may be estimated at perhaps a factor of 2. For an ideally sharp line the contrast between minimum line intensity and continuous background should be $1 - R^2/(1-R)^2$; with $R = 0{\cdot}87$, the value we may assume for the eclipse observations on Koster, this gives an increase of the contrast of ~ 15. But since the corona line is actually much broader (~ 1 A) than the instrumental width ($\sim 0{\cdot}2$ A) and has a characteristic Doppler broadening shape, the contrast is again decreased by a factor of say 6. Taking all together this brings the contrast of line to background to about $20 \times 15/6 \times 2 \times 6 = 4 : 1$. But this value relates to an average phase of the solar cycle, whereas we were working at a very low minimum in an unusually unfavourable cycle. No measures were available to show how weak λ 5303 really had become, but it seemed reasonable to expect about $\frac{1}{20}$ of the value above (**34**, Fig. 12). So we had to be prepared for a contrast as low as 1 : 5, and this subsequently proved to be of the right order. Using an artificially broadened emission line, it was confirmed by special tests in Cambridge that the photographic emulsion and the method of developing employed later at Koster would give reasonable results for rather low contrasts of this order.

Observations on Syd Koster.—The Cambridge eclipse party was located on the small granite island of Syd Koster about 15 km off the west coast of the Swedish mainland not far from Strömstad. We considered it unwise to use the

sensitive interferometer optics in a temporary hut or tent as is usually done with apparatus at a solar eclipse. Fortunately a private house with a substantially built cellar on granite ground was available where we could set up the apparatus, shielded beautifully from weather and temperature changes, and where in fact we had most of the essential features of a good laboratory. Water and electricity supplies were available in the house and the cellar was easily blacked out to give a photographic dark room and a darkened room for optical work. The Sun's light was reflected through one of the cellar windows by a 40 cm coelostat and an auxiliary mirror. The slight loss of light by this double reflection was a small price to pay for the good laboratory conditions under which we were able to work. The whole arrangement proved very satisfactory and can be strongly recommended for similar purposes, provided seeing requirements are not too critical. The temperature changes over the whole day were always lower than 1 deg. C and it was a great advantage to be able to make adjustments and tests quite independently of weather conditions. The whole equipment was set up quite simply as in the Cambridge laboratory on standard optical bench rails and fittings (reproduction in (**35**)). Instead of pillars of brick or concrete some of the expedition's bigger cases were used, loaded with rocks, and these proved to be very solid.

We had some doubts as to whether to use the interferometer adjusted with the fringe system centred on the Sun or in an eccentric position. The centre position would have the advantage that one might obtain perhaps one or two fringes right round the corona at more or less constant photographic density, and could obtain measurements of possible radial velocities much more easily. On the other hand, it is well known that it is not practicable to adjust an interferometer so that a given fringe has exactly some desired diameter. Thus it could easily happen that the first visible fringe would just miss the most interesting part of the corona. In any case not more than about two fringes could be expected to show. The eccentric position on the other hand gave far more chance of covering the whole corona with a system of fringes, without much loss in resolving power. After experience one of us had gained in 1953 with similar observations on the coronagraph of the Pic du Midi, and since our exposure times were relatively short, we decided to try both arrangements and to change from one adjustment to the other during totality itself.

The fringe system was centred on the solar image a few minutes before second contact, and then, after totality had started and the first three frames had been exposed, the fringes were moved to the eccentric position by inserting a prepared wedge under the interferometer mounting. Two more frames were taken with this adjustment.

During totality, the coelostat and auxiliary mirror outside the house were in charge of Mrs von Klüber, whilst the observers inside the cellar took the eclipse exposures and the calibration and test exposures. The corona was photographed through a thin high layer of irregular cirrus cloud under which was another thin layer of fairly fast-moving broken-up cumulus. The clouds interfered rather seriously with the first and second exposures; for the rest the seeing must have improved considerably.

Shortly before totality a set of intensity marks was photographed on the beginning of the film using an accurately calibrated Hilger rhodium step filter (using L_2 for imaging) with an artificial continuous light source, and through an interference filter similar to the one used in the eclipse itself. The wave-length

range of spectrum and the exposure times were quite close to those of the actual eclipse photographs. Then a few minutes before the eclipse, several sets of comparison fringes from the mercury lamp were exposed on the same film in the centred fringe position. During totality the following set of exposures was made on the corona:

Frame 1	exposure 10^s	centred fringes
2	20^s	
3	60^s	
Frame 4	exposure 25^s	eccentrically placed fringes
5	10^s	

Immediately after the eclipse another set of mercury test fringes was photographed on the same film, this time in the eccentric position, before the interferometer had been touched. The interferometer was then brought back to the centred adjustment and additional mercury fringes were taken exactly as at the beginning. Lastly a duplicate set of calibration marks was printed on the end of the film. As the contrast of the λ 5303 line against its background was expected to be very low, the film was developed for high contrast in a tank with continuous agitation, for five minutes at 20 deg. C in undiluted Kodak D19b developer. The photographic quality of the film (and of a second control film) was found, after the development, to be very good. The eleven different photographs of the mercury fringes showed that the optical adjustment had remained good throughout, while the intensity marks testified to the general photographic quality.

Films. Frame 1.—This frame was taken at the beginning of the eclipse with 10^s exposure time and seems to have been considerably affected by cloud. It is very under-exposed and far weaker than frame 5 taken later with the same exposure time. The innermost part of the corona is clearly visible but its image nowhere reaches the distance of the third interference ring, the first which would have been visible, i.e. no fringe could be expected to show and none is visible.

Frame 2.—The density of this frame, exposed for 20^s, is still rather weak compared with the fourth frame, which had a similar exposure time, and clouds must still have interfered. The prominences P_1 and P_2 (Figs. 7, 8) can be clearly seen and offer a good method for correctly orientating the photograph. On the east side the corona extends just to the third fringe which can be traced very weakly but quite clearly, as indicated in Fig. 7. The fringe seems to be sharper in the N.E. quadrant and more diffuse in the S.E. quadrant. On this frame the west side of the corona is much weaker and only a trace of the third fringe can be seen in the N.W. quadrant. The corona nowhere reaches the fourth interference ring. It does not seem worth while to measure this film.

Frame 3.—This frame had the longest exposure, 60^s, and as transparency of the sky had now become much better it shows the highest density. The centre of the fringe system coincides well with the Sun's centre. The first and second rings were calculated to fall well within the solar image, the second being very near to the Sun's limb. In spite of the rather high density, the third fringe can be seen distinctly on the east side of the corona, as indicated in Fig. 7, which was drawn from this film. This fringe appears to be rather sharp in the N.E. quadrant and a small kind of knot can be seen at P.A. 60°, of the kind well known to observers with the Lyot coronagraph. In the region of the equator

the contrast to the background density becomes very low, so that the fringe can be seen only under low magnification. In the S.E. quadrant the contrast increases again to fairly good visibility; the fringe seems here to be definitely broader and more diffuse than in the N.E. quadrant. Also the widths seem to vary a little from place to place and these variations are apparently not caused by slight intensity variations of the underlying corona. As all the comparison fringes from the mercury isotope lamp taken shortly before and just after the eclipse on the same film and with the same adjustment proved to be excellent, this behaviour of the fringes is probably real.

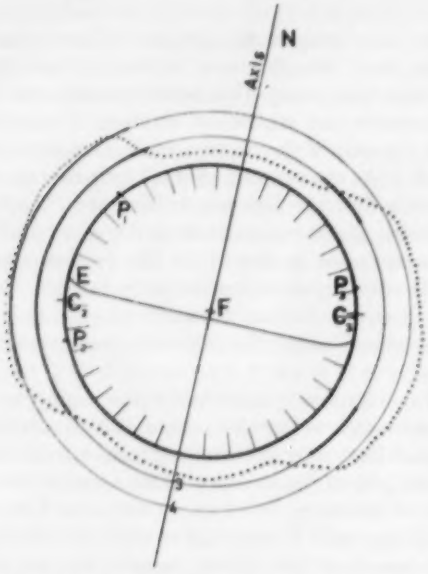

FIG. 7.—*Sketch indicating the centred interference fringes visible on Frame 3. Dotted line: outer contour of the corona image on this frame. Thin line: position of the third and fourth interference fringes. Heavy line: visible parts of interference fringes from λ 5303. F: centre of interference system. P_1, P_2, P_3: positions of prominences. C_2, C_3: positions of second and third contact.*

In the surroundings of the north and south pole no fringe is visible, but it cannot be expected, because at this distance from the Sun's limb the film is practically clear, as can be seen from the isophotes indicated (dotted line) in Fig. 7. The density of the corona image on the west side is higher than on the east side. In the region occupied by the third interference ring the corona is definitely over-exposed. Nevertheless the third ring can be traced quite well in the N.W. and S.W. quadrants if a low magnification is used, although with low contrast. These parts of the fringe have about the same widths as in the S.E. quadrant but since the density is too high and the contrast too low they cannot be measured here with sufficient accuracy.

The fourth ring at the east side is clearly visible at the outer edge of the corona image where the density of the film is already too low for reliable measurement. On the west side this ring is hardly to be seen at all in spite of the fact that the

density there is still quite sufficient. This is in agreement with our other frames; all of them show the fringes far more distinctly on the east side than on the west side of the Sun.

Frame 4.—Fig. 8 was sketched from this frame. It is well exposed; indeed the inner parts of the corona are rather over-exposed. The eccentric fringe system is easily and clearly visible on the east side of the corona. The density on the west side is higher and the (photographic) contrast of the fringes therefore much lower. From micrometric measurements of the visible parts the whole system of eccentric fringes can be easily constructed as indicated on Fig. 8, their centre

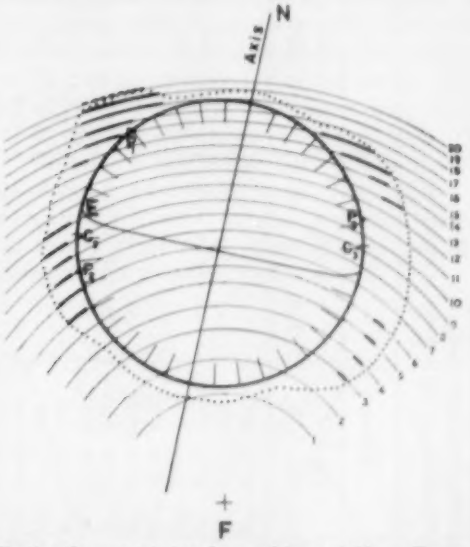

FIG. 8.—*Sketch indicating the eccentric interference fringes visible on Frames* 4 *and* 5. *The figures at the right-hand side indicate the fringe numbers. Other notation as for Fig.* 7.

being at F. The well-known law that the squares of the radii are in arithmetical progression is satisfied by these measures extremely well. In Fig. 8 all parts of the interference fringes which could be seen and measured without difficulty on Frame 4 are drawn in heavy line. The dotted curve again indicates roughly the outer isophote on this film. It is clear from this frame, and also from the next Frame 5, that the fringes avoid the region near the equator where as far as photographic density is concerned they should show up easily. The same is true for the polar regions. This behaviour is just what one would expect if one takes into account what we know of the average intensity distribution of the green corona line in this phase of the solar cycle (**14**). Near the Sun's limb on both east and west sides the density of the film is very high, the (photographic) contrast therefore low, and it gets progressively more difficult to trace the fringes as the limb is approached. This frame has produced most of the measurements of Table I.

Frame 5.—This is also a very good exposure, its density being much higher than that of Frame 1 which was exposed for the same length of time (10^s) but which apparently was taken through clouds. All the fringes indicated in Fig. 8 can

TABLE I

Half-widths of the λ 5303 corona line from micrometric or microphotometric measurements of the fringes

vis. = *measurements by micrometer only;*
phot. = *measurements by microphotometer;*
P.A. = *approximate position angle;*
D = *distance from Sun's limb;*
A = *whole width at half intensity in angstroms.*

Frame 3				Frame 4						Frame 5					
	vis.				vis.			phot.			vis.			phot.	
Fringe	P.A.	D	A	Fringe	P.A.	D	A	P.A.	D	A	P.A.	D	A	P.A.	D	A
3	50°	2′·5	0·94	19	38°	2′·3	0·8									
3	80°	2′·5	0·90	19	55°	4′·0	0·7	43°	2′·5	0·8						
3	110°	2′·5	0·95	18	38°	0′·9	1·4	41°	1′·2	1·3	32°	0′·6	1·3			
3	130°	2′·5	1·1	18	48°	1′·9	0·84				46°	1′·6	1·0	40°	1′·4	1·0
3	240°	2′·5	0·95	18	60°	4′·2	0·79							47°	2′·0	1·1
3	320°	2′·5	1·05	17	52°	1′·1	0·87	53°	1′·5	1·1	46°	0′·5	1·2	42°	0′·4	1·4
				17	60°	2′·2	0·96	60°	2′·2	1·2	55°	1′·4	1·1	48°	0′·8	1·3
				16	64°	2′·0	0·82	58°	1′·0	1·4						
				16	330°	0′·4	1·4				330°	0′·5	1·7			
				16	318°	2′·5	1·1				322°	1′·4	1·2			
				15	318°	0′·8	1·6				320°	0′·5	1·7			
				15	310°	2′·6	1·5				313°	1′·6	1·4			
				11	96°	1′·3	1·1									
				10	103°	1′·1	1·1	108°	2′·7	1·1						
				9	109°	1′·0	1·3	111°	1′·9	1·0	108°	0′·5	1·1	109°	0′·9	1·4
				8	116°	1′·0	1·3	118°	2′·0	1·0	115°	0′·5	1·1			
				7	122°	0′·7	0·8				122°	0′·6	1·0			
				7	123°	1′·0	1·0									
				6	130°	0′·9	0·9									

clearly be seen; but here they can be traced practically down to the limb of the Sun. Again the density of the west side is higher and the contrast of the fringes is there diminished. Measurements of this film are also included in Table I and form a valuable supplement to those determined from Frame 4.

Measurement of the films.—The various sets of mercury comparison fringes taken on the same film before and after the eclipse were measured visually with the micrometer and then with the recording microphotometer. Both pre- and post-eclipse images proved to be of the best quality, in keeping with those obtained in the tests in Cambridge and on Koster before the eclipse. The interferometer therefore was in perfectly good condition during the eclipse itself. The half-widths of the fringes, which were examined specially in the neighbourhood of the fifteenth fringe, where most of the later measurements of the corona line were made, was found to be 0·21 A, i.e. about $\frac{1}{20}$ of the range. This is equivalent to a resolving power of 26 000 and, from resolving power $= 3 \cdot m\sqrt{R}/(1-R)$, in good agreement with an effective reflectivity R of 87 per cent. It is also in good agreement with the theoretical half-width (**36**) which from $\Delta\lambda(1-R)/\pi \cdot R$, where $\Delta\lambda$ is the range of 4·04 A, would be expected to be 0·18 A. These extremely sharp mercury isotope interference fringes give the instrumental profile immediately without further correction. Fig. 9 shows two of them drawn to correct scale and in correct relation to their range.

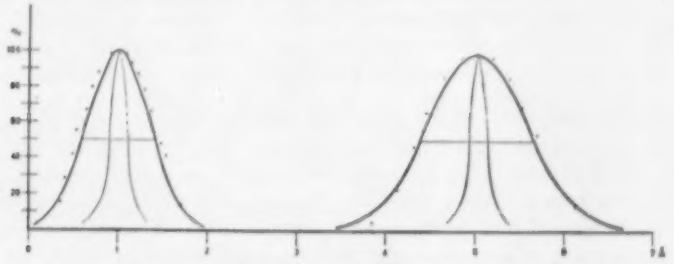

FIG. 9.—*Example of two line contours of λ 5303 from Frame 4 drawn in correct relation to the range (4·04 A) of the interferometer. The dots indicate actually observed values. The full curve indicates the line contour after correcting for the limited resolving power of the photometer. The line contour of the mercury isotope comparison fringe is given by the thin line.*

From Frame 3 the widths of the third fringe of λ 5303 could be measured with the micrometer in different parts of the corona. The results are in Table I. The density of this frame is too high to give reliable microphotometric records, so that only the micrometric measurements are given here.

On Frames 4 and 5 micrometric measurements of the fringe widths could be obtained without difficulty for many selected points. These measurements are to be found also in Table I. They give immediately, without further reduction, fairly reliable values for the widths of the green line at different parts of the corona. Lyot (**9, 10**) made his first measurements of this line with a slit spectrograph in a similar manner. As the range of the interferometer was known accurately and the separation of the fringes can be measured also very well, the scale value for converting the measurements into angstroms provided no difficulty. On the other hand, the high density gradient within the image of the corona was a source of difficulty in the measurements. This was of course expected, but since we had to face so many other uncertain factors concerning exposure time and contrast

we had deliberately avoided taking special precautions against this effect, so as not to introduce more complication than necessary into the experiment. It was for this reason that we had planned to get frames of different exposure times.

But even if one takes into account the density gradient in comparing Frames 4 and 5 (which have altogether different densities) with each other there is not much doubt that the line appears to be much broader quite near to the limb of the Sun than further out. On the average this is confirmed by tracings made on several fringes with the Cambridge self-recording microphotometer. Owing to the fact that the coronal image was rather small, the photographic density high and the fringes narrow, it was found difficult to obtain these tracings without loss of resolving power. The graininess of the emulsion on the other hand did not cause much trouble. The many intensity calibrations on the film permitted reduction of the photometer tracings to intensities in the usual manner. As mentioned already, the fringes are superimposed on a background with a rather steep density gradient. A difficulty was, therefore, encountered similar to that in the photometric investigation of faint components very near to a strong spectrum line. But in spite of this, by carefully taking into account the slope of the background, fairly good intensity curves could be obtained of suitably selected parts of the fringe. The possibility was even considered as to whether to apply a correction for the density gradient with relation to width of the photometer slit. The necessary procedure was described long ago by Rayleigh (**37**). This correction for x_0 can be written in the form

$$\frac{\epsilon^2}{3}\left(\frac{1}{\tau}\cdot\frac{d^2\tau}{dx^2}\right)_{x_0},$$

where ϵ is the half-width of the slit of the spectrograph, and $\tau(x)$ the coefficient of transmission of the emulsion at the point x_0. But the correction was found to be very small and not very certainly determined, so it was omitted. Besides recording the fringes of the corona line, tracings were made of the corresponding eccentric fringes of the mercury comparison, with the same setting of the microphotometer, which gave the instrumental width as produced by the photometer. The intensity distribution in the fringes of both corona line and mercury lamp could be represented sufficiently well by an error curve,

$$s(\Delta\lambda) = a\exp\left[-\left(\frac{\Delta\lambda}{\gamma}\right)^2\right].$$

Using the instrumental half-width, the observed half-widths of the corona line were corrected in the usual way (**38**), by taking the difference of the respective squares of the denominator in the exponential expression. Because of the relatively high resolving power provided by the interferometer these corrections were rather small, and in good agreement with corrections derived for the special case of a Fabry–Perot interferometer by Minkowski and Bruck (**39**). The corrected half-widths are in Table I. This procedure for the reduction is open to some criticism. It would have been better to approximate to the observed curves by a two-parameter type of expression, to take better account of the wings. This more elaborate reduction definitely becomes necessary if one has to deal with the intensity distribution of a Fabry–Perot pattern for reflectivity <80 per cent where the wings are no longer negligible. But in our case the wings cannot be determined with sufficient accuracy anyhow and an application of a Voigt function as suggested by v. d. Hulst and Reesinck (**40**) would not have been justified.

The photometrically derived widths are on the whole in fairly good agreement with the purely micrometric measurements. But there seems to be a slight tendency for the photometric values to be larger than the micrometric ones. Fig. 9 shows an example of the fringe contours in two successive fringes from Frame 3, drawn in correct proportion to the range of the interference system and normalized to peak intensity 100. The profiles of the mercury isotope comparison fringes as produced by the interferometer are shown by the thin curve. The observed points for the corona fringes are given by dots and the heavy lines denote the contours after correction had been applied for the instrumental profile. Taking into account the rather small scale of our image, its high density and the limited contrast of the fringes, photographed under most unfavourable conditions, we do not feel justified in putting too much weight on these preliminary measures or in drawing any far-reaching conclusions from them. Also it seems inadvisable to attempt to deduce macroscopic movements by Doppler shifts from this material, for this really needs a larger image, and probably would be better done with the centred fringe system. The present measures however seem to indicate a decrease of the line widths with increasing distance from the Sun, an effect also indicated in coronagraph measurements by Waldmeier (**13, 14, 15**). On the other hand, other observers' measures of the red line $\lambda 6374$ seem not to show such a decrease (**12**), though this would also be expected. The line widths appear rather large on some parts of the fringes and this behaviour is revealed simply by visual inspection of the fringes under a low power. In spite of the not very favourable photometric conditions mentioned above, it seems improbable that there would be any large systematic falsification of the widths by photographic effects; and there seems no doubt whatever that the interferometer worked perfectly well. The mean error of the values given in Table I must be estimated as at least 0·1 A, and even larger for those values where the contrast was very low. But in any case even where the values seem to be somewhat doubtful there always seems to be the tendency towards the larger value.

If one supposes that the width of the line is due entirely to temperature broadening, the temperature can be derived easily from the expression $T = \mu\xi^2/2R$ with the molecular weight $\mu = 56$ (Fe), R the gas constant and ξ the velocity derived from Doppler effects from the half-widths. This would lead to a temperature T of $\sim 2{\cdot}2 \times 10^6$ to 5×10^6 with most of the values round about $2{\cdot}5 \times 10^6$ in the range of 1·3 to 1·05 solar radii from the Sun's centre. In a recent paper Allen (**41**) has pointed out that temperatures derived by direct spectroscopic measurements of line widths seem to be slightly larger than those derived by other methods. This may point to high turbulent velocities in the corona on a macroscopic (but still rather small) scale. But with most of the previous spectroscopic values a rather high correction had to be applied because of the large instrumental widths, while a simple Gaussian approximation was used for the observed curve, so that some of them may have been under-corrected (**40**).

Spectroscopic measurements of the width of the green line with a coronagraph were obtained as early as 1931 by Lyot (**9**) in the second order of a Rowland plane grating, giving a dispersion of 7·5 A/mm, but a resolving power of only 8000. Further measurements with a coronagraph have been published by Waldmeier (**14, 15**). He found the half-widths to be about 1·3 A, but used a resolving power as low as 4000 ($\sim$ 1·3 A), so that his measures required rather large corrections.

In an active region of the corona he found in 1945 (**15**) half widths between 1·56 and 0·96 A, but again the resolving power was low (~1 A), and the necessary corrections therefore were still rather high. In 1942 Lyot, using a grating spectrograph attached to the Pic du Midi coronagraph, obtained resolving power 20 000 (0·27 A) at a dispersion 4 A/mm (**12**). Measurements of the green line with this instrument have not yet been published, but for the red line λ6374 Dollfus has given a number of measurements with a resolving power of 0·3 A, giving a temperature of 2×10^6 at 1·1 radii from the Sun's centre. Measurements of Righini (**42**) at the eclipse of 1936, with a slit spectrograph giving a width of 3·8 A for the green line, are not reliable, as the author himself points out, because of the low resolving power of the instrument. At the 1941 eclipse Kaliniak (**4**) obtained some measurements from a rather faint interference pattern from the green line, using a Fabry–Perot interferometer in front of the slit of a prism spectrograph. The range of the interferometer was ~8 A, reflectivity ~70 per cent, and the resolving power, therefore, could not have been larger than ~5000 or approximately 1 A. In this case again a rather large correction for the observed profile was needed which actually could have been obtained only by extrapolation as no suitable exposed reference line was available. He has derived line widths of 1·4 A from his observations. Apparently no other measurements of the widths of the green line during an eclipse have so far been published.

General comments.—The main aim of the present work was to establish the practicability of this method of investigating the corona during an eclipse. With the experience outlined here there is no more doubt that valuable observations of this kind can be made at most eclipses, assuming exposure times of 1 minute or more are possible. Desirable improvements, some of which we had omitted deliberately to avoid too many complications for the first test, should be outlined here:

1. A factor of 2 in exposure time could be gained if an emulsion could be obtained with its peak sensitivity centred exactly at λ5303 (see Fig. 6), but no emulsion with bigger graininess should be chosen. This might be achieved, perhaps, by sensitizing dyes of the cyanin or carbocyanin type, but the emulsion has to be carefully balanced for spectral and general sensitivity and account has to be taken of the dye added to reduce halation.

2. Another factor of between 2 and 3 could be gained if a special dielectric filter were used. Alternatively a wide-angle Lyot filter would be very useful and might give an improvement by a factor of 1·6.

3. The corona should be imaged on at least double the scale used here, the easiest method being to use a longer focal length for L_3.

4. It is most important that the steep gradient near the innermost part of the corona should be smoothed out to facilitate the attainment of higher accuracy in the photometry. This could be done by introducing near G either a specially designed circular absorption filter as pointed out long ago by Michailov (**43**) or alternatively a rotating sector of suitable form.

5. Our observations were made at a most unsuitable phase of the solar cycle when the green line was extremely weak. At the time of the eclipse we knew from routine measurements, kindly transmitted by radio from the Wendelstein (**44**), that even under excellent sky conditions great difficulty was encountered in detecting the green line with the Lyot coronagraph. The average intensity variation of the green line with the solar cycle is well known from many thousands

of observations made with Lyot coronagraphs (**34**). In favourable circumstances the line may be 10 or more times brighter than at the time of our observations. The continuous light of the corona (K-corona) seems also to alter with the phase of the solar cycle, the brightness at maximum may be about twice that at minimum (**45, 46**). This would mean that near maximum solar activity not only the intensity but also the contrast of the green line with respect to its continuous background should rise appreciably, making interferometric investigations correspondingly easier. It is difficult to estimate how much we may have lost on Koster by thin cloud, even during the exposures of Frames 3, 4 and 5, but the experience of other observers nearby supports our belief that we may have lost a factor of at least 2 in intensity. Altogether, therefore, there should be good chances for observations of this kind at a phase of higher solar activity.

6. The intensity of the red corona line $\lambda 6374$ according to (**34**) should be sufficient to give fringes during an eclipse, provided a suitable interference filter were available. We had hoped for such observations on Koster, but had unfortunately been unable to obtain the right filter in time. The observations might be made with the same arrangement as described above by simply changing from a green to a red interference filter during totality itself.

7. If an interference filter is used it should be coated, if possible, directly on a suitable coloured glass filter to cut out undesirable secondary maximum. This would avoid having an extra filter in the optical arrangement, which may always give trouble by unwanted reflections. As there is a tendency for these interference filters to change their wave-length of peak transmission with time, they must be checked by a spectrograph of rather large dispersion shortly before totality. It should be possible now to obtain such filters with an equivalent width of about 10 A, a peak transmission ~ 50 per cent and a peak to off-peak transmission ratio of 10^3 (**42**).

Acknowledgments.—We are indebted to the Joint Permanent Eclipse Committee for the expenses of the expedition to Syd Koster and further to the Bausch and Lomb Optical Company, Rochester, to Dr B. H. Billings of Baird Ass. Inc., Cambridge (Mass.), and to Messrs Hilger and Watts Ltd, London, for the production of special narrow-band interference filters for this work, to the Research Laboratory of Kodak Ltd, Harrow, for producing the special emulsion used for our observations and to the Oxford University Observatory for the loan of a 12-inch astrographic lens. We are also most grateful to Lektor B. Svenonius, Boras, for his assistance in a preliminary survey of possible observing sites and for much help given us by the local population of the island. We should specially thank Mr Eric Hansson, to whom we caused much inconvenience during our occupation of his cellar, house and garden, but whose assistance in this and other ways was an indispensable factor ensuring the success of our observations.

The Observatories,
Madingley Road,
Cambridge:
1955 *March* 14.

University Observatory,
St Andrews.

References

(1) H. Buisson, Ch. Fabry and H. Bourget, *Ap. J.*, **40**, 241, 1914.
(2) W. P. Wright and H. D. Curtis, *Sproul Obs. Publ.*, 11 (no year quoted).
(3) J. A. Carroll, *Nature*, **159**, 666, 1947.
(4) A. A. Kaliniak, *Rep. Solar Eclipse Exp. of* 1941 *Sept.* 21, Akademia Nauk S.S.S.R., Moscow, 1949, p. 352.
(5) P. J. Treanor, *The Observatory*, **70**, 179, 1950.
(6) A. H. Jarrett, *Investigations concerning semi-reflecting films, with special reference to interferometry*. Thesis, St Andrews Univ., 1952.
(7) A. H. Jarrett and H. von Klüber, *Nature*, **169**, 790, 1952.
(8) A. H. Jarrett, *Zeits. f. Astrophys.*, **34**, 91, 1954.
(9) B. Lyot, *C.R.*, **194**, 443, 1932.
(10) B. Lyot, *C.R.*, **202**, 392, 1936.
(11) B. Lyot, *M.N.*, **99**, 580, 1939.
(12) A. Dollfus, *C.R.*, **236**, 996, 1953.
(13) M. Waldmeier, *Zeits. f. Astrophys.*, **20**, 323, 1941.
(14) M. Waldmeier, *Zeits. f. Astrophys.*, **21**, 85 and 120, 1941.
(15) M. Waldmeier, *Mit. Sternwarte Zürich*, No. 149, 1947.
(16) H. Brück and D. A. Jackson, *Proc. Roy. Soc.* A, **216**, 183, 1953.
(17) H. Kuhn and R. A. Wilson, *Proc. Roy. Soc.* B, **63**, 745, 1950.
(18) B. Lyot, *Ann. d'Ap.*, Nos. 1 and 2, 1944.
(19) J. W. Evans, *J.O.S.A.*, **39**, 229, 1949.
(20) H. A. Tanner and L. B. Lockhart, *J.O.S.A.*, **36**, 70, 1946.
(21) P. Cotton, *Ann. de Phys.*, **12**, 209, 1947.
(22) M. Banning, *J.O.S.A.*, **37**, 792, 1947.
(23) L. N. Hadley and D. M. Dennison, *J.O.S.A.*, **37**, 451, 1947; **38**, 483, 1948.
(24) W. Grotrian, *Zeits. f. Astrophys.*, **7**, 26, 1933.
(25) E. B. Armstrong, *Contr. Armagh Obs.*, No. 10, 1953; *Journ. Atm. and Terr. Physics*, **3**, 274, 1953.
(26) Bausch-Lomb Opt. Soc. Rochester Leaflet, D.248, 1953.
(27) Kodak Data Booklet SE-3—Scientific Plates.
(28) F. Gehrcke and O. Reichenheim, *Ber. Deut. Phys. Ges.*, p. 209, 1906.
(29) K. Burns and W. F. Meggers, *Publ. Allegh. Obs.*, **6**, No. 7, 105, 1927.
(30) W. E. Meissner, *J.O.S.A.*, **32**, 191, 1942.
(31) C. Candler, *Modern Interferometers*, p. 290, London, 1951.
(32) F. Dyson and R. v. d. R. Woolley, *Eclipses of the Sun and Moon*, p. 145, Oxford, 1937.
(33) H. C. van de Hulst, *The Sun* (ed. G. P. Kuiper), p. 267, Chicago, 1953.
(34) M. Waldmeier, *Die Sonnenkorona*, p. 27, Basel, 1951.
(35) H. von Klüber, *Naturwissenschaften*, **42**, 3, 1955.
(36) W. E. Meissner, *J.O.S.A.*, **32**, 183, 1942.
(37) Lord Rayleigh, *Scient. Papers*, **1**, p. 135, Cambridge, 1899.
(38) A. Unsöld, *Physik der Sternatmosphären*, pp. 212–213, Berlin, 1938.
(39) R. Minkowski and H. Bruck, *Zeits. f. Physik*, **95**, 299, 1935; also S. Tolansky, *High Resolution Spectroscopy*, p. 162, London, 1947.
(40) H. C. van de Hulst and J. J. M. Reesinck, *Ap. J.*, **106**, 121, 1947.
(41) C. W. Allen, *Rep. on Progress in Physics*, **17**, 135, 1954.
(42) G. Righini, *Zeits. f. Astrophys.*, **21**, 158, 1941.
(43) A. Michailov, *Vierteljahresschrift der Astr. Gesellschaft*, **65**, 290, 1930.
(44) R. Müller, *The Observatory*, **74**, 222, 1954.
(45) H. C. van de Hulst, *B.A.N.*, **11**, 135, 1950.
(46) K. Saito, *Ann. Tokyo Astr. Obs.*, **3**, 3, 1950.
(47) S. J. Sullivan and E. E. Barr, *J.O.S.A.*, **44**, 352, 1954.

RADIAL VELOCITIES OF CEPHEID VARIABLE STARS IN THE SOUTHERN HEMISPHERE

D. W. N. Stibbs

(Communicated by the Radcliffe Observer)

(Received 1955 March 27)

Summary

Radial velocity determinations have been made on a uniform system for 55 cepheid variables in the Southern Hemisphere. Velocity curves have been drawn from 830 observations secured at phases well distributed over the light curves of the variables, and the normal velocities have been determined graphically by the method of equal areas.

The plates for radial velocity were obtained with the Cassegrain spectrograph of the 74-inch Radcliffe reflector, the dispersion of the spectrograms being 49 A/mm at Hγ. The velocity system to which the determinations refer has been examined by means of 39 spectrograms of 9 standard velocity stars, mostly giants, and 46 spectrograms of 9 supergiants obtained during the cepheid programme. The Radcliffe velocities of the standard velocity stars were found to be in very satisfactory agreement with velocities on the Lick System.

The radial velocity observations presented in the paper complete an extension of Joy's work to southern cepheids, with photographic magnitudes brighter than $10^{m}\cdot5$ at minimum light, contained within a hitherto largely unobserved quadrant of galactic longitude.

Introduction.—The results of a comprehensive programme of spectroscopic observations of cepheid variable stars, carried out at the Mount Wilson Observatory by A. H. Joy (**1**), were published in 1937. Joy's programme completed a survey of cepheids north of declination $-40°$ and brighter than the fifteenth photographic magnitude at minimum light. Radial velocity curves were obtained for 106 stars brighter than $14^{m}\cdot5$ at minimum light from observations conveniently distributed in phase, and the normal velocities were found by the method of equal areas from schematic velocity curves drawn through the observations. Joy also gave provisional normal velocities for twenty-two additional cepheids for which velocity curves could not be drawn, either through lack of sufficient data, or uncertainty in the ephemerides of the light curves. This brought the number of cepheids with known radial velocities to one hundred and fifty-five. In a discussion which followed the publication of the observations, Joy (**2**) gave a table of velocities for 156 cepheids, one additional star having been brought into the list. Apart from some redeterminations by Sanford (**3**), Struve (**4**), and Herbig and Moore (**5**), it appears that no further contributions have since been made to the list of cepheid velocities.

Joy's list contains very few stars in the sector of galactic longitude extending from about $l=230°$ to the longitude of the galactic centre near $l=325°$. This sector contains many cepheids, but only a few of the brightest had been observed,

and in some cases the observations from which the normal velocities were calculated had been obtained at phases inadequately distributed over the periods. It has not been possible until recently to secure further observations in this part of the galaxy on account of its southern declination. In this communication an account is given of a programme of observations of the radial velocities of fifty-five cepheid variables, with photographic magnitudes brighter than $10^{m}\cdot5$ at minimum light, contained in this largely unobserved quadrant of galactic longitude.

1. *Spectroscopic equipment and observational procedure*

The observations were made at the Cassegrain focus of the 74-inch Radcliffe reflector, using the two-prism spectrograph (**6**) designed by Professor Redman. The prisms of the spectrograph are of light flint, and are set for minimum deviation at λ 4200 A which is the central ray through the camera system. There are four camera combinations giving linear dispersions of 21, 29, 49 and 86 A/mm at $H\gamma$, designated for convenience the a, b, c and d cameras respectively. The spectrograph is provided with a curved slit for use with all cameras. A sensitive thermostat ensures that the temperature of the spectrograph is adequately controlled. The specifications for the prisms and the a, b and c cameras were chosen so that the spectrograms would closely resemble those obtained with the Cassegrain spectrograph of the Dominion Astrophysical Observatory, Victoria, B.C.

TABLE I

Approximate exposure times for Radcliffe spectrograms with dispersion 49 A/mm at Hγ

Plates	Photographic magnitudes	Exposures in minutes
Ilford Process	$5^{m}\cdot0$	7
	$6^{m}\cdot0$	20
Ilford Special Rapid	$7^{m}\cdot0$	30
Ilford Special Blue Sensitive	$7^{m}\cdot5$	20
Ilford Zenith Astronomical	$8^{m}\cdot0$	25
Kodak 103aO	$9^{m}\cdot0$	20
	$10^{m}\cdot0$	60
	$10^{m}\cdot5$	100

The c-camera was used throughout the observing programme, the standard slit-width being 0·075 mm, projecting to 0·018 mm on the plate. The stars were trailed to and fro along the slit in right ascension to give a spectrum of width 0·20 mm. Approximate exposure times for the photographic plates used in the programme are given in Table I for these standard widths. The limiting photographic magnitude for cepheids in the observing list was set somewhat arbitrarily at $10^{m}\cdot5$. Increased accuracy could have been gained by using a higher dispersion for the brighter stars, but this could not have been achieved without loss of

observing time incurred by changing from one camera to another. Accordingly, it was decided to use the same camera for all stars, regulating the exposure times for the brighter stars by the use of slower photographic plates. In this way the velocities of the brightest cepheids were automatically determined with the greater accuracy made possible by the fine grain and high contrast of the slower emulsions. At the same time, uniformity was maintained in the measurements and reductions by using spectra with the same dispersion throughout the programme.

An iron arc comparison spectrum was used, the iron arc lines being impressed on each side of the stellar spectrum both before and after each stellar exposure, and in some instances during the exposure as well. The separate exposures on the iron arc were of nearly equal duration. The practice was regularly followed of checking the collimation of the iron arc beam with due care before observations were made with the spectrograph. In making the observations an attempt was made to minimize the effect of atmospheric dispersion across the slit of the spectrograph by guiding on the blue core of the stellar image on the slit by means of a filter clamped over the guiding eye-piece. This was only possible for the brighter stars in the observing list, and was only necessary when the excellence of the seeing conditions demanded its use.

Most of the plates were calibrated for intensities by means of a tube sensitometer employing a filter for average calibration in blue light.

2. *Measurement and reduction of the spectrograms*

The spectrograms were measured for radial velocity on the projection micrometer of the Radcliffe Observatory. This machine, the design of which is due to Redman (**7**), gives a total magnification from plate to the projected image of about forty diameters, the projected field being about 2·5 mm of the plate. The plates were measured in the usual way, both in the direct and reverse positions.

Iron arc lines.—A total of thirty-five arc lines were included in a selected list of comparison lines in the wave-length range 3920 A to 4529 A. Both strong unblended lines and weak lines were included in the list to ensure that the Hartmann correction curve would be sufficiently well defined for all likely densities of the arc spectra. The arc exposure times were chosen to give a measurable density for the line λ4529 A. Weak, rather than strong, arc densities were favoured as they were found to be more suitable for measurement by the projection method.

Stellar lines.—The wave-length standards recommended by the Dominion Astrophysical Observatory (**8**) for the determination of radial velocity for solar-type stars from low dispersion spectrograms have been used. These wave-length standards give correct dynamical velocities for objects in the solar system, and stellar velocities on the Lick System for spectral types F4 to K8.

Reduction.—The reduction of the plate measurements was carried out in the usual way. The constants in the Hartmann formula were found from the measured positions of iron arc lines on a sample of spectrograms taken under a variety of conditions. The Hartmann formula for the average conditions was found to be entirely satisfactory for the reduction of all the spectrograms. The following procedure was adopted. The wave-lengths of the iron arc lines, and the stellar lines for zero velocity, were first transformed into micrometer readings by means of the Hartmann formula. The difference between the observed

and computed micrometer readings for the arc lines then gave a correction curve for the reduction of the dispersion on the plate to the standard dispersion given by the formula. The Doppler displacements of the stellar lines from the tabular values of the micrometer readings for zero velocity were then converted into velocities by means of factors computed for each line by differentiation of the Hartmann formula. Finally, the velocities were reduced to the Sun by correcting for diurnal rotation whenever necessary, and for annual motion by means of the 24-hourly changes in the rectangular coordinates of the Sun given in the *Nautical Almanac*. No correction for curvature was applied to the velocities as an investigation by Wesselink (**6**) showed that the curved slit of the spectrograph compensated adequately for the curvature introduced by the optical system, the residual correction for curvature being less than 0·1 km/sec in the photographic region.

3. *Standard velocity stars and standard wave-lengths*

The extent of the list of standard velocity stars for inclusion in the observing programme was determined by the following considerations. In the first place, the observations were begun soon after the spectrograph had been installed at the Cassegrain focus of the 74-inch reflector, and a periodic check on the performance of the spectrograph was necessary, particularly after adjustments had been made to the spectrograph itself or to the secondary mirror of the telescope. Secondly, the suitability of the Victoria wave-length standards for radial velocity work with the Radcliffe spectrograph required verification on account of the dependence of the effective wave-lengths of blended lines upon the dispersion of the spectrograph and its diffraction pattern. Thirdly, the wave-lengths had not previously been shown to be entirely satisfactory for supergiant stars throughout the range

TABLE II

Standard stars

Radial velocities and differences

Spectral type	General Catalogue number	Radial velocities					Differences	
		Radcliffe	No.	Lick	No.	Gen. Cat.	R−L	R−C
dF3*	10083	+36·5	5	+37·8	8	+37·8	−1·3	−1·3
Go	9331	− 5·3	4	− 5·1	9	− 4·7	−0·2	−0·6
gG1	3303†	−13·2	4	−13·8	19	−13·5	+0·6	+0·3
gG5	11158	−10·2	7	−10·0	6	−10·6	−0·2	+0·4
gKo	3246†	+21·5	3	+20·0	5	+20·5	+1·5	+1·0
sgKo	6628	−13·6	4	−12·7	4	−11·9	−0·9	−1·7
gK1	7398†	+36·3	3	+35·3	5	+35·3	+1·0	+1·0
gK3	5344†	+72·1	3	+71·2	4	+70·9	+0·9	+1·2
gK4	853†	+32·4	6	+33·9	4	+34·8	−1·5	−2·4

* This star was originally selected on the basis of the HD classification F5.

† I.A.U. standard velocity stars in equatorial regions.

F4–K8, only one star, α Persei with spectral type cF4, having been examined when the Victoria wave-length standards were originally determined (**8**). A list of non-variable c-stars covering the entire range F4–K8 was therefore necessary in order to ascertain if the recommended wave-lengths gave satisfactory velocities for these cepheid-like spectra. Two sets of standard velocity stars, primary standards and supergiants, with spectral types distributed as well as possible throughout

the range F4–K8 and located in both equatorial and southern regions were chosen in order to meet these requirements.

3.1. *Primary standards.*—The radial velocities of nine standard velocity stars covering the range F5–K4 were determined from 39 spectrograms. No evidence was found for flexure effects in the individual plate velocities, in agreement with other tests for flexure which have since been carried out (**6**). The mean velocities are given in Table II, with the velocity differences Radcliffe *minus* Lick (R − L) and Radcliffe *minus* General Catalogue (R − C). The nine stars are listed in the Catalogue as having *a*-quality velocities.

The mean difference R − L for the standard stars considered is 0·0 km/sec, the mean differences R − C being −0·2 km/sec. Since the Mount Wilson General Catalogue gives velocities on the Lick System, two sets of differences would be the same for a sufficiently large sample of stars. The stars in the sample are almost entirely giants, and the inference is that Radcliffe velocities for giants do not differ significantly from velocities on the Lick System. The velocity differences for the stars examined are shown in Fig. 1.

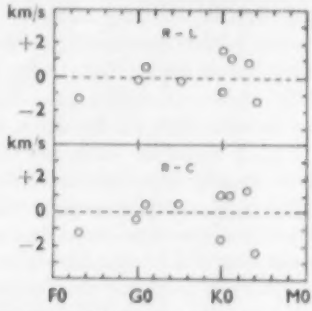

FIG. 1.—*Velocity differences Radcliffe minus Lick (R − L) and Radcliffe minus Mt Wilson General Catalogue (R − C) for standard velocity stars.*

TABLE III

Radial velocities of supergiant stars

Spectral type	General Catalogue number	Radial velocities							
		Radcliffe	No.	Lick	No.	Mt Wilson	No.	Gen. Cat.
cF3	11022	+ 5·7	3	...	...	+ 9·2	3	+ 9·7b
cF4†	7287	− 7·9	5	...	...	−10·8	4	− 9·1b
cF6	7734	−25·4	5	...	...	−22·0	5	−21·5b
cG1	14847	+ 4·2	6	+ 4·8	4	− 2·2*	4	+ 3·2b
cG5	12659	−26·6	7	−25·9	9	...	...	−25·9a
cK0	11657	+ 2·7	5	...	...	+ 1·4	2	+ 1·0c
cK1‡	540	−14·8	3	...	...	−12·7	3	−13·2b
cK5	10998	+ 6·5	5	...	...	+ 1·6	3	+ 1·1b
cK5	18	−40·9	7	−41·9	13	−42·0§	4	−42·0a

* The Mount Wilson velocities for No. 14847 (HD 222574) are −11, −6, +8, +1, probably variable (*Ap. J.*, **111**, 221, 1950). The Radcliffe velocities are +6, +4, +2, +4, +4, +6, and do not support much variation.

† cF4 in *Ap. J.*, **70**, 207, 1929; gF5 in General Catalogue.

‡ cK1 in *Ap. J.*, **111**, 221, 1950; gK0 in General Catalogue.

§ Lick Catalogue gives velocity for No. 18 (HD 225212) as variable. The Radcliffe velocities are −41, −41, −39, −42, −38, −43, the last value being the mean of two plates taken at the same epoch.

3.2. *Supergiant stars.*—The radial velocities of nine non-variable c-stars with spectral types ranging from cF3 to cK5 were determined from 46 spectrograms. The velocities are given in Table III together with the Lick and Mt Wilson velocities, and the velocities in the General Catalogue. From the velocity differences we obtain the following mean values with sign: Radcliffe *minus* Lick, −0·1 km/sec; Radcliffe *minus* Mt Wilson*, +0·2 km/sec; Radcliffe *minus* General Catalogue, 0·0 km/sec.

Two of the nine supergiants have velocities listed in the General Catalogue as *a*-quality, six being *b*-quality, and one *c*-quality. The limits of probable error and the mean probable errors corresponding to these designations in the Catalogue are respectively as follows:—*a*, ±0·9, ±0·5; *b*, ±2·0, ±1·2; *c*, ±5·0, ±2·5 km/sc. The velocity differences Radcliffe *minus* Lick and Radcliffe *minus* Catalogue are satisfactorily small for the two stars with *a*-quality velocities, also for the only *b*-quality velocity for which Lick observations are available. For the remaining six stars, the comparison Radcliffe *minus* Catalogue rests entirely on corrected Mt Wilson velocities. The Radcliffe velocities for three of these, Nos. 540, 7287 and 11657, lie within ±2 km/sec of the Catalogue values and are in satisfactory agreement within the limiting probable error for *b*-quality velocities. For the remaining three stars, Nos. 7734, 10998 and 11022, the velocity differences are greater than one might have expected in view of the generally good agreement with velocities on the Lick System. The velocity differences are shown in Fig. 2 together with the differences Mt Wilson *minus* Lick for eight northern supergiants observed by Joy (1, p. 355) for the standardization of the Mt Wilson velocities of cepheid variables.

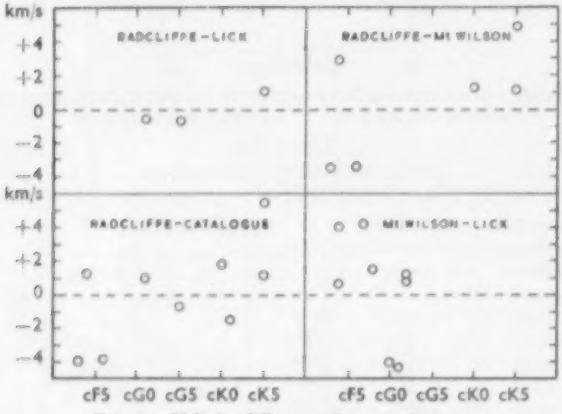

FIG. 2.—*Velocity differences for supergiant stars.*

3.3. *Standard wave-lengths.*—In the calculation of the radial velocities of primary standards and supergiant stars, the velocity given by each line in the Victoria list of standard wave-lengths† was determined without reference to the spectral type of each star. The mean plate velocities were then obtained from the recommended selection of lines. In some instances, additional lines were either rejected or given half-weight in the calculation of the plate velocity, the

* The discordant velocity difference for No. 14847 has been omitted in finding the mean difference Radcliffe *minus* Mt Wilson. See Table III for a note on this star.

† The discordant line λ 4482 A has not been used.

criterion being principally the difficulty experienced in obtaining a satisfactory measurement on the line as recorded when the plate measurements were made. Rejections based only on the size of line residuals were avoided as far as possible. In the case of the supergiant stars, the criteria for selection and rejection of lines were the same as for the primary standards, except that rejection based on the size of residuals was considered advisable in some instances, particularly for lines suspected of dependence upon luminosity class.

TABLE IV

Line residuals for standard giants and supergiants

Line λ (A)	Standard giants			Supergiants		
	Residuals km/s ± p.e.	Plates No.	Stars No.	Residuals km/s ± p.e.	Plates No.	Stars No.
4092	...	...	...	+4·3 ± 0·4	33	6
4307	...	...	...	−4·0 ± 0·7	23	4
4325	−5·8 ± 0·8	15	3	−6·8 ± 0·7	23	4
4340	+5·1 ± 0·6	15	3	+6·6 ± 0·6	23	4

The velocity residual for each line in the wave-length table was obtained by finding the average, over all spectrograms for a given star, of line velocity *minus* mean plate velocity from selected lines. The line residuals were then averaged over stars within the valid intervals of spectral type. It was found that there were only four lines with velocity residuals of 4 km/sec or greater. The residuals for these lines and their probable errors are given in Table IV in which is also listed the number of stars within the recommended intervals of spectral type and the total number of plates involved in the calculations.

The largest residuals for both giants and supergiants are shown by the lines λ4325 and λ4340. These two lines are blends for which the recommended wave-lengths are empirical, that is, wave-lengths which are adjusted to give a velocity in agreement with other lines, the adopted value being a wave-length which reduces to zero the average residual for stars within the recommended interval of spectral type. For these two lines the intervals are F4–G7 and F4–G5 respectively.

An examination of the Mt Wilson spectral types for the stars used in the Victoria work on standard wave-lengths reveals that within the interval F4–G7 the stars are a mixture of luminosity classes, comprised of three dwarfs, two giants and one supergiant. Now the dependence of the effective wave-length of the line λ4325 A on luminosity was suggested in the Victoria work on the supergiant α Persei, but it does not appear to have been recognized that the effective wave-length as given has been derived from three dwarfs and two giants. According to Evans (**9**) the recommended wave-length for this line appears to be satisfactory for dwarfs. The present work suggests that it is not suitable for giants and supergiants. It is clearly desirable that in setting up the system of standard wave-lengths due regard should be paid to the luminosity classes of the standardizing objects.

The effective wave-lengths for the interval F4–G5 apparently depend upon two dwarfs, two giants and one supergiant. Two blended lines are given for this interval, λ4307·994 A and λ4340·441 A. The former wave-length is the weighted mean position of solar lines due principally to Fe I, Ca I and Ti I. The Fe I line is coincident with a line at λ4307·05 A due to Ti II, which, presumably being stronger in the spectra of supergiants, will reduce the effective wave-length of the blend. This is confirmed by the negative sign found for the velocity residual for this line.

The only blends in the Victoria wave-length table which involve lines used in spectroscopic absolute magnitude work are λ4215 A containing lines due to Fe I and Sr II, and λ4340 A containing Hγ. The latter is, however, only used for absolute magnitudes for K and M type giants, and is recommended for radial velocities only for types F4–G5. The velocity residual for λ4215 A was found to be satisfactorily small for both giant and supergiant types in spite of the fact that the intensity ratio $\lambda\lambda$4215/5250 is a well-established measure of luminosity. The line λ4314 A due principally to Fe I, Sc II and Ti II was suspected of dependence upon luminosity in the Victoria work on α Persei, but the average residual for this line for stars in the range from cF4 to cK8 has been found in the present investigation to be small. The residuals for individual stars in the range may, however, be quite large.

These considerations suggest that for supergiant spectra there is some justification for rejecting measures of the lines λ4307 A and λ4314 A which differ markedly from the plate velocity. For these lines the wave-lengths are the weighted mean positions of the blended components, but the lines λ4325 A and λ4340 A have wave-lengths which are adjusted to give the correct velocity. It was considered impracticable to make a satisfactory adjustment of these wave-lengths for cepheid variables in view of the fact that the line spectrum is abnormal (**10**) on the ascending branch of the light curves although closely corresponding to a supergiant of luminosity class Ib at minimum light. It was decided to discard the lines $\lambda\lambda$4325, 4340 rather than attempt to make further adjustments to their effective wave-lengths since such wave-lengths, even if correctly adjusted, cannot add much weight to a plate velocity, although they might be useful for normal spectra when some of the calibrating lines are for some reason not accessible.

TABLE V

Effective wave-lengths used for the determination of radial velocities of cepheid variables

Wave-length in angströms	Spectral interval	Wave-length in angströms	Spectral interval
3961·537	F4–K8	4215·686	F4–K0
4005·244	K0–K8	4254·348	F4–K8
4030·645	G0–K8	4260·488	K0–K8
4034·494	K0–K8	4307·994	F4–G5
4045·765	F4–K8	4314·683	F4–K8
4071·738	F4–K8	4404·745	F4–K8
4092·478	G0–K8	4415·137	F4–K8
4132·230	F4–K8	4461·810	G5–K8

4. *Cepheid variables*

The programme of observations of cepheid variables was carried out with due attention to the need for securing spectrograms at phases well distributed over the light curves. In order to facilitate the computation of the phases, and hence the selection of stars for observation, tables were constructed which gave, for each star on the programme, thirty-one multiples of the reciprocal period. The phase of the light variation on any night in a given month could then be written down at once by adding the phase shift for the night in question to the phase at midnight on the last night of the preceding month. These predicted phases were used to estimate the photographic magnitudes from the light curves, and hence the exposure times required. The light elements given in the Russian Catalogue of Variable Stars(**11**)were used. Elements for the star CPD $-60°4739$, which is not contained in the Catalogue, were kindly supplied by the Riverview College Observatory.

The observing programme was limited to cepheids brighter than photographic magnitude $10^m{\cdot}5$ at minimum light. Fifty-five cepheids were observed on 112 nights, a total of 830 spectra being secured. The published magnitudes were found to be not entirely dependable, and the estimation of exposure times was frequently more a matter of judgment than of calculation. In some cases, the ephemerides were not accurate enough for the prediction of phases, notably for the large-amplitude cepheids T Antliae, U Carinae, VY Carinae, AQ Puppis and RZ Velorum. In these cases provisional corrections to the computed phases were made with the help of rough velocity curves deduced from plate measurements made during the observing programme.

4.1. *Radial velocities and velocity curves.*—The radial velocities of the cepheids were determined from the effective wave-lengths given in Table V, using approximate spectral types for each phase. The spectral types given in the Russian Catalogue, mostly from Harvard classifications, were used. In cases where the data are insufficient, spectral types at maximum and minimum light were taken from the period–spectrum relations of Code (**12**), the approximate types at intermediate phases being then obtained from the range in type and the phase. The radial velocities are given in Table VI in which the following data are tabulated: (i) the Radcliffe plate number with the designation C for Cassegrain and c for the camera used, (ii) the Julian Date of observation, (iii) the geocentric

TABLE VI

Radial velocity observations of cepheid variables

Plate Cc	Epoch JD	Phase P	Velocity km/sec	Plate Cc	Epoch JD	Phase P	Velocity km/sec
	T Ant	JD 2434000			V496 Aql	JD 2433000	
694	122·28	0·77	+18·0	249	871·44	0·81	+12·7
720	130·28	·12	+36·3	261	875·43	·40	+ 6·4
730	133·26	·63	+ 4·2	276	881·42	·28	+ 4·3
744	137·23	·30	+47·2	290	897·43	·63	+18·2
763	145·24	·66	+ 7·1	300	900·34	·06	− 2·6
838	167·25	·38	+48·9	308	903·36	·50	+ 6·1
860	174·26	·57	+ 5·8	319	906·33	·94	+ 5·8
918	197·19	·45	+45·5	338	913·37	·97	+ 0·7
930	200·20	0·96	+30·3	352	928·31	0·17	+ 0·3

Plate Cc	Epoch JD	Phase P	Velocity km/sec
	V496 Aql (*continued*)		
359	934·29	0·05	+ 1·3
370	937·30	·49	+ 5·4
383	943·27	·36	+ 6·1
391	955·24	·27	+ 1·8
408	962·23	·15	− 3·9
421	965·25	·59	+10·3
808	1157·66	·86	+ 6·4
894	1183·61	·67	+ 9·4
920	1197·61	·73	+ 9·8
960	1219·50	·94	− 5·4
977	1223·41	·52	+ 6·9
1012	1231·49	0·71	+14·6
	l Car JD 2434000		
493	16·60	0·94	+ 7·4
499	20·50	·05	−15·9
504	22·56	·11	−16·3
512	25·46	·19	−16·4
516	27·61	·25	−12·6
522	29·42	·30	−11·9
530	31·51	·36	− 5·3
539	44·44	·73	+16·0
543	53·38	·98	− 1·5
546	57·48	·09	−18·5
575	77·40	·65	+15·1
585	80·39	·74	+19·7
603	85·38	·88	+15·7
671	110·41	·58	+11·1
681	113·32	·66	+16·8
685	117·34	·78	+22·7
862	175·16	·41	− 5·9
868	176·17	·43	− 1·9
874	177·16	·46	+ 0·3
880	179·16	·52	+ 5·2
885	181·16	0·58	+ 8·5
	U Car JD 2433000		
179	827·25	0·36	+14·0
185	829·25	·41	+ 7·7
192	831·24	·46	−19·2
201	834·29	·54	−24·0
213	840·27	·70	−17·7
227	844·29	·80	− 4·8
577	1077·56	·82	− 2·3
587	1080·51	·90	− 9·6
694	1122·34	·98	+ 6·3
720	1130·34	·18	+23·8
730	1133·35	·26	+23·2
744	1137·29	·36	+27·5
764	1145·35	·57	−24·0
825	1163·32	·03	+ 8·8
838	1167·30	·14	+10·3
860	1174·30	0·32	+25·0
	V Car JD 2433000		
440	973·60	0·21	+ 6·9
448	984·59	0·85	+ 6·1
452	986·59	0·15	+ 7·2
458	988·58	·45	+19·0
474	996·53	·63	+34·1
480	998·53	·93	+ 3·2
484	1000·54	·23	+ 9·5
497	1018·46	·91	+ 2·7
500	1020·56	·22	+11·7
506	1022·50	·51	+24·2
513	1025·49	·96	+ 6·0
517	1027·58	·27	+11·3
521	1029·54	·56	+27·5
531	1031·48	·85	+ 5·4
558	1062·35	·46	+15·7
576	1077·37	·71	+34·8
608	1088·32	·34	+14·5
642	1098·27	·83	+15·9
669	1110·28	·62	+23·4
678	1113·23	·06	+ 1·8
683	1117·21	0·66	+30·4
	Y Car JD 2434000		
547	57·50	0·09	−17·0
602	85·49	·78	− 3·5
610	88·49	·61	+ 2·8
626	92·50	·71	+ 1·2
669	110·39	·62	+ 3·3
694	122·32	·90	+ 4·0
720	130·33	·10	−26·3
744	137·26	·01	− 8·3
763	145·27	·21	− 7·4
899	191·27	0·85	+ 4·7
	ER Car JD 2433000		
167	822·28	0·78	− 6·3
180	827·26	·42	−25·1
185	829·26	·68	−12·4
192	831·24	·94	− 3·1
201	834·28	·33	−29·4
213	840·28	·11	−25·1
227	844·30	·63	−17·1
548	1057·56	·26	−28·0
577	1077·58	·86	0·0
602	1085·59	·90	+ 6·3
628	1092·54	·80	− 6·5
645	1101·47	·95	−10·3
650	1102·48	·08	−24·4
684	1117·40	·02	−20·5
694	1122·35	·66	−11·7
806	1157·32	·19	−31·8
825	1163·33	·97	−10·4
891	1183·29	0·56	−20·7
	GI Car JD 2433000		
167	822·30	0·28	−28·1
180	827·29	·40	−26·8
186	829·29	·86	−14·8
193	831·26	0·10	−31·3

Plate Cc	Epoch JD	Phase P	Velocity km/sec
	GI Car (*continued*)		
201	834·30	0·99	−20·3
213	840·30	·34	−32·1
588	1080·54	·57	−16·7
678	1113·39	·98	−24·3
684	1117·39	·88	−14·4
694	1122·35	·00	−22·6
730	1133·39	·50	−21·2
763	1145·33	·19	−27·4
807	1157·35	·90	−12·6
838	1167·31	·15	−31·3
860	1174·33	·74	−12·9
899	1191·30	·57	−18·2
930	1200·30	0·60	−16·0
	IT Car JD 2434000		
678	113·37	0·56	−19·7
730	133·37	·21	− 6·1
744	137·30	·73	−22·5
806	157·33	·39	− 8·9
825	163·36	·19	− 9·1
860	174·31	·64	−22·8
886	181·23	·56	−15·3
891	183·29	·84	−19·0
899	191·28	·90	−18·1
918	197·25	·69	−19·6
930	200·28	·09	− 9·4
945	206·25	·88	−19·4
950	207·23	0·01	−17·6
	UX Car JD 2433000		
155	818·23	0·35	+12·6
167	822·20	·43	+20·2
179	827·20	·79	+24·3
185	829·21	·34	+11·8
192	831·20	·88	+ 7·8
201	834·22	·70	+22·9
216	841·21	·59	+20·6
227	844·23	·41	+10·8
576	1077·48	·76	+24·8
602	1085·46	·92	− 8·7
653	1104·52	·10	− 2·2
693	1122·25	·92	− 6·0
720	1130·31	·10	− 7·5
744	1137·25	·99	− 4·8
763	1145·26	·16	− 1·3
825	1163·21	·04	− 8·5
838	1167·29	·15	− 1·5
899	1191·24	·65	+26·0
918	1197·22	0·27	+ 6·5
	VY Car JD 2433000		
155	818·26	0·30	+ 0·3
179	827·24	·77	+17·5
185	829·24	·88	−31·5
192	831·23	·98	−27·8
213	840·26	0·46	+13·2
227	844·27	0·67	+16·0
547	1057·52	·92	−31·1
577	1077·54	·97	−28·6
588	1080·48	·13	−10·2
626	1092·52	·76	+ 2·3
678	1113·34	·86	−33·1
683	1117·32	·07	−15·6
744	1137·27	·12	−13·9
763	1145·28	·54	−26·8
860	1174·28	·07	−16·9
918	1197·23	0·28	+ 3·4
	V Cen JD 2433000		
181	827·40	0·14	−35·9
186	829·36	·49	−12·8
193	831·32	·85	−36·7
202	834·37	·40	−16·8
214	840·36	·49	−11·2
228	844·39	·23	−21·3
246	871·19	·11	−30·0
259	875·19	·83	−44·6
275	881·21	·93	−39·7
611	1088·60	·68	− 2·2
645	1101·44	·02	−32·0
746	1137·54	·58	− 5·3
808	1157·56	·23	−16·7
888	1181·46	·58	− 2·1
900	1191·38	·39	−13·0
989	1226·19	·72	−18·4
1022	1233·20	0·99	−31·6
	AZ Cen JD 2434000		
588	080·56	0·98	−16·5
679	113·42	·21	−10·7
684	117·43	·46	− 9·3
694	122·36	·99	−18·1
721	130·36	·48	− 6·5
730	133·41	·43	− 3·6
744	137·32	·65	−15·9
765	145·36	·15	− 7·7
826	163·40	·77	−19·5
886	181·29	·34	− 4·4
918	197·27	0·31	− 0·5
	UZ Cen JD 2434000		
679	113·46	0·05	+10·3
684	117·52	·26	−20·1
694	122·40	·73	+ 0·1
765	145·38	·62	− 8·8
860	174·35	·31	−25·5
886	181·24	·38	−20·7
930	200·33	·10	+ 9·4
945	206·28	·89	+ 6·2
960	219·23	0·77	+ 4·2

Plate Cc	Epoch JD	Phase P	Velocity km/sec
	XX Cen JD 2433000		
175	825·18	0·85	−24·7
176	826·21	·94	−23·3
179	827·18	·03	−25·1
182	828·19	·12	−30·3
185	829·18	·22	−19·1
189	830·18	·30	−19·8
192	831·18	·40	−11·6
195	832·18	·49	+ 2·5
200	833·18	·58	+11·5
201	834·18	·67	− 6·8
695	1122·21	·00	−26·1
722	1130·25	·72	−17·2
731	1133·28	·00	−33·3
989	1227·27	0·55	− 2·0
	V339 Cen JD 2433000		
156	818·39	0·87	−36·8
180	827·38	·82	−34·2
680	1113·64	·06	−32·8
686	1117·60	·48	−12·7
695	1122·65	·01	−30·7
722	1130·62	·85	−29·4
732	1133·60	·16	−33·4
746	1137·51	·58	− 6·5
766	1145·56	·43	−14·1
807	1157·53	·69	−10·5
826	1163·49	·32	−27·4
839	1167·46	·74	−26·6
888	1181·44	·22	−33·2
893	1183·48	·43	−19·2
919	1197·41	0·91	−37·8
	V378 Cen JD 2434000		
721	130·56	0·35	−24·6
731	133·53	·81	−10·7
745	137·46	·42	−22·6
765	145·53	·67	−16·9
807	157·48	·52	−16·9
839	167·41	·06	−18·3
861	174·41	·14	−23·2
888	181·40	·22	−24·2
893	183·43	·54	−13·0
975	223·29	·71	−12·7
1009	231·21	0·94	− 9·6
	V381 Cen JD 2433000		
175	825·19	0·00	−49·6
176	826·19	·19	−38·7
179	827·19	·39	−28·4
182	828·19	·59	−13·1
185	829·19	·78	−19·1
192	831·19	·18	−41·4
201	834·20	·77	−16·1
274	881·19	·02	−49·9
722	1130·60	·13	−42·1
730	1133·57	·71	−17·7
746	1137·48	0·48	−23·5

Plate Cc	Epoch JD	Phase P	Velocity km/sec
	V381 Cen (*continued*)		
919	1197·39	0·28	−37·8
930	1200·41	0·88	−39·6
	V419 Cen JD 2434000		
548	57·61	0·31	−14·5
577	77·63	·94	− 8·5
588	80·62	·48	−25·0
628	92·57	·65	−24·9
684	117·47	·17	−14·2
694	122·38	·06	−10·2
721	130·39	·52	−19·9
731	133·39	·07	− 8·3
745	137·34	·78	−17·1
899	191·32	·57	−23·2
918	197·29	·66	−22·5
950	207·26	0·46	−24·5
	CPD −60° 4739 JD 2434000		
549	57·63	0·92	−13·4
560	62·64	·81	−11·9
587	80·65	·01	−21·5
604	85·64	·90	−16·9
609	88·62	·43	−12·8
627	92·65	·15	−15·8
647	101·64	·75	− 5·1
653	104·60	·28	−14·1
672	110·42	·31	−14·8
686	117·61	·59	− 4·2
695	122·63	·48	−11·9
807	157·50	·68	− 6·1
839	167·44	0·45	− 9·3
	R Cru JD 2433000		
155	818·28	0·50	− 7·8
180	827·33	·05	−28·9
186	829·33	·39	−13·5
193	831·29	·73	+ 5·7
202	834·34	·25	−23·7
214	840·34	·28	−16·0
227	844·34	·97	−30·9
602	1085·63	·39	−14·8
610	1088·59	·90	− 7·6
645	1101·52	·12	−29·1
679	1113·54	·18	−23·9
695	1122·48	·71	− 1·7
731	1133·44	·60	− 4·8
765	1145·47	0·66	− 5·2
	S Cru JD 2433000		
156	818·33	0·70	+ 4·4
180	827·35	·62	+ 5·6
186	829·35	·05	−23·1
193	831·31	·47	− 0·4
214	840·35	·40	− 9·0
228	844·38	·25	−15·4
647	1101·62	0·10	−27·4

Plate Cc	Epoch JD	Phase P	Velocity km/sec
	S Cru (*continued*)		
731	1133·51	0·90	− 1·5
745	1137·44	·74	+ 8·9
807	1157·45	·01	−21·8
839	1167·39	·13	−22·0
893	1183·41	·54	+ 1·8
988	1227·19	·88	+ 7·1
1009	1231·18	0·73	+ 9·4
	T Cru JD 2433000		
156	818·34	0·66	+11·8
169	822·35	·26	−10·3
180	827·32	·00	−20·2
186	829·32	·29	−14·1
193	831·28	·58	+ 7·8
202	834·33	·04	−19·2
213	840·32	·93	−16·6
227	844·33	·52	− 2·9
602	1085·61	·36	− 8·1
610	1088·57	·80	+ 7·6
628	1092·59	·39	− 7·2
645	1101·50	·72	+ 7·4
650	1102·60	·88	− 1·6
653	1104·58	·18	−19·4
679	1113·53	·50	− 1·8
695	1122·46	·83	+ 0·7
765	1145·46	0·24	−15·2
	X Cru JD 2434000		
695	122·57	0·85	−13·0
721	130·52	·13	−30·7
731	133·48	·60	−27·6
745	137·42	·24	−35·8
765	145·50	·54	−28·1
807	157·43	·46	−33·5
839	167·37	·05	−20·3
860	174·38	·18	−35·3
886	181·38	·30	−34·2
893	183·38	·63	−23·2
919	197·36	·88	−12·3
989	227·22	0·68	−21·1
	AG Cru JD 2434000		
628	92·62	0·24	− 7·1
646	101·58	·57	+ 6·1
680	113·59	·70	+15·3
684	117·58	·74	+13·9
695	122·52	·03	−21·2
721	130·48	·10	−20·1
731	133·46	·88	−19·0
745	137·40	·90	−23·9
765	145·48	·01	−24·4
807	157·40	·12	−12·6
838	167·34	·71	+10·6
886	181·36	·36	+ 0·4
893	183·36	·88	−18·9

Plate Cc	Epoch JD	Phase P	Velocity km/sec
	AG Cru (*continued*)		
899	191·34	0·96	−22·6
930	200·40	·32	− 6·3
960	219·30	·25	− 7·4
975	223·25	0·28	− 3·4
	β Dor JD 2433000		
459	990·44	0·41	+20·5
461	992·43	·61	+26·4
461	994·40	·81	− 1·2
470	995·36	·91	+ 1·0
470	996·37	·01	+ 3·4
481	998·33	·21	− 0·4
483	1000·35	·41	+18·4
491	1014·40	·84	+ 0·0
493	1016·39	·04	− 3·0
495	1018·42	·24	+ 1·4
496	1018·33	·24	+ 0·5
499	1020·29	·44	+21·5
504	1022·33	·65	+20·4
512	1025·42	·96	+ 0·9
516	1027·32	·16	− 6·8
516	1027·33	·16	− 7·7
522	1029·41	·37	+10·1
530	1031·32	·56	+31·5
533	1033·37	·77	+ 1·6
533	1033·38	·77	+ 1·8
585	1080·25	·53	+26·6
625	1092·20	·76	+ 4·8
625	1092·21	0·75	+ 4·5
	R Mus JD 2433000		
156	818·36	0·95	−13·2
180	827·34	·14	− 5·6
186	829·34	·41	− 4·1
193	831·30	·67	+27·3
202	834·35	·08	− 6·4
214	840·34	·88	+ 0·9
228	844·36	·41	+ 3·5
610	1088·60	·93	− 9·5
646	1101·54	·66	+17·9
680	1113·55	·26	− 0·7
684	1117·55	·79	+27·2
721	1130·50	·51	+ 3·2
745	1137·38	·43	− 2·5
891	1183·33	0·54	+ 4·0
	S Mus JD 2434000		
610	88·56	0·08	− 0·6
679	113·52	·66	+28·0
745	137·38	·13	+ 3·7
764	145·44	·97	− 2·2
887	181·34	·69	+24·4
892	183·34	·89	+10·1
945	206·31	0·27	+ 6·6

Plate Cc	Epoch JD	Phase P	Velocity km/sec
	RT Mus JD 2434000		
695	122·44	0·26	−10·0
721	130·45	·86	− 6·2
745	137·36	·10	−13·9
765	145·41	·71	+14·2
807	157·37	·58	+12·4
886	181·31	·34	− 0·3
891	183·31	·99	−19·2
918	197·32	·53	+ 5·8
930	200·36	·51	+ 7·3
950	207·32	·77	+14·6
975	223·21	0·92	−14·9
	S Nor JD 2433000		
247	871·26	0·83	+ 9·5
260	875·25	·24	− 5·3
275	881·27	·85	+10·5
288	897·22	·49	+ 0·5
298	900·20	·79	+23·6
307	903·19	·10	− 2·2
317	906·19	·41	−10·0
328	910·21	·82	+22·2
339	913·21	·13	− 3·5
352	928·21	·66	+12·9
359	934·20	·28	− 9·1
370	937·22	·79	+22·6
887	1181·52	·64	+18·0
901	1191·42	·65	+18·4
931	1200·44	·58	+ 9·9
975	1223·33	·92	− 0·8
1009	1231·34	·75	+19·5
1022	1233·24	·94	+ 3·5
1022	1233·25	0·94	+ 1·3
	BF Oph JD 2433000		
259	875·28	0·94	−47·5
274	881·29	·42	−23·4
288	897·24	·34	−31·5
298	900·22	·08	−52·6
308	903·22	·81	−21·6
317	906·21	·55	−16·5
338	913·24	·28	−39·2
352	928·22	·96	−48·1
383	943·21	·64	− 4·5
893	1183·54	·72	−15·2
900	1191·46	·67	−11 6
919	1197·46	·14	−40·1
945	1206·33	·32	−40·8
960	1219·47	0·56	−21·4
	κ Pav JD 2433000		
248	871·39	0·48	+47·1
262	875·41	·92	+30·9
273	881·40	0·58	+45·4

Plate Cc	Epoch JD	Phase P	Velocity km/sec
	κ Pav (*continued*)		
289	897·39	0·34	+31·0
297	900·32	·66	+45·2
309	903·33	·99	+17·9
318	906·35	·33	+35·7
340	913·40	·10	+26·4
352	928·33	·75	+53·2
360	934·32	·41	+38·4
392	955·26	·82	+52·5
398	959·26	·15	+25·1
409	962·25	·48	+43·5
423	965·27	·81	+48·9
432	967·24	0·03	+24·8
	AP Pup JD 2433000		
362	934·61	0·55	+25·2
374	937·61	·14	+ 4·4
383	943·61	·32	+ 6·4
394	955·59	·87	+32·5
412	962·55	·04	+ 0·8
422	965·54	·63	+23·8
431	967·53	·02	+ 5·9
435	968·51	·22	+ 7·4
440	973·50	·20	+ 1·2
443	976·50	·79	+36·3
446	984·51	·36	+10·3
452	986·50	·76	+34·7
458	988·51	·15	+ 5·4
462	992·54	·94	+22·0
468	994·50	·33	+ 5·9
474	996·44	·71	+33·1
480	998·46	·11	+ 1·3
484	1000·42	·49	+16·8
497	1018·41	·03	+ 7·5
500	1020·37	·42	+11·3
506	1022·39	·82	+32·9
669	1110·26	·10	+ 2·8
825	1163·17	0·50	+19·3
	AQ Pup JD 2433000		
497	18·38	0·21	+31·3
506	22·43	·35	+38·2
517	27·46	·52	+51·5
521	29·47	·58	+56·0
531	31·42	·65	+62·0
544	53·42	·38	+36·4
576	77·32	·18	+37·9
586	80·28	·28	+30·6
720	130·19	·95	+89·2
730	133·20	·05	+82·1
763	145·20	·45	+39·9
806	157·21	·85	+81·6
891	183·19	0·72	+71·3

Plate Cc	Epoch JD	Phase P	Velocity km/sec
	AT Pup JD 2433000		
422	965·59	0·41	+27·5
440	973·59	·61	+31·2
443	976·57	·06	+12·9
452	986·53	·55	+34·4
458	988·53	·85	+52·0
463	992·56	·46	+31·5
476	996·46	·04	+ 5·9
480	998·48	·35	+22·1
484	1000·44	·64	+38·8
506	1022·46	·94	+19·8
521	1029·36	·98	+10·1
547	1057·34	·18	+16·0
558	1062·33	·93	+27·2
576	1077·35	·18	+20·4
586	1080·32	·62	+32·3
608	1088·30	·82	+56·8
720	1130·22	·12	+14·0
825	1163·18	·06	+10·0
838	1167·19	·66	+36·6
860	1174·24	·72	+41·0
886	1181·18	0·76	+49·2
	WX Pup JD 2434000		
506	22·36	0·83	+47·6
517	27·40	·39	+57·6
531	31·36	·84	+48·5
558	62·30	·30	+50·5
576	77·26	·97	+41·6
608	88·26	·20	+45·6
626	92·28	·65	+66·7
645	101·27	·66	+74·3
669	110·22	·66	+74·5
678	113·20	·99	+38·4
806	157·18	·91	+35·3
838	167·17	0·03	+41·1
	U Sgr JD 2433000		
249	871·41	0·57	+ 5·4
261	875·40	·16	−14·3
276	881·39	·05	− 5·1
288	879·37	·32	+ 0·2
298	900·31	·85	+22·2
308	903·32	·30	− 5·2
317	906·32	·74	+12·9
338	913·36	·79	+ 8·6
359	934·28	·89	+24·7
370	937·27	·33	− 5·9
383	943·25	·22	− 4·9
391	955·22	·14	−19·6
408	962·22	·03	− 4·4
421	965·22	·48	+ 7·8
888	1181·58	·55	+ 8·4
901	1191·55	·03	− 8·1
1012	1231·37	0·94	+21·0

Plate Cc	Epoch JD	Phase P	Velocity km/sec
	W Sgr JD 2433000		
248	871·37	0·77	− 3·3
277	881·38	·09	−42·7
289	897·36	·19	−42·5
299	900·30	·58	−30·2
309	903·30	·97	−32·3
318	906·30	·37	−20·5
328	910·31	·90	− 6·9
340	913·34	·29	−33·0
371	937·27	·44	−21·4
902	1191·52	·92	−27·1
921	1197·58	0·72	−18·1
	X Sgr JD 2433000		
248	871·36	0·36	−16·8
262	875·33	·93	−19·2
273	881·33	·78	− 1·6
297	900·26	·48	− 0·2
309	903·26	·91	− 1·4
318	906·26	·34	−13·3
328	910·29	·91	−14·4
340	913·33	·35	−16·3
384	943·23	·61	+ 3·8
390	955·21	·46	− 8·2
902	1191·51	·02	−27·2
946	1206·39	·14	−25·1
961	1219·41	·00	−31·0
974	1223·35	·56	− 9·4
1011	1231·35	0·70	− 6·5
	RV Sco JD 2433000		
181	827·46	0·88	− 2·2
187	829·50	·22	−35·6
194	831·37	·53	−19·3
203	834·43	·03	−38·1
247	871·27	·11	−37·7
259	875·26	·77	+ 2·2
274	881·28	·76	+ 1·3
288	897·23	·39	−17·4
308	903·21	·38	−23·3
317	906·20	·87	− 3·9
328	910·22	·54	−11·0
338	913·23	·03	−34·3
919	1197·45	·92	−24·4
975	1223·34	·20	−28·2
989	1227·30	0·85	+ 3·6
	RY Sco JD 2433000		
261	875·36	0·69	− 7·2
276	881·36	·99	− 9·6
288	897·33	·78	− 2·8
298	900·28	·92	−10·4
308	903·28	·07	−18·7
317	906·27	·22	−32·6
338	913·26	0·56	−21·9

Plate Cc	Epoch JD	Phase P	Velocity km/sec
	RY Sco (*continued*)		
352	928·26	0·30	−33·6
359	934·25	·59	−19·0
920	1197·55	0·56	−21·9
	V482 Sco	JD 2433000	
246	871·31	0·82	+17·5
259	875·30	·70	+28·5
274	881·31	·03	+ 0·1
288	897·27	·56	+18·8
298	900·24	·21	− 6·7
308	903·24	·87	+15·2
317	906·23	·54	+18·6
338	913·28	·09	+ 0·3
352	928·24	·39	+ 8·6
359	934·22	·72	+28·6
370	937·24	·38	+ 9·7
722	1130·66	·10	− 0·2
746	1137·57	·63	+23·1
893	1183·57	·79	+26·8
945	1206·37	·82	+21·9
989	1227·32	·45	+12·3
1027	1234·18	·96	− 2·5
1027	1234·19	0·97	− 1·0
	V500 Sco	JD 2434000	
732	133·66	0·04	−23·2
746	137·63	·47	− 2·0
766	145·66	·33	−15·8
808	157·66	·62	+ 4·8
826	163·60	·25	−23·1
839	167·52	·67	+ 2·8
888	181·55	·18	−22·6
920	197·50	·89	−27·7
947	206·44	·85	−32·5
989	227·35	·10	−21·1
1012	231·41	·53	+ 4·6
1022	233·30	0·74	− 5·3
	V636 Sco	JD 2433000	
169	822·52	0·62	+ 6·5
194	831·39	·92	+15·5
203	834·44	·37	− 0·1
228	844·46	·85	+15·3
246	871·30	·80	+12·2
259	875·29	·38	− 3·5
274	881·30	·27	−10·8
288	897·26	·62	+ 8·2
298	900·23	·05	−13·1
308	903·23	·49	+ 1·8
317	906·22	·94	+11·2
328	910·24	·53	+ 3·0
746	1137·60	·98	− 2·3
764	1145·62	·16	−13·9
893	1183·51	·74	+ 8·0
900	1191·48	0·91	+12·7

Plate Cc	Epoch J.D.	Phase P	Velocity km/sec
	V636 Sco (*continued*)		
919	1197·46	0·79	+12·9
931	1200·46	·23	− 9·6
945	1206·35	·10	− 7·6
960	1219·39	·01	− 0·2
975	1223·34	0·60	+ 4·2
	R TrA	JD 2433000	
181	827·41	0·48	− 4·5
187	829·38	·06	−23·5
193	831·33	·64	+11·8
202	834·38	·54	+ 5·1
228	844·42	·50	+ 1·3
246	871·20	·40	− 7·3
259	875·20	·58	− 3·8
274	881·22	·36	− 6·1
722	1130·65	·95	−18·5
732	1133·63	·83	+ 1·0
746	1137·55	·99	−27·9
919	1197·42	·65	+ 3·0
931	1200·43	·54	+ 1·1
1022	1233·19	0·20	−20·8
	S TrA	JD 2433000	
187	829·39	0·01	−12·3
194	831·34	·32	+ 8·3
202	834·39	·80	+28·8
228	844·42	·39	+10·3
246	871·21	·63	+27·6
259	875·22	·26	+ 0·2
260	875·21	·26	− 3·8
275	881·24	·21	− 8·1
732	1133·64	·13	− 9·0
746	1137·56	·75	+26·7
764	1145·61	·02	− 9·3
809	1157·58	·91	− 4·0
839	1167·48	·48	+10·9
888	1181·47	·69	+22·3
989	1227·29	·94	−11·9
1009	1231·33	0·58	+15·0
	U TrA	JD 2433000	
187	829·47	0·73	− 2·5
194	831·35	·46	−24·0
203	834·42	·66	− 5·2
228	844·44	·56	−16·3
246	871·23	·99	+ 9·7
259	875·23	·55	−21·8
274	881·25	·89	− 1·9
328	910·20	·16	−29·9
338	913·20	·33	−32·1
370	937·21	·68	−10·6
766	1145·59	·81	− 3·1
888	1181·49	·79	+ 3·6
919	1197·44	·00	+ 1·7
975	1223·32	0·08	+ 3·0

Plate Cc	Epoch JD	Phase P	Velocity km/sec
	T Vel JD 2433000		
474	996·58	0·34	− 0·7
480	998·59	·77	+28·8
484	1000·59	·20	+ 1·6
497	1018·50	·06	− 1·3
506	1022·53	·93	− 3·9
513	1025·53	·58	+16·0
531	1031·57	·88	+ 4·8
534	1033·54	·30	− 0·9
537	1042·52	·24	− 4·1
544	1053·51	·61	+21·4
547	1057·39	·44	+10·3
558	1062·40	·52	+18·3
576	1077·42	·76	+28·3
586	1080·36	·40	+ 8·7
608	1088·34	·12	− 4·5
626	1092·38	·99	− 7·9
669	1110·31	·85	+13·1
743	1137·18	·64	+19·9
806	1157·24	·97	−10·0
891	1183·22	0·56	+23·3
	V Vel JD 2434000		
498	18·61	0·10	−43·3
507	22·60	·02	−44·7
521	29·62	·62	−16·0
547	57·45	·99	−46·5
559	62·54	·16	−42·5
586	80·45	·25	−35·5
602	85·43	·39	−25·9
608	88·40	·07	−45·8
626	92·47	·00	−53·0
653	104·44	·74	− 6·8
669	110·37	·10	−40·4
678	113·31	·77	−10·3
683	117·26	·68	−12·6
693	122·24	·81	−13·3
720	130·26	·65	−13·8
743	137·21	·24	−38·6
899	191·22	0·59	−15·8
	AH Vel JD 2433000		
363	934·62	0·58	+31·8
371	937·62	·29	+21·2
413	962·57	·19	+21·7
420	964·61	·68	+31·8
423	965·58	·90	+21·1
432	967·58	·38	+22·4
438	970·60	·09	+19·8
439	973·57	·80	+31·9
444	976·55	·50	+32·8
447	984·57	·40	+27·1
453	986·57	·87	+25·8
457	988·59	·35	+27·0
464	992·60	0·30	+26·2

Plate Cc	Epoch JD	Phase P	Velocity km/sec
	AH Vel (*continued*)		
469	994·57	0·76	+33·5
477	996·51	·22	+22·9
482	998·52	·70	+35·2
485	1000·36	·16	+22·2
501	1020·42	·88	+22·4
587	1080·34	·05	+21·6
609	1088·29	·93	+16·8
625	1092·35	·90	+22·0
627	1092·33	·89	+18·2
670	1110·27	·13	+17·8
890	1183·16	0·38	+34·5
	AX Vel JD 2433000		
405	960·60	0·01	+ 8·2
412	962·56	·76	+21·1
419	964·59	·45	+32·6
422	965·56	·92	+10·0
431	967·56	·69	+42·5
437	971·58	·24	+18·9
440	973·55	·00	+18·0
443	976·52	·15	+18·1
446	984·54	·24	+26·2
452	986·56	·02	+10·1
458	988·55	·79	+24·7
474	996·49	·85	+22·3
480	998·50	·63	+31·4
484	1000·50	·40	+29·8
497	1018·52	0·36	+28·0
	BG Vel JD 2434000		
498	18·60	0·93	+ 1·2
521	29·60	·52	+12·4
532	31·60	·80	+15·5
535	42·50	·38	+ 6·3
547	57·42	·53	+17·7
558	62·46	·26	+17·6
586	80·43	·86	+ 5·8
608	88·38	·01	− 4·2
626	92·45	·59	+25·2
650	102·44	·04	− 0·7
669	110·36	·18	+ 5·6
678	113·29	·60	+25·2
693	122·22	·89	+ 1·9
720	130·24	·05	− 1·2
743	137·20	·06	− 1·5
806	157·27	·96	+ 1·4
838	167·21	·39	+12·0
891	183·24	0·70	+24·0
	RZ Vel JD 2433000		
452	986·60	0·97	+45·3
457	988·60	·07	+16·0
480	998·56	·56	+27·4
484	1000·57	0·65	+35·6

Plate Cc	Epoch JD	Phase P	Velocity km/sec
	RZ Vel (*continued*)		
517	1027·60	0·98	+40·3
523	1029·57	·08	+14·0
529	1031·54	0·17	− 2·8
	SV Vel JD 2434000		
730	133·31	0·76	+26·7
744	137·28	·04	−10·0
763	145·31	·61	+23·8
795	153·34	·18	−17·0
806	157·30	·46	+ 7·3
825	163·30	·88	+ 3·3
891	183·26	·30	− 5·2
930	200·24	·50	+ 9·7
945	206·21	·93	+ 3·7
950	207·20	0·00	− 1·4

Plate Cc	Epoch JD	Phase P	Velocity km/sec
	SX Vel JD 2434000		
586	80·41	0·01	+21·8
608	88·36	·85	+15·2
626	92·40	·27	+30·2
642	98·33	·89	+22·1
669	110·33	·15	+22·9
678	113·26	·45	+41·1
683	117·24	·87	+23·3
693	122·19	·39	+34·4
730	133·23	·54	+44·1
743	137·19	·96	+19·7
763	145·22	·80	+16·4
806	157·26	·06	+25·0
825	163·19	·68	+38·5
886	181·21	·57	+48·2
899	191·19	0·61	+51·1

phase of the light variation at the time of mid-exposure, calculated from the ephemerides in the Russian Catalogue, and (iv) the radial velocity. The cepheids are arranged in alphabetical order and the observations for a given cepheid in chronological order. The thousands part of the epoch in Julian days is given next to the star name. To this should be added the number of days given in the epoch column.

TABLE VII

Observational data for cepheid variables in the Southern Hemisphere

Star	m_{pg}	Period (days)	Spectral type	Normal velocity km/sec	Velocity range km/sec	No. of plates
T Ant	8·8–10·4	5·9071	G2	+29·5	45	9
V496 Aql	8·5– 9·1	6·8069	G5	+ 5·2	14	21
l Car	5·0– 6·0	35·532	F8–Ko	+ 1·4	40	21
U Car	6·4– 8·0	38·749	F9–K3	+ 0·4	52	16
V Car	8·2– 8·9	6·6967	Go–K2	+16·1	32	21
Y Car	8·2– 8·7	3·6398	F5	− 5·8	24	10
ER Car	7·6– 8·0	7·7178	F8	−18·1	34	18
GI Car	8·7– 9·1	4·4306	F8	−21·4	20	17
IT Car	8·3– 8·7	7·5356	F7–K2	−14·0	18	13
UX Car	8·3– 9·4	3·6823	F4–G5	+10·4	34	19
VY Car	8·3– 9·4	18·961	F9–Ko	− 1·2	59	16
V Cen	7·1– 8·2	5·4940	F5–G5	−22·3	39	17
AZ Cen	8·8– 9·4	3·2127	F3–Go	−12·3	19	11
UZ Cen	9·1–10·0	3·3343	F2–G5	− 5·1	38	9
XX Cen	7·9– 9·0	10·956	F6–Ko	−15·7	35	14
V339 Cen	9·0–10·1	9·466	...	−24·3	31	15
V378 Cen	9·6– 9·8	6·4587	F5–G5	−17·7	17	11
V381 Cen	7·8– 8·5	5·0789	F6–G7	−30·8	39	13
V419 Cen	8·7– 9·3	5·5103	Ko	−17·2	17	12
CPD −60° 4739	7·2– 7·5	5·6218	F8	−12·8	16	13
R Cru	7·4– 8·3	5·8256	F6–G7	−13·5	34	14
S Cru	7·3– 8·0	4·6900	F5–G5	− 6·6	36	14
T Cru	7·5– 8·1	6·7332	G1–G5	− 6·0	34	17
X Cru	9·4–10·0	6·2199	Go–Ko	−25·0	25	12

Star	m_{pg}	Period (days)	Spectral type	Normal velocity km/sec	Velocity range km/sec	No. of plates
AG Cru	9·0– 9·8	3·8374	F5	− 4·5	39	17
β Dor	4·5– 5·7	9·8426	F2–F9	+ 8·1	36	23
R Mus	7·2– 8·1	7·5102	F9–G6	+ 3·8	43	14
S Mus	7·3– 7·6	9·6587	F8–G4	+11·8	29	7
RT Mus	9·1–10·1	3·0862	...	− 1·8	36	11
S Nor	6·7– 7·5	9·7530	F8–G2	+ 3·3	34	19
BF Oph	7·6– 8·8	4·0679	F8–K2	−31·4	45	14
κ Pav	4·5– 5·5	9·0838	F5–G5	+37·6	32	15
AP Pup	7·6– 8·7	5·084	G0	+17·9	33	23
AQ Pup	8·8–10·7	29·92	K5	+59·8	61	13
AT Pup	8·0– 9·4	6·6648	...	+28·8	50	21
WX Pup	9·1–10·1	8·9393	G0	+53·4	35	12
U Sgr	6·9– 8·0	6·7449	F7–G5	+ 3·9	44	17
W Sgr	5·0– 6·4	7·5947	F2–G6	−26·4	44	11
X Sgr	5·0– 6·1	7·0122	F5–G9	−13·7	32	15
RV Sco	7·0– 8·1	6·0613	F5–G5	−18·3	39	15
RY Sco	9·4– 9·6	20·314	F9–G7	−18·4	37	10
V482 Sco	8·1– 8·9	4·5278	F5	+11·1	32	18
V500 Sco	9·7–10·4	9·3163	...	−13·8	36	12
V636 Sco	7·3– 8·1	6·7963	G5	+ 0·8	29	21
R TrA	7·2– 7·8	3·3893	F6–G4	− 9·1	35	14
S TrA	7·0– 7·7	6·3236	F6–G8	+ 6·6	42	16
U TrA	8·0– 8·8	2·5683	F4–G2	−13·7	41	14
T Vel	8·8– 9·2	4·6398	G0–G5	+ 8·0	39	20
V Vel	8·2– 8·8	4·3710	F8–G5	−28·7	39	17
AH Vel	5·8– 6·3	4·2272	F8p	+26·0	17	24
AX Vel	8·5– 9·2	2·5925	F8	+24·2	27	15
BG Vel	9·0– 9·6	6·9235	G5	+10·9	30	18
RZ Vel	6·6– 9·2	20·396	G8	+25·5	57	7
SV Vel	8·7–10·7	14·097	F8–K0	+ 4·5	49	10
SX Vel	8·8– 9·7	9·5499	G5	+30·9	32	15

The observations were plotted according to phase, and schematic or smooth curves, whichever seemed appropriate, were drawn through the velocity points. The radial velocity curves are given in Figs. 3, 4, 5, 6 and 7. Normal velocities were found from the curves by the method of equal areas. Using a planimeter, the residual area was found for *figure of eight* loops for three assumed, and approximately correct, values of the normal velocity, the velocity for zero residual area being then found graphically to the nearest 0·1 km/sec. The uncertainty in the normal velocity depends mostly upon how well the velocity curve is defined by the observations. The estimated average probable error of a single normal velocity is of the order of 1 km/sec. The normal velocities are given in Table VII with other relevant data.

4.2. *Comparison with Lick.*—Five cepheid variables for which definitive velocity curves had been obtained by the Lick Observatory from high dispersion spectrograms, taken at a much earlier epoch, were included in the programme in order to check the constancy of the normal velocities and, if possible, the shape of the velocity curves. The stars in question are the five brightest cepheids in the Southern Hemisphere, each having noteworthy features: *l* Carinae for its long period, 35·5 days, and for suspected irregularities in the velocity curve (**13**); β Doradus for its high galactic latitude, −32°·3, and the unusual shape of its

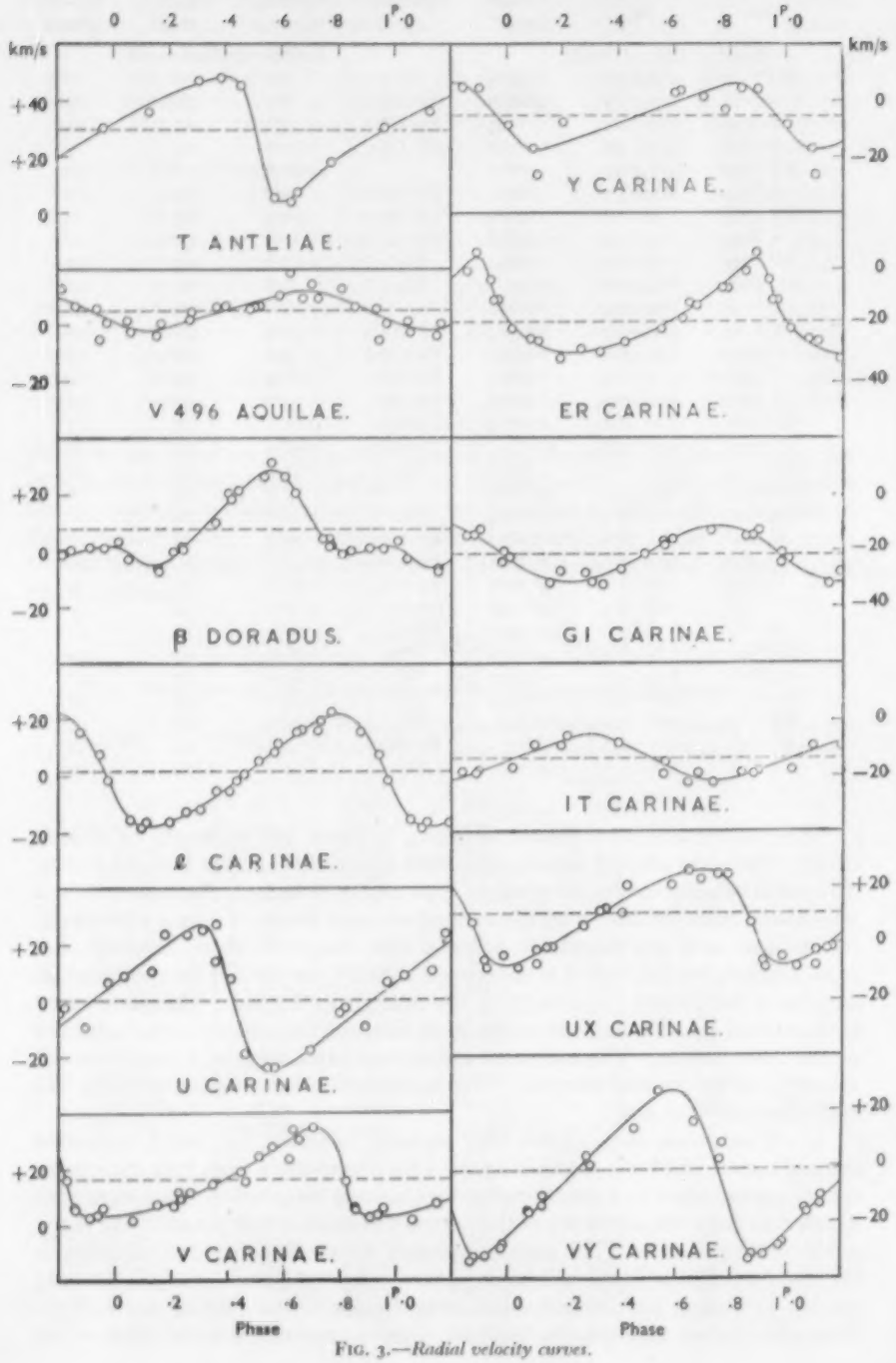

FIG. 3.—*Radial velocity curves.*

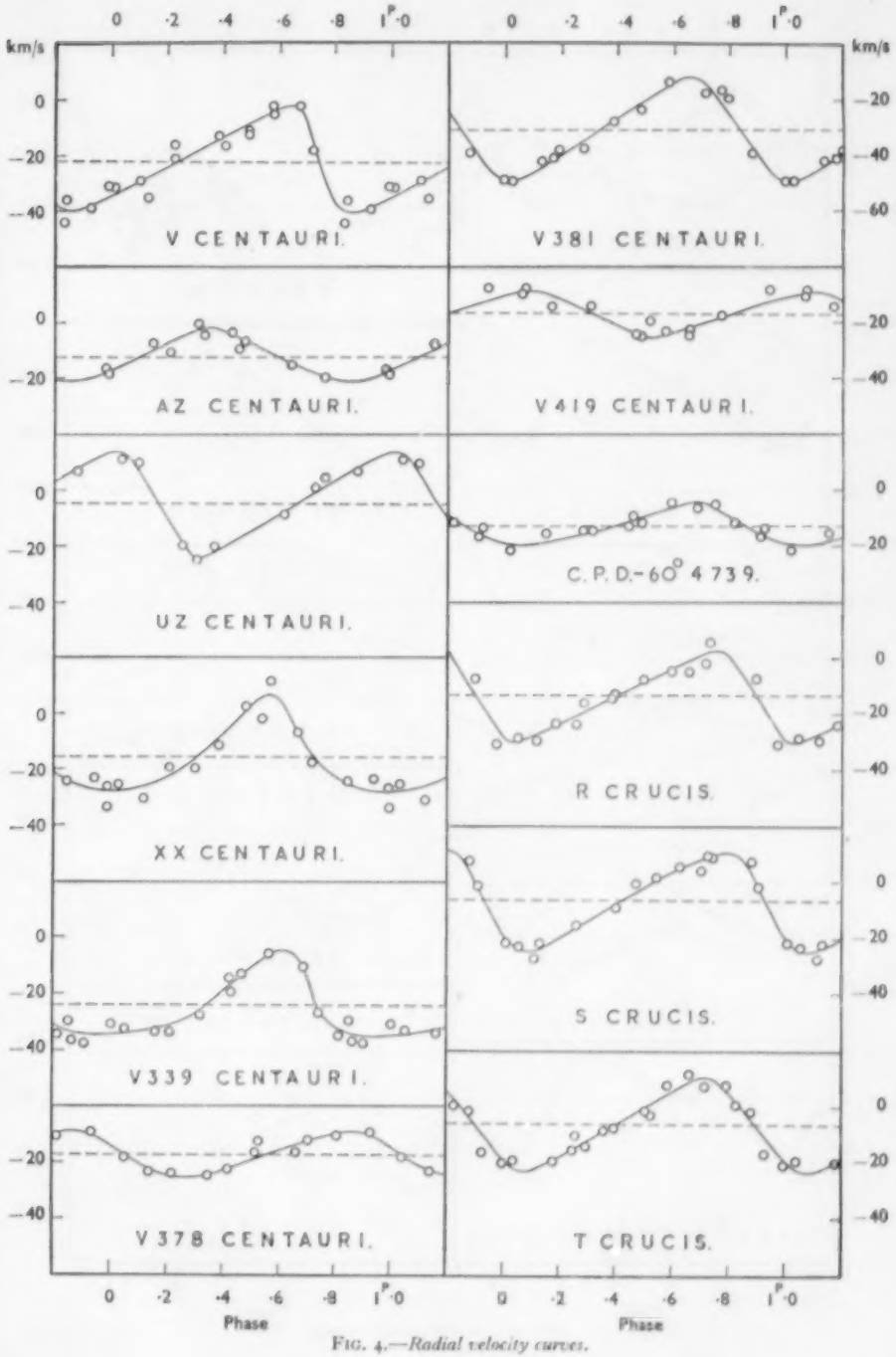

FIG. 4.—*Radial velocity curves.*

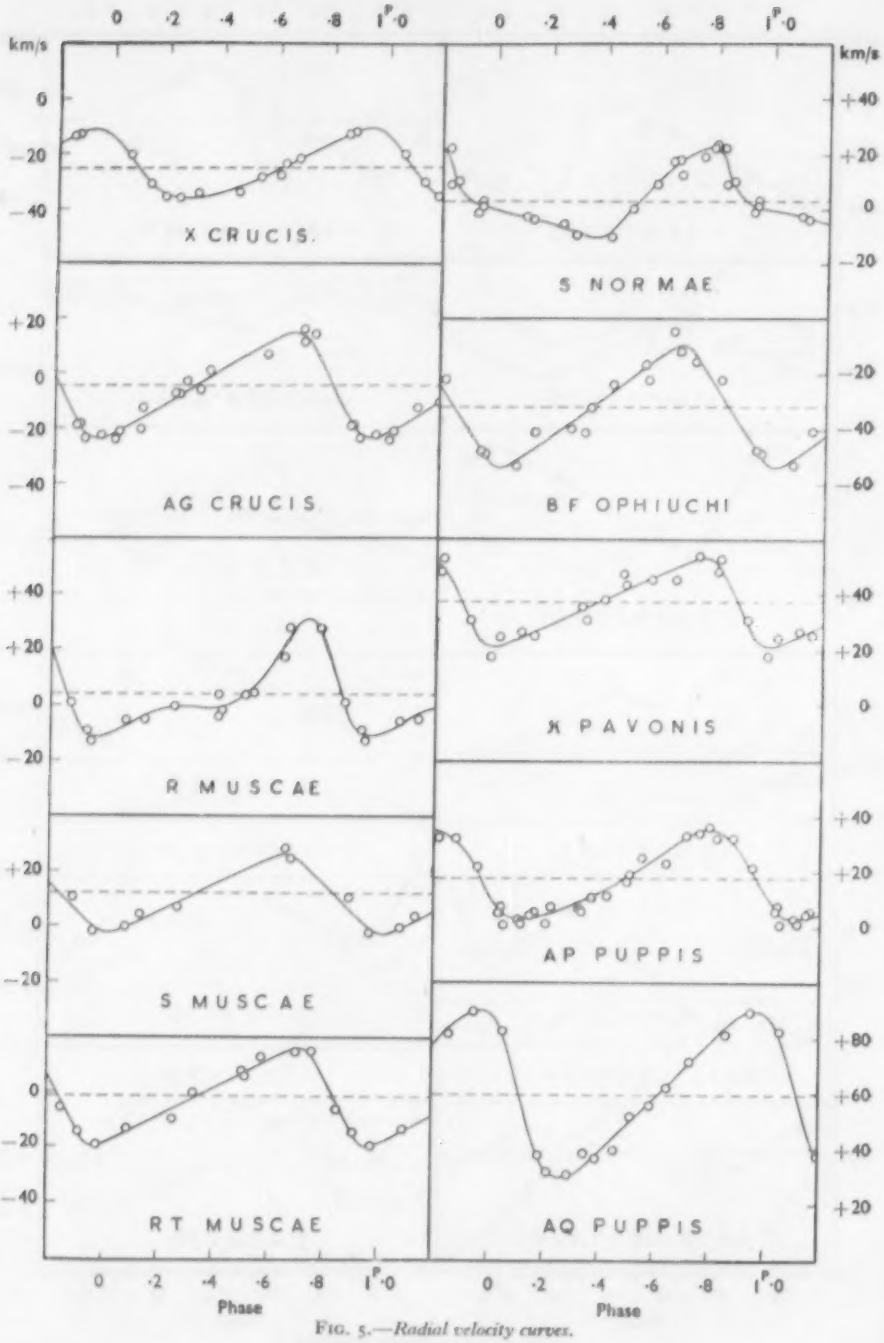

FIG. 5.—*Radial velocity curves.*

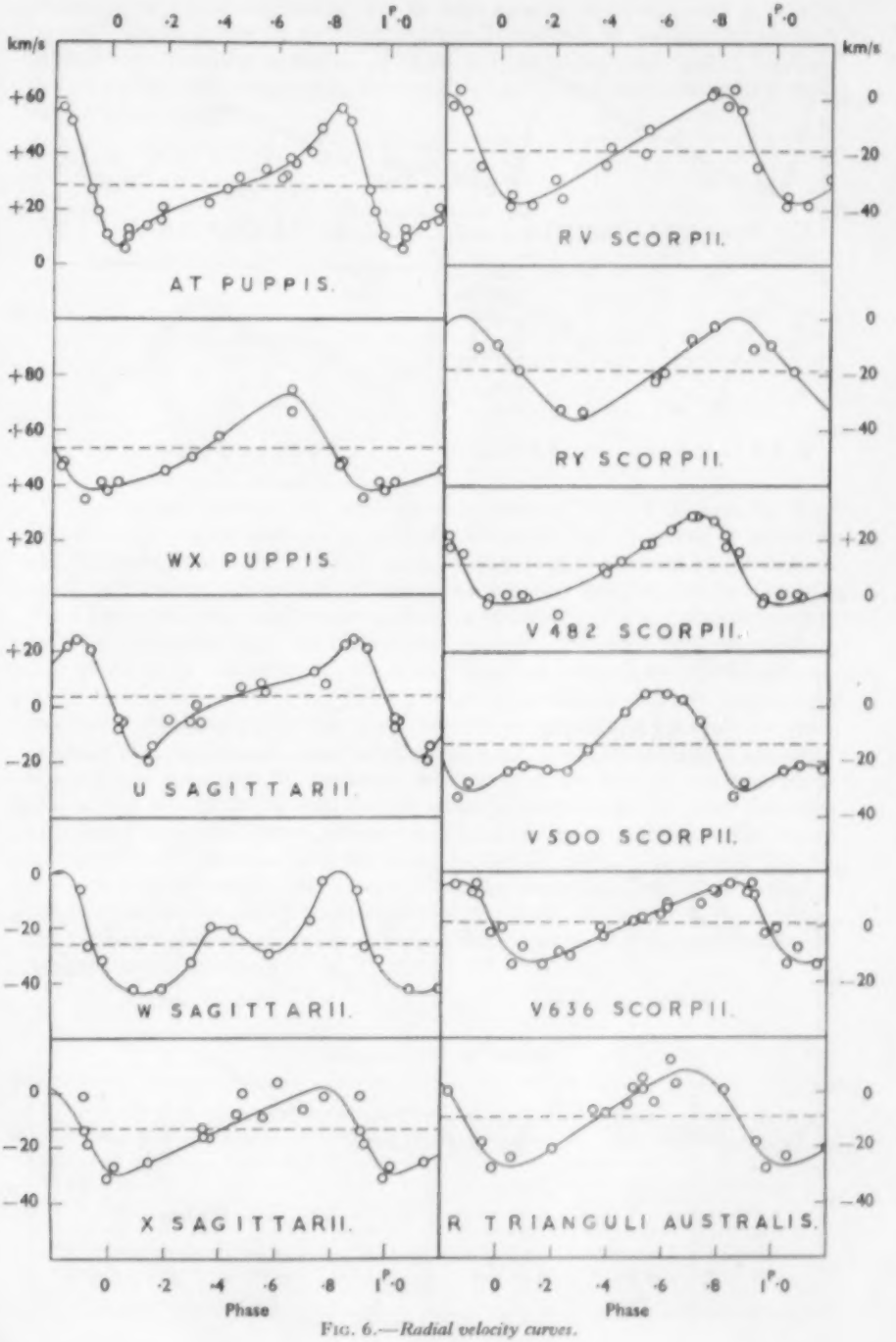

FIG. 6.—*Radial velocity curves.*

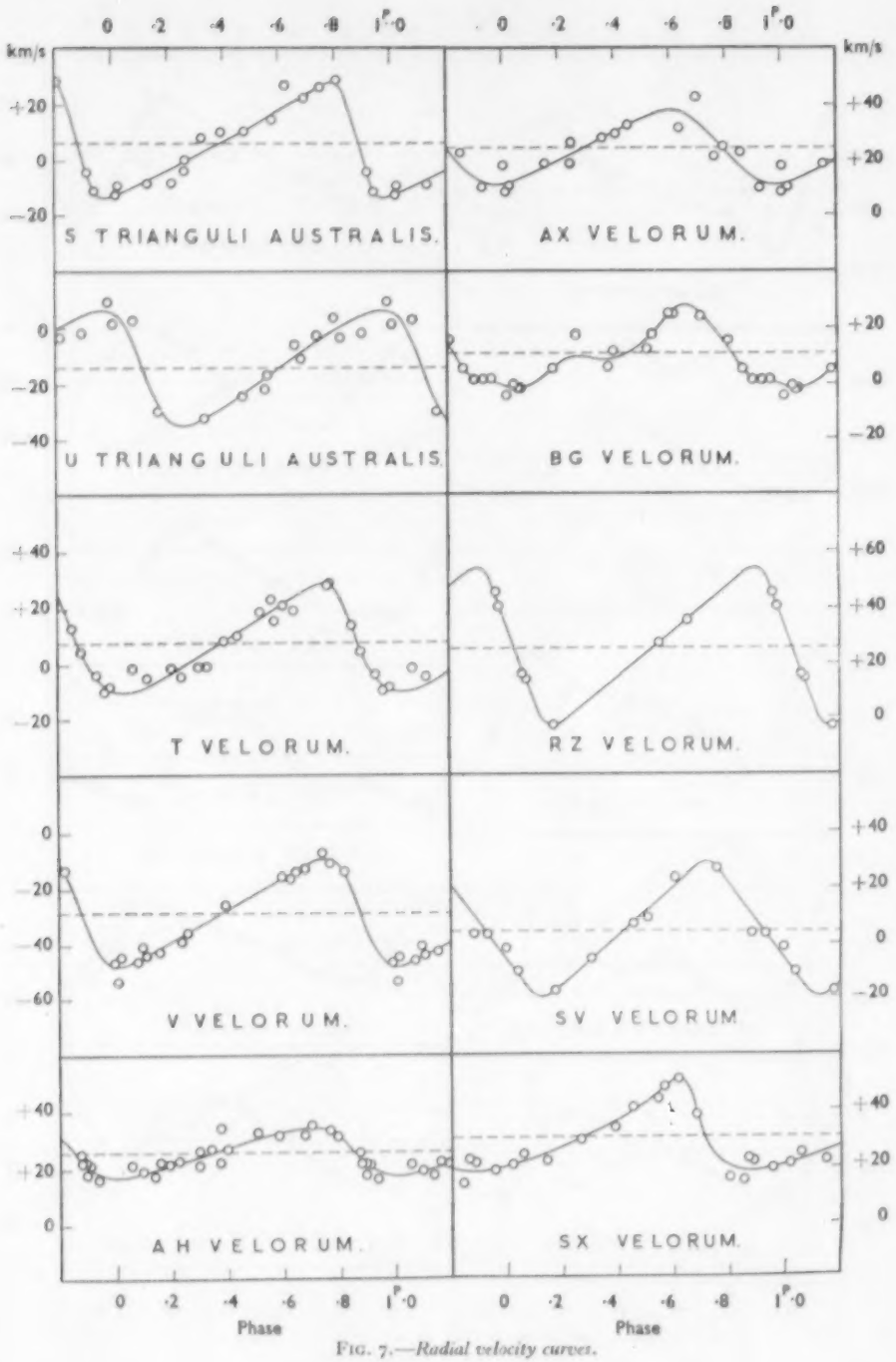

FIG. 7.—*Radial velocity curves.*

velocity curve (**14**); κ Pavonis for its high galactic latitude, $-26°.3$, and its recently proposed identification (**15**) as a type II cepheid; W Sagittarii for the well-established variability in the shape of its velocity curve (**16**); and X Sagittarii for the early epoch, 1904–1905, of the one and only set of observations (**17**) made for its radial velocity.

TABLE VIII

Comparison with Lick

Star	Radcliffe km/sec	Lick km/sec	R − L km/sec
l Car	+ 1·4	+ 4·0	−2·6
β Dor	+ 8·1	+ 7·4	+0·7
κ Pav	+37·6	+36·5	+1·1
W Sgr	−26·4	−26·2	−0·2
X Sgr	−13·7	−13·5	−0·2

The normal velocities for these stars are given in Table VIII with the Lick velocities for comparison. The velocity difference for *l* Carinae is probably significant in view of the fact that Jacobsen (**13,** p. 261) obtained evidence for a small variation in the normal velocity from separate solutions for two epochs. For β Doradus, the normal velocity differs inappreciably from the value previously found by Applegate (**14**), and the remarkable shape of the velocity curve in Fig. 3 was found to be practically identical with the Lick curve from high dispersion spectrograms taken in 1920. The present observations support Applegate's conclusion that the normal velocity of β Doradus is constant, and provide adequate evidence that the shape of the velocity curve is still much the same as it was some thirty years ago. For W Sagittarii, the hump in the velocity curve at phase $0^{p}.4$ in Fig. 6 is probably real. It coincides with the phase at which Jacobsen (**16**) found a similar feature which was considered to be variable. The hump is slightly more pronounced in the present observations but the normal velocity is practically the same. No unusual features were noted about the velocity curves for κ Pavonis and X Sagittarii. For the latter, the scatter in the observations is larger than for the other stars, possibly on account of the poor quality of the lines in the spectrum.

TABLE IX

Comparison with Mt Wilson

Star	Radcliffe km/sec	Plates No.	Mt Wilson km/sec	Plates No.	R − Mt W. km/sec
BF Oph	−31·4	14	−31·5	9	+0·1
WX Pup	+53·4	12	+49·0	8	+4·4
U Sgr	+ 3·9	17	− 2·0	8	+5·9
RV Sco	−18·3	15	−17·5	12	−0·8
RY Sco	−18·4	10	−17·5	10	−0·9

4.3. *Comparison with Mt Wilson.*—The cepheid programme included five variables between declinations $-19°$ and $-34°$ for which Joy obtained schematic velocity curves. The velocities for these stars are listed as *b*-quality in the Mt Wilson General Catalogue. The normal velocities and the number of observations used in their determination are given in Table IX. For the purpose of this discussion, Joy's phases have been recalculated with the ephemerides used in the present work. This results in a small shift in the velocity curves without changing the normal velocities.

The velocity differences Radcliffe *minus* Mt Wilson for BF Oph, RV Sco and RY Sco are satisfactorily small. The two series of observations for BF Oph and RV Sco combine to give well-defined composite curves, but for RY Sco a reduction of $0^{P}\cdot18$ in the computed phases of the Radcliffe observations is necessary for coincidence between the two curves. Apparently the ephemeris for RY Sco, which contains a squared term, predicts the light maximum about 3·7 days too early at the present epoch.

The velocity differences for WX Pup and U Sgr are larger than one might expect for *b*-quality velocities for which the maximum probable error is $\pm 2{\cdot}0$ km/sec. A comparison of the individual observations in both series is necessary before it can be decided if there have been any significant changes in the velocity curves and the normal velocities. Joy's velocity curves for these two stars are given in Fig. 8 with the Mt Wilson and Radcliffe observations.

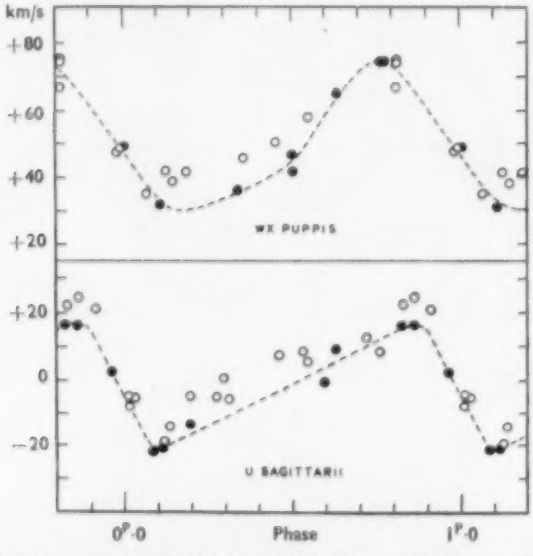

FIG. 8.—*Comparison between Radcliffe and Mt Wilson velocities for WX Puppis and U Sagittarii. Open circles and filled circles denote Radcliffe and Mt Wilson observations respectively. Joy's velocity curves are shown by broken lines.*

The phases of the Radcliffe velocities for WX Pup have been increased by $0^{P}\cdot16$ in order to bring the two series of observations into coincidence on the descending branch of the velocity curve. Evidently the ephemeris for WX Pup is not accurate enough for the present epoch on account of an uncertain period given

only to four decimal places. The present shape of the velocity curve is definitely not the same as Joy's curve which, in the interval of phase between $0^{P}\cdot15$ and $0^{P}\cdot5$, lies about 10 km/sec below the Radcliffe observations. The difference in the shape of the velocity variation at the two epochs depends almost entirely upon three of Joy's observations with dispersion 120 A/mm for two phases within the interval in question. It would appear that there is not much evidence to suggest that there has been any appreciable change in the normal velocity or the shape of the velocity curve for WX Pup in the interval of 17 years between the mean epoch of the two series of observations. Turning now to the case of U Sgr, it is evident from Fig. 8 that Joy's velocities combine satisfactorily with the Radcliffe velocities. Joy's schematic velocity curve gives a very satisfactory fit to the Mt Wilson observations, but it is clearly inadequate for the combined observations. The difference is greatest in the interval of phase from $0^{P}\cdot2$ to $0^{P}\cdot6$ in which there are no Mt Wilson velocities. The Radcliffe observations, by contributing seven velocities in the same interval, confirm the evidence from the shape of the light curve that a schematic curve is not likely to give a satisfactory representation of the velocity variation.

Conclusion.—It may be concluded from the discussion on the standardization of the velocities that the observations described in the paper have given a homogeneous set of velocity determinations in a system which differs inappreciably from the Lick System of radial velocities. The normal velocities of cepheid variables presented in the paper may be introduced with confidence into other radial velocity data, such as Joy's data for cepheid variables in the northern hemisphere, which also differ inappreciably from the Lick System.

Acknowledgments.—The work described in the paper was carried out during the author's tenure of the Radcliffe Travelling Fellowship in Astronomy at the Radcliffe Observatory, Pretoria, and the University Observatory, Oxford. Grateful acknowledgment is due to the Radcliffe Observer, Dr A. D. Thackeray, whose helpful consideration made possible the completion of the observational programme and the measurement of the spectrograms in Pretoria. The writer is deeply indebted to Professor H. H. Plaskett for his interest and constant encouragement during the protracted calculations for radial velocity, and the subsequent work on velocity standards and the cepheid velocity curves, all of which was carried out at the University Observatory, Oxford.

The work is, in a very real sense, the fruit of the labours of Dr H. Knox-Shaw under whose energetic directorship the Radcliffe Observatory and the 74-inch telescope, the first in the Southern Hemisphere, were successfully established in Pretoria.

University Observatory,
Oxford:
1955 *March.*

References

(1) A. H. Joy, *Ap. J.*, **86**, 363, 1937.
(2) A. H. Joy, *Ap. J.*, **89**, 356, 1939.
(3) R. F. Sanford, *Ap. J.*, **114**, 331, 1951.
(4) O. Struve, *Ap. J.*, **102**, 232, 1945.
(5) G. H. Herbig and J. H. Moore, *Ap. J.*, **116**, 348, 1952.
(6) M. W. Feast, A. D. Thackeray and A. J. Wesselink, *Mem. R.A.S.*, LXVII, Pt. II, 52, 1955.

(7) R. O. Redman, *M.N.*, **99**, 686, 1939.
(8) J. K. Macdonald, *J.R.A.S. Canada*, **42**, 220, 1948.
(9) D. S. Evans, *Monthly Notes Astron. Soc. S.A.*, **13** (No. 3), 25, 1954.
(10) O. Struve, *The Observatory*, **65**, 270, 1944.
(11) B. V. Kukarkin and P. P. Parenago, *General Catalogue of Variable Stars* (Moscow), 1948.
(12) A. D. Code, *Ap. J.*, **106**, 309, 1947.
(13) T. S. Jacobsen, *P.A.S.P.*, **46**, 255, 1934.
(14) D. Applegate, *L.O.B.*, **13**, 12, 1927.
(15) O. J. Eggen, private communication.
(16) T. S. Jacobsen, *L.O.B.*, **12**, 150, 1926.
(17) J. H. Moore *L.O.B.*, **5**, 111, 1909.

THE BRIGHT DOUBLE-LINED ECLIPSING VARIABLE CV VEL

Sergei Gaposchkin

(Communicated by Cecilia Payne-Gaposchkin)

(Received 1955 March 21)

Summary

The star HD 77464 found by Feast to be a spectroscopic binary is shown by photometric observations to be an eclipsing variable with the same period as that established by Feast. The essential elements are: Min = 2434091^{d}·302 + 6^{d}·892ϵ, Max = 6^{m}·61, m_1 = 7^{m}·28, m_2 = 7^{m}·25; D = 0^{p}·08; r_1 = 0·126 = 4·26 ○; r_2 = 0·123 = 4·16 ○; μ_1 = 5·618 ○, μ_2 = 5·418 ○; M_{pg1} = −1^{m}·78, M_{v1} = −1^{m}·55; M_{pg2} = −1^{m}·67, M_{v2} = −1^{m}·45; Sp_1 = B2·8, Sp_2 = B3·2.

The dimensions of this new system may support the idea that there exists a group of progressively lower mass all along and below the main sequence beginning with the Wolf Rayet stars and ending at the late A spectral class.

1. The bright star HD 77464 (8^{h} 57^{m}; −51° 10′, 1900) of spectral class B3 (Harvard) has been announced by M. W. Feast (1) as a spectroscopic binary with a period of about seven days and with similar components. Although the spectroscopic elements have characteristics which do not suggest that the orbit may be so inclined as to produce alternating eclipses as seen from the Earth, I have examined the star's brightness.

2. From inspection of several hundred plates in the Harvard Collection, I have estimated the brightness of the star. This photographic material suffers from heterogeneity; the location of the star in a thick nebulous region of the Milky Way, and the relatively long exposures of the plates, produced a halo around the image, but in spite of these difficulties the variation of the star's brightness is easily perceived.

3. The comparison stars are collected in Table I.

TABLE I

Comparison stars for HD 77464

HD	Pg mag.	Steps	Source of mag.
	m		
77653	5·32	15·0	(2)
76230	6.35	7·8	(2)
76968	7·23	2·0*	(2)
77305	7·52	0·0†	(3)

* Definitely variable. † Has a faint companion.

All my observations are given in Table II expressed in steps. The relation between the steps and the magnitudes is expressed in the form

$$\text{Ipg} = 6^{m}\cdot30 + 0^{m}\cdot15(8 - x),$$

where x is the number of steps.

4. Feast's period seems to be correct. I have observed few minima but observations at the beginning and end of the Harvard series fit the predicted minima. For the middle of the interval I have many plates taken with AX, AY, and AK telescopes, which, however, have appreciable differences in colour sensitivity. This factor, together with the brightness of the variable and the

TABLE II

Photographic observations of HD 77464

JD 2 400 000+	Units	JD 2 400 000+	Units	JD 2 400 000+	Units
d		d		d	
14 979·804	2·25	17 342·534	6	20 620·493	4·5
984·862	6	523·869	6	627·490	3·5
15 089·683	6	579·814	5·5	635·511	6
159·498	6	651·662	6	950·667	6
337·827	6·5	711·531	6	986·514	5·5
465·618	2·25	965·769	5·5	21 005·520	5
469·616	5·5	18 030·598	6	012·474	6
516·582	5·5	033·612	6	136·988	5·5
526·512	6	065·535	5·5	311·581	5·5
719·854	6	068·552	6	314·561	4·5
767·812	6·5	331·779	6·5	316·546	5·5
810·660	5·5	367·408	3·5	332·580	6
817·666	6	370·371	5·5	663·612	5·5
880·532	6·5	375·414	5·8	22 045·609	6
885·531	5·5	385·617	5·5	424·621	5·5
16 015·894	5·5	395·368	6	23 163·772	3·5
073·785	6	405·365	6	174·567	4
079·778	5·5	421·517	6	180·517	6
118·822	6	434·512	5	189·568	5·5
120·734	6	440·389	6	489·627	6·5
183·637	5	626·502	5·8	519·581	5·5
197·624	6	749·253	6	536·358	3
204·606	6	750·548	6	544·620	6
239·549	6	814·507	5·5	784·764	5·5
242·521	6	821·497	6	793·669	6
249·567	6	989·858	5·8	822·625	6
253·538	6	19 029·779	6	902·525	6
387·890	6·5	450·699	5·5	919·496	5·5
435·787	5	488·589	5·5	24 136·751	6
489·684	5·5	500·568	6	198·634	6·5
549·705	5·5	507·569	6	270·507	4·5
589·677	5·5	511·560	5	283·503	5·5
591·619	5·5	512·563	6	527·679	6
603·575	5	513·523	6	538·627	6
612·542	6	526·550	6·5	563·676	6
636·552	5	543·507	6	635·512	2·5
649·509	5·5	546·512	6	643·501	5·5
663·521	6	557·567	6	653·501	6
785·832	6	803·726	6	830·857	6·5
789·869	6	889·531	6	25 246·459	6·5
823·783	6	889·571	6	273·430	6·5
855·685	5·5	896·527	6	327·456	6·5
856·835	6	927·546	6	361·443	6·5
907·651	6	843·518	6	27 955·219	6
918·598	5·5	20 185·695	5·5	28 222·338	5
976·506	6	237·569	6	276·298	6
17 237·665	5·5	238·569	3·8	339·219	6·5
283·548	5·5	250·521	6	344·219	6
331·512	6	278·504	6	566·417	5·5
17 340·565	4·5	20 295·516	6	28 625·372	6

TABLE II (*continued*)

JD 2 400 000 +	Units	JD 2 400 000 +	Units	JD 2 400 000 +	Units
d		d		d	
28 633·367	6	32 648·364	6·5	33 111·446	5·5
639·299	6	711·379	6·5	307·405	5·5
695·282	6	713·445	6·5	332·303	6·5
776·610	5·5	714·434	6·5	360·421	6·5
822·582	6 ?	726·323	6·5	367·605	1·8
875·552	6·5	730·465	4	409·345	5·5
897·360	6	731·414	6	416·354	4·5
932·286	6·5	879·403	6·5	417·410	6·5
961·490	6	882·251	2	423·402	6·5
987·346	6·5	882·401	6·5	438·389	5·5
29 017·376	5·5	888·248	6·5	440·403	5·5
066·205	6	891·357	6·5	441·416	4·5
141·612	6	908·346	6·5	444·367	6
203·508	6	913·325	6	452·445	6
254·532	6·5	915·318	6·5	472·505	6·5
319·342	6	916·432	3·5	662·378	6·5
348·352	6·5	951·412	6·5	664·465	6·5
373·360	6·5	977·415	6·5	708·289	6·5
419·216	6	998·404	6	708·355	6
433·220	6	33 000·389	6·5	719·211	2
486·016	6·5	005·395	6	719·375	3·5
32 128·403	5·5	011·379	6·5	735·325	6
129·402	6·5	025·384	6·5	750·251	2·5
271·385	6	026·595	3·5	823·665	5·5
293·381	6	029·380	6·5	834·642	6·5
315·384	6	033·402	1·7	34 039·354	4·5
590·355	6·5	034·545	6	044·402	5·5
593·353	6	053·562	6	071·367	6
594·347	6	063·534	6·5	076·456	5·5
626·368	5	071·585	5·5	091·302	1·5
626·403	4·5	085·520	5·5	098·403	4
641·423	5·5	090·466	4·5	099·368	6·5
644·375	5	094·450	6·5	120·425	5·5
32 646·385	5	33 097·437	6·5	34 121·413	6

surrounding galactic absorption, makes the plates of little value. Nevertheless, they seem to indicate that the observed minima in this intermediate interval deviate from the predicted ones. This observation, if real, would suggest the existence of a third body.

5. Fig. 1 represents my observations reduced according to the period given by Feast. The maximal brightness, the depths of the minima and the duration of the eclipse were first expressed in steps and then transformed into magnitudes. The narrowness of the minima, the limited number of the plates, and the relative length of the period account for the fact that few observations fall in the interval of both minima. Nevertheless, if the photometric scale is correct, the light curve is quite sufficient to obtain important dimensions of the system. The elements of the light curve are:

$$\text{Min} = \text{JD } 2434091^{d}\cdot302 + 6\cdot892\epsilon$$
$$\text{Max} = 6^{m}\cdot61$$
$$m_1 = 7^{m}\cdot28$$
$$m_2 = 7^{m}\cdot25$$
$$D = 0^{P}\cdot08 \text{ (computed)}$$

Comparison with the spectroscopic orbit reveals that the slightly heavier and larger component is eclipsed during the deeper minimum (phase $\simeq 0^{P}.5$).

6. The relative elements are the following:

Ratio of the radii of the components	0·98
Ratio of their surface brightnesses	1·034
Ratio of their luminosities	1·10
Inclination of the orbit	88° 14′
Relative radius of the larger component	0·126
Relative radius of the smaller component	0·123

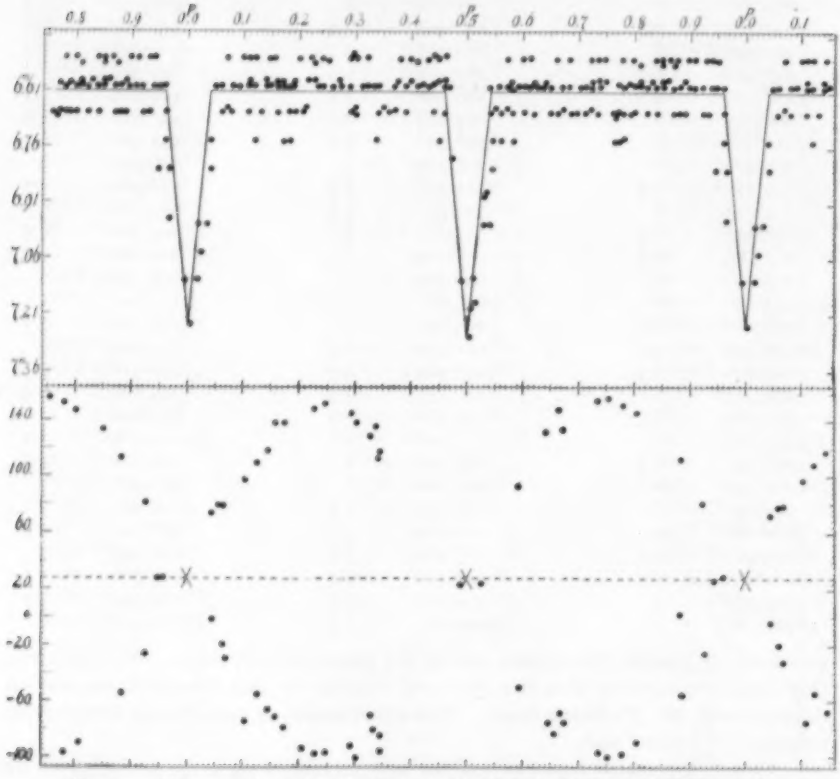

FIG. 1.—*Light curve (above) and radial velocities (below) of HD 77464 (HV 11109).*

The abscissae are phases in terms of the period. The ordinates are magnitudes (above) and velocities in km/sec (below). The dotted line refers to the velocity of the system. The crosses represent the intersection of the orbital velocities and phases of predicted minima.

By using some of the spectroscopic results of Feast, the minimal masses and the distance between the centres, the final absolute dimensions of this system may be obtained. Assuming the Sun's radius to be $0{\cdot}6951 \cdot 10^{6}$ km, then

Radius of the larger component is	$4{\cdot}26_{\odot}$
Radius of the smaller component is	$4{\cdot}16_{\odot}$
Mass of the larger component is	$5{\cdot}618_{\odot}$
Mass of the smaller component is	$5{\cdot}418_{\odot}$

If the spectrum of the system during its maximal brightness is B3, then the individual spectra of the components may be computed from the observed difference of their surface brightnesses, as B2·8 for the larger component, and B3·2 for the smaller.

And finally, taking the corresponding temperatures (**4**) as 17 530 deg. and 17 090 deg., their absolute photographic and visual magnitudes may be computed:

Absolute photographic magnitude of the larger component	$-1^{m}\cdot78$
Absolute photographic magnitude of the smaller component	$-1^{m}\cdot67$
Absolute visual magnitude of the larger component	$-1^{m}\cdot55$
Absolute visual magnitude of the smaller component	$-1^{m}\cdot45$

6. *Conclusions.*—HV 11109 is interesting in the definiteness of its dimensions, which is the result of the two deep minima and the lack of a pronounced ellipticity. There are some ten systems having approximately the same spectral class but none of them has both of these advantages.

The new system is remarkable in that its masses and to some extent the radii are smaller than the majority for the same spectral class. If Feast's spectral classification, B2, is accepted, the low masses will be even more striking. Perhaps this system demonstrates the existence of a group of low mass all along the main sequence whose upper end is formed by the Wolf Rayet stars (about ten solar masses), and whose lower part goes through the system of UX Monocerotis with its spectral class of A7 and its mass below that of the Sun.

When this paper was in proof, the writer's attention was called to the discovery of the star's variability by van Houten (**5**), who, however, did not give the correct period.

Harvard College Observatory,
Cambridge 38,
Mass., U.S.A.
1955 *March* 15.

References

(**1**) M. W. Feast, *M.N.*, **114**, 246, 1954.
(**2**) C. Payne-Gaposchkin, *Harv. Obs. Mimeogram*, Series III, No. 1, 1938.
(**3**) S. Gaposchkin, *Harv. Ann.*, **89**, No. 9, 1937.
(**4**) S. Gaposchkin, *H.R.*, **201**, 1941.
(**5**) C. J. van Houten, *Leid. Ann.*, **20**, No. 7, 1950.

NOTE ON A SET OF MODELS FOR UNMIXED STARS

A. E. Roy

(Communicated by the Director, University Observatory, Glasgow)

(Received 1955 March 24)

Summary

An erroneous equation in a previous paper is corrected and leads to the conclusion that the radii of the unmixed stars are smaller and the effective temperatures higher than was formerly indicated.

---

1. *Introduction.*—In a previous paper (**1**) the present author derived a set of point-convective models of a star with a range of discontinuities of molecular weight between core and envelope. It was found that the radius of such a star could increase by a factor of ten owing to the exhaustion of hydrogen during evolution.

It has been pointed out to the author by Dr Donald E. Osterbrock of Mt Wilson and Palomar Observatories that the use of equation (3.10) is erroneous in the present case where a discontinuity in molecular weight arises at the interface between core and envelope. Equation (3.10) was adopted from equation (14) of a paper by C. M. and H. Bondi (**2**). Equation (14), correct in that paper, requires modification when used with discontinuous model stars.

The error, in fact, arises earlier. In equation (3.03) of the previous paper (**1**) the contribution from the discontinuous jump in density across the interface between core and envelope was forgotten.

The equation should be

$$\ln \frac{\rho_c}{\rho} = \int_u^\infty \frac{1-N}{S}\, du + \ln \frac{\mu_e}{\mu_c}. \tag{1.01}$$

This changes expression (3.10) to the following:

$$\ln \frac{P_c r_s}{\rho_c G M_s} = \ln Q - u + \int_0^u \frac{Q}{S}\, du + \int_u^\infty \frac{N}{S}\, du + \ln \frac{\mu_e}{\mu_c}. \tag{1.02}$$

This correction leaves the set of tables calculated from the homology equations unchanged but changes the final reductions by which R/R_a, L/L_a and T_c/T_{ca} were found. If R'/R_a, L'/L_a and T_c'/T_{ca} refer to the corrected values, then they are given by the following expressions:

$$\left.\begin{aligned} R'/R_a &= R/R_a \left(\frac{\mu_e}{\mu_c}\right)^{\alpha_4 \alpha_5}, \\ L'/L_a &= L/L_a \left(\frac{\mu_e}{\mu_c}\right)^{(4\beta-\alpha)\alpha_4\alpha_5}, \\ T_c'/T_{ca} &= \left(\frac{\epsilon_N}{\epsilon_{Na}} \cdot \frac{A}{A_a} \cdot \frac{\mu_e}{\mu_c}\right)^{\alpha/(\alpha-\beta)} \left(\frac{\epsilon_a}{\epsilon_{aa}}\right)^{\beta/(\alpha-\beta)} \frac{R_a}{R'}, \end{aligned}\right\} \tag{1.03}$$

where α, β, a_4, a_5, etc. are defined as before and R/R_a, L/L_a are given in Fig. 1 of the previous paper (**1**). The changes in R/R_a, L/L_a, T_c/T_{ca} for a discontinuity in molecular weight of $\mu_c/\mu_e = 2{\cdot}64$ are given in Table I below.

TABLE I

$\mu_c/\mu_e = 2{\cdot}64$

	Uncorrected (paper 1)	Corrected from (1.03)
R/R_a	10	3·00
L/L_a	1·35	2·46
T_c/T_{ca}	1·24	0·42

An unmixed model for $\mu_c/\mu_e = 2{\cdot}091$ was interpolated from the corrected values and compared with a similar model kindly sent to the present author by Dr D. E. Osterbrock. The results agreed, showing that the numerical part of paper (**1**) is accurate, viz. the set of models for unmixed stars calculated from the homology equations.

2. *Conclusion.*—The fact that the radius of such a model does not increase by a factor of ten and the luminosity by a factor of 1·35 during evolution changes the H–R diagram of such stars obtained in the previous paper (**1**). The changes in $\log T_c/T_{ca}$ and $m - m_a$ are shown below for $\mu_c/\mu_e = 2{\cdot}64$ where suffix a refers to the Cowling model.

TABLE II

$\mu_c/\mu_e = 2{\cdot}64$

	Uncorrected (paper 1)	Corrected
$\log T_c/T_{ca}$	−0·45	−0·12
$m - m_a$	$-0^m{\cdot}33$	$-0^m{\cdot}98$

Thus as μ_c/μ_e grows from 1 to 2·64, the star does not move into the red giant region of the H–R diagram but remains relatively close to the line AB. The previous conclusion that the two populations of mixed and unmixed stars do not mingle in the H–R diagram remains unchanged.

My thanks are due to Dr Osterbrock for drawing my attention to this matter.

University Observatory,
Glasgow W. 2:
1955 *March* 18.

References

(1) A. E. Roy, *M.N.*, **112**, 484, 1952.
(2) C. M. and H. Bondi, *M.N.*, **109**, 62, 1949.

NOTE ON THE OBSERVED DIFFERENCES IN SPOTTEDNESS OF THE SUN'S NORTHERN AND SOUTHERN HEMISPHERES

H. W. Newton and A. S. Milsom

(Communicated by the Astronomer Royal)

(Received 1955 April 14)

Summary

The variation with time of the relative spottedness of the Sun's two hemispheres, north and south, is examined by means of a simple index over a period embracing eleven 11-year sunspot cycles. There are changes from cycle to cycle which, although not random, appear to have no definite period. There is the suggestion of a dependence of the pattern of the excess spottedness, north or south, upon the degree of activity of any particular cycle. The results indicate no dependence upon a 22-year cycle.

Introduction.—Sunspot observers have long been aware of persisting periods, extending for months and occasionally to years, when there has been a marked inequality in the spottedness of the two hemispheres of the Sun, north and south.* The presence of any systematic or periodic behaviour of this phenomenon, if established, would be of interest as a new observational feature of sunspot behaviour and of immediate interest to current theories of sunspots. The time covered by the data hitherto considered has been too short to suggest other than a random behaviour in the difference already noted between the spottedness of the two solar hemispheres.

There are, however, now available from the Royal Greenwich Observatory the northern and southern annual mean daily areas of sunspots (corrected for the effect of surface foreshortening and expressed in millionths of the Sun's hemisphere) from 1874 to 1954, thus comprising seven complete sunspot cycles.† It seems therefore worth while pointing out in this note certain features now apparent in this N – S spot occurrence over the period of 80 years covered by the Greenwich observations, and seeing to what extent the features can be recognized in the older records extending back to 1833. The Greenwich observations will be discussed first.

* Newcomb, S., *Ap. J.*, **13**, 13, 1901, who drew attention to a general excess of southern spots from 1856 to 1898. Royal Observatory, Greenwich, *M.N.*, **63**, 452, 1903. It is noted that for the two cycles ending 1902, the northern spots predominated during the rising phase and the southern spots towards the end of the cycle. Brunner-Hagger, W. and Liepert, A., *Astronomische Mitteilungen*, No. 140, p. 556, 1941. The authors have studied the distribution of log N/S within each cycle irrespective of time (1853–1939). Maunder, E. W., *M.N.*, **82**, 534, 1922. Kiepenheuer, K. O., *The Sun*, ed. G. P. Kuiper, p. 336, Chicago, 1953.

† The annual volumes of the *Greenwich Photoheliographic Results* have not yet been issued by H.M.S.O. after 1945. A special volume that will contain the collected data 1874–1954 is in course of publication, entitled "*Greenwich Sunspot and Geomagnetic-Storm Data, 1874–1954*". The requisite tables 1946 to 1952 inclusive have also been published in *Monthly Notices*.

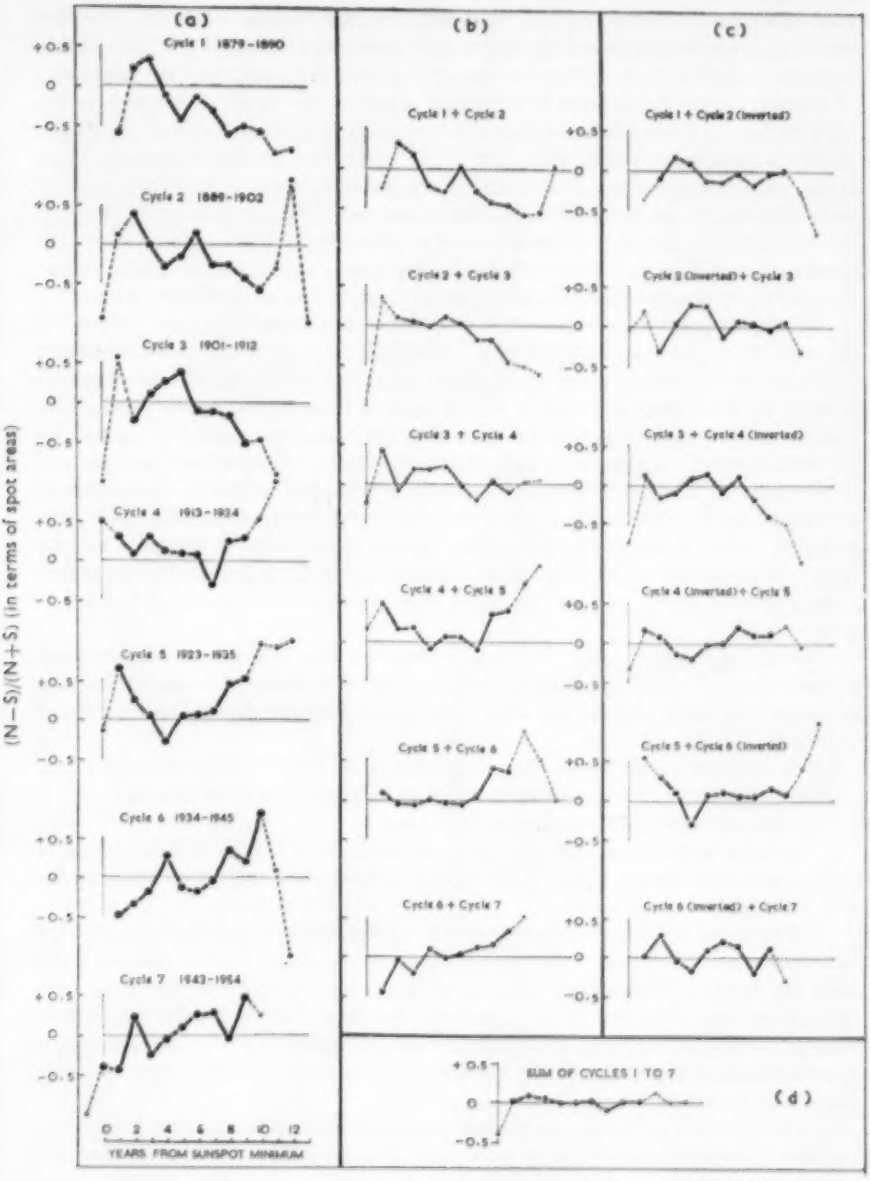

FIG. 1.—*(a) Yearly values of* $(N-S)/(N+S)$ *(in terms of area) for each of the seven cycles 1879–1954. Points where* $N+S<100$ *units of area are joined by broken lines. (b) Means of adjacent cycles shown in Fig. 1 (a). (c) Means of adjacent cycles shown in Fig. 1 (a), alternate cycles inverted. (d) Mean of the seven cycles shown in Fig. 1 (a).*

Data.—Using the Greenwich values of the annual mean daily areas of sunspots, the difference E_A of the ratios N/(N + S) and S/(N + S) has been taken for each year and plotted in Fig. 1 (*a*) for the seven sunspot cycles. In each case, the time origin has been adopted as the year of sunspot minimum, as given by Zürich sunspot "numbers" in agreement with the Greenwich areas and the frequency of spotless days. Any epoch of minimum is admittedly partly dependent on the old cycle as well as the new but is better for our purpose than the epoch of maximum, which is sometimes rather indefinite as in cycle No. 3. At minimum, there is the well-known overlap in latitude of the old-cycle spots in low latitudes and the new-cycle spots in latitudes usually above 20°. The spots in the period of the overlap have therefore been allocated to their appropriate cycles. Although these points in Fig. 1 (*a*) at or near minimum appear significant in giving trends, the points are numerically of low weight because of low sunspot frequency.

Greenwich areas of faculae.—It is of interest to compare the yearly values of E_A with those derived from faculae. Although faculae in the general sunspot zones are closely related to the spots, their dark streaks or masses (on the negative) present to the measurer a very different feature from the sunspots themselves. Moreover, faculae are longer-lived than their associated sunspots, but are usually visible only within three or four days of the Sun's limb. Areas of faculae measured at Greenwich, divided according to the northern and southern hemispheres, are available* for deriving a similar ratio to that for the spots for the years 1874 to 1916. The agreement of the values given respectively by sunspots and by faculae is remarkably close (Fig. 2), and indicates that the departures of the points from a smooth curve in Fig. 1 (*a*) are not due to observational errors but are of solar origin.

Counts of sunspots 1832 *to* 1874.—Prior to the Greenwich observations commencing in 1874 April, there are no published areas of sunspots divided according to hemisphere, but there are the following dependable series of drawings:

Schwabe's records 1826 to 1867 preserved at the Royal Astronomical Society.

Carrington's published observations 1853 November to 1861 March.†

Spörer's published observations 1861–1879.‡

The Kew series of photographs§ extend from 1862 to 1873 but the whole of the observations do not appear to have been published in the form necessary for this investigation.

Before using any of these older records it was first ascertained from the extensive Greenwich records whether the yearly values of E_A derived from sunspot areas were satisfactorily represented by similar values E_N, obtained by counting each spot group once, whether it was seen for a few days only or for the whole disk passage. A recurrent group was counted as another group (i.e. as in the Greenwich results, in which the return group has a separate number). All groups seen only for one day were excluded.

As indicated by the high degree of correlation exhibited in Fig. 3 between E_A and E_N over the period 1874 to 1954, it appears well justified to extend the

* E. W. Maunder, *Memoirs of British Astronomical Association*, Vol. XXIII, p. 57.

† R. C. Carrington, *Observations of the Spots on the Sun from November* 9, 1853, *to March* 24, 1861, *made at Redhill*, 1863.

‡ G. Spörer, *Publicationen der Astronomische Gesellschaft*, **13** (Leipzig, 1874); **13**, Fortsetzung (Leipzig 1876); *Pub. Astrophys. Obs., Potsdam*, No. 1, **1**, Part I; No. 5, **2**, Part I.

§ *Phil. Trans.*, **159**, 1, 1869; **160**, 389, 1870.

data backwards from 1874 by means of spot counts, north and south. Schwabe's published observations in *Astronomische Nachrichten* give counts for the whole disk only, so that counts of spot groups, according to hemisphere, have had to be made on the original drawings. From about 1832, these drawings were made

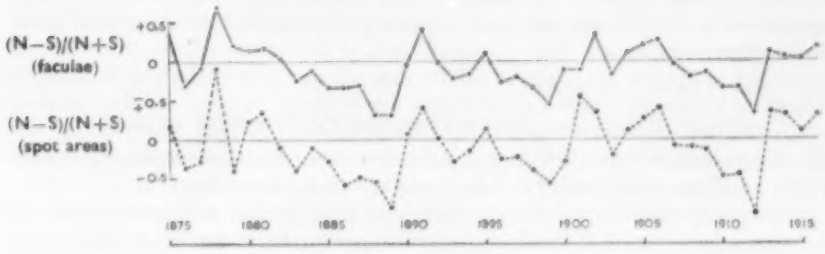

FIG. 2.—*Comparison of* $(N-S)/(N+S)$ *(faculae) (full curve) with* $(N-S)/(N+S)$ *(spot areas) (broken curve) 1875–1916.*

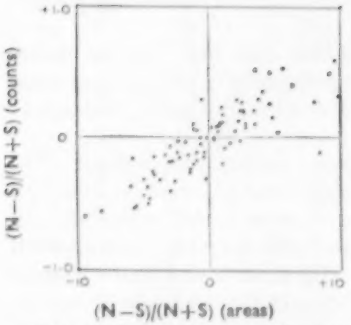

FIG. 3.—*Scatter diagram to show correlation of* $(N-S)/(N+S)$ *(spot counts) and* $(N-S)/(N+S)$ *(spot areas).*

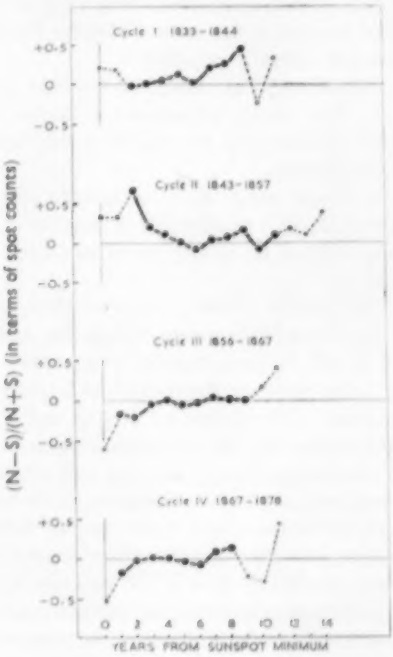

FIG. 4.—*Yearly values of* $(N-S)/(N+S)$ *(in terms of spot counts) for each of the four cycles 1833–1878. Points where* $N+S<50$ *are joined by broken lines.*

on a scale that was substantially constant, the solar disk being represented by a circle 2·1 inches in diameter. Copies of the Stonyhurst Disks reduced to the same scale were used to read off the latitudes of the spots. Permission to examine the records was kindly given by the Royal Astronomical Society. The counts

were made wholly by one of us (A. S. M.) but sample checks were made. As in the Greenwich counts, a group, whether of short or long duration, was counted once, group numbers having been assigned in the records both by Schwabe and Spörer. Counts were similarly made from the published records of Carrington, Spörer, and the Kew publications. After finding that there was satisfactory agreement of E_N over the few years common to these last three series of data, those adopted were

1833 to 1867 Schwabe,

1866 to 1878 Spörer (these overlap with the Greenwich records).

The Schwabe data from 1826 to 1832 inclusive were not used, owing to uncertainty in the position of the north point of the image on the drawings.

The yearly values of E_N thus derived from 1833 to 1878 are plotted in Fig. 4, the time origin of each of the four cycles being adopted, as before, as the year of sunspot minimum. The separation of old- and new-cycle spots has been made, according to their respective latitudes, as was done for the Greenwich data.

Discussion.—Although it is believed that a reasonably homogeneous series of data is here presented from 1833 to 1954, we prefer to discuss first the last seven 11-year cycles covered by the Greenwich observations for which the daily record is virtually complete.

Examining Fig. 1 (*a*), we see that using an index derived from areas (E_A):

1. The values are subject to rather large fluctuations. It has been shown, however, that these are real since they are reproduced by the faculae and *numbers* of spot groups.

2. If for each cycle a straight line be drawn that best fits the points (unweighted), a progressive change of slope from negative to positive (the sense being defined by taking north as positive) is apparent from Cycle 1 through to Cycle 7.

The reality of this change of slope is confirmed by Fig. 1 (*b*) and (*c*). The former displays the means of adjacent pairs of cycles (1 and 2 : 2 and 3 . . . 6 and 7), and it will be seen that the progressive change of slope is still preserved. In Fig. 1 (*c*), however, the procedure has been repeated with alternate cycles inverted (i.e. 1 and -2 : -2 and 3 : . . . -6 and 7), and a progression is no longer apparent. If these data did not represent a significant variation in the behaviour of each of the two hemispheres, then this procedure of inverting alternate cycles could not be expected to alter the character of the results obtained in Fig. 1 (*b*). Fig. 1 (*d*), which gives the mean curve for all seven cycles, is informative, especially in showing that over the period of nearly eighty years the amount of spottedness is very nearly the same in the two hemispheres throughout the averaged cycle.

3. The slowly changing pattern of E_A from cycle to cycle implies that the relative behaviour of the two hemispheres is maintained in successive cycles, with no indication of an alternation as might have been suspected from the 22-year cycle of magnetic polarities.

With these fairly definite features shown from Cycles 1 to 7 covered by the Greenwich observations of spot areas, it is obviously desirable to extend the observations backwards in time by means of the data provided by the earlier sunspot observers. The results of the differences in the ratios of spot counts $N/(N+S)$ minus $S/(N+S)$, E_N, are plotted in Fig. 4, which is directly comparable with Fig. 1 (*a*).

It seems that the progressive change of slope of E_A is not continued back in time as might have been expected if the progression in Fig. 1 (*a*) had been part of a periodic change. There is, however, one feature of interest concerning the whole series extending over 120 years, exhibited in Fig. 5. Excluding points for which N + S was less than 50, numerical values of the slope of each cycle using E_N throughout have been derived by calculating the slopes from each point to the centre of the curve and taking the mean, each point being weighted in proportion to its distance from the centre (this method, for the present purpose, is sufficiently accurate). Each of the eleven values thus obtained is plotted in Fig. 5 using full circles. In the same diagram is plotted for comparison the annual mean daily sunspot number (R) of the maximum year for the appropriate cycle. There appears to be a marked correlation between the two curves. Thus a very active cycle as defined by a high maximum (either of R or mean daily spot area) tends to be associated with a positive slope, i.e. the southern hemisphere is the more spotted at the beginning of the cycle and the northern at the end.

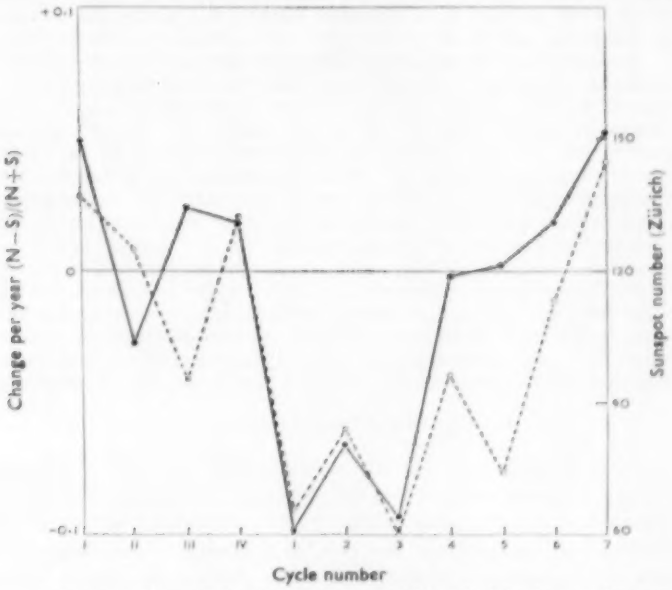

FIG. 5.—*Full curve : slopes of* $(N - S)/(N + S)$ *(counts) for each of the eleven cycles* 1833–1954. *Broken curve : annual mean sunspot number for the maximum year of each cycle.*

Conclusions.—The observational results discussed above suggest that the relative amount of spottedness of the northern and southern hemispheres of the Sun follows some pattern which cannot be accounted for in terms of the random fluctuations that would be expected in the data. This pattern does not appear, however, to be periodic. The spot areas of the homogeneous series of Greenwich photographic observations extending now over seven complete 11-year cycles suggested at first that a periodic change might be present. But on extending the observations backwards to 1833 by means of the records of the visual observers of sunspots, Schwabe, Carrington, and Spörer, the promising pattern given by the Greenwich results 1874–1954 does not appear to be continued, though the limited period (four cycles, 1833–1878) leaves this a little inconclusive.

A definite result that emerges is that over the whole period of observation (120 years) there is no suggestion of any effect related to the 22-year cycle of the magnetic polarities of sunspots. The apparent correlation between the computed slopes given by E_N values for each cycle and the height of the peak of the cycle is noteworthy.

A detailed statistical analysis of the data would be desirable to establish the degree of significance of each of the effects suggested here, and perhaps also to enquire into other possible effects given by these data. It is hoped that this note will stimulate such work.

Our thanks are due to the Astronomer Royal for permission to publish this note. We are also indebted to Mr T. Gold, Chief Assistant, for his interest and helpful discussion.

Royal Greenwich Observatory,
Herstmonceux Castle, Sussex:
1955 *March.*

INTERFEROMETRIC MEASUREMENTS OF WAVE-LENGTHS

II. Measurements at 6500 A and a general discussion of the solar red shift

M. G. Adam

(Communicated by the Director of the University Observatory, Oxford)

(Received 1955 April 18)

Summary

It has been suggested that the largest wave-length displacement of solar lines to the red will be observed for resonance lines. To test this prediction the wave-lengths of a number of lines, including the calcium inter-system resonance line $4^1S–4^3P$, have been measured in the 6500 A region by the method of circular channels. Contrary to the theoretical prediction the resonance line has the smallest red shift which has yet been observed.

This resonance line is very faint and it appears to exemplify the phenomenon (frequently referred to by Burns) of a variation in line displacement with line strength. In a discussion of the red shifts at 6500 A, together with the earlier results at 5080 A and 6020 A, it is clear that line strength is the dominating factor affecting the shifts. In order to make a quantitative examination of this effect over all wave-length regions, line strengths are expressed in equivalent " ergs ", a unit proportional to the absolute energy absorbed by the line. If Δ (milliangstroms) is the solar red shift at wave-length λ it is shown that there is a linear relation between Δ/λ^2 and the logarithm of the equivalent " ergs ", a relationship which is applicable at all wave-lengths. 158 solar red shifts measured in the Allegheny Observatory —Bureau of Standards work are analysed in exactly the same way as the 20 Oxford results. These confirm the empirical relationship over a wave-length range extended by 1000 A, and a greatly increased range of line strengths.

Introduction.—The red shift observed for the solar lines is attributed to a combination of the predicted relativity shift and possible low-pressure collisional shifts due to neutral hydrogen. The relativity shift is precisely determined as a wave-length change of 2·12 parts in 10^6, but the collisional shifts, which are of the same general order of magnitude, are so uncertain in exact magnitude and sign as to prevent any real confirmation of this theory of the solar red shifts. The least uncertain collisional shift is that for a resonance line. For such a line we should expect a collisional shift to the red (**19**), and therefore a solar red shift in this case in excess of the relativity shift.

The work now described extends the earlier measurements (**1**) to the red in a region which includes a resonance line. Section I gives an account of the determination of absolute wave-lengths for solar and vacuum-arc lines by the method of circular channels, and the results obtained. In Section II the red shifts, now determined over a considerable range in the visible spectrum, are discussed. It is found that the outstanding observational characteristic of the solar red shift is its dependence upon line strength, rather than on any other factor.

Section I

Wave-length determinations

1.1. *Region.*—In selecting a region the first requirement is that it should contain a resonance line measurable both in the solar spectrum and in the laboratory source. A study of Miss Moore's Multiplet Table (**15**) shows that while there are 60–70 resonance lines of neutral elements in the solar spectrum between 4000 and 7000 A, the number of lines possible for the present problem is nearer to 10. The resonance line finally selected was the calcium inter-system combination line $4^1S–4^3P^o$ at 6572·8 A. The line is unfortunately rather faint in the Sun (Rowland number 1), but such an inter-system line should be intrinsically narrow, and we need not fear broadening due to hyperfine structure, since ^{40}Ca, for which the nuclear magnetic moment is zero, is 97 per cent of naturally occurring calcium. The line is fairly easily obtained in the vacuum arc, the only disadvantage being again that it is somewhat faint. The region 6580 A has the very great advantage that it is close to the primary standard at 6438 A, so that uncertainties in the measured wave-lengths on account of chromatic variation of phase change, camera focal length, and shift of pattern centre are all negligible.

In the 6580 A region the lines given in the lower part of Table I have been measured in the solar spectrum. The faint water-vapour line and the faint iron lines have been included to give an idea of the accuracy obtainable, for lines of intensity comparable with that of the calcium line. The seven lines in the upper part of Table I have been measured to extend the solar observations in the red, and to give some measures of the red shift of calcium lines generally, in case of any peculiarities in the behaviour of the element. The two calcium lines in this region are the measurable lines closest to the resonance line. Columns 1, 2 and 3 in Table I are from the Rowland Revision (**23**). The next four columns are from the 1928 I.A.U. table of standard solar wave-lengths (**24**); they show the recommended wave-length, the measures of St John, of Babcock and of Burns, Meggers and Kiess in the Allegheny Observatory—Bureau of Standards work. In column 7 the A.O.–B.S. measures have been augmented by the values in brackets from the A.O.–B.S. papers (**7, 9, 10**) where the I.A.U. table has no entries.

Table I

Measured lines in the solar spectrum

Rev. Rowland Table			I.A.U.	St John	Babcock	A.O.–B.S.
El.	Int.	Wave-length in A	1928			
w.v.	1	6490·798	...	...	...	(·790)
Ca	6	6493·796	·788	...	·788	·789
Fe	8	6495·001	4·994	·994	·993	·995
Fe	2	6496·480	...	...	...	(·469)
Ba^+	4	6496·916	...	...	...	(·911)
Fe	1	6498·954	·945	...	·945	·945
Ca	4	6499·663	·654	...	·655	·654
Fe	5	6569·232	·224	...	·224	·223
Ca	1	6572·804	...	...	...	(·786)
Fe	1	6574·243	...	...	...	(·234)
w.v.	1	6574·854	...	...	...	...
Fe	2	6575·045	...	...	...	(·022)
Fe	6	6592·934	·926	...	·926	·926
Fe	4	6593·892	...	...	...	(·881)

1.2. *Observational procedure.*—The method of circular channels has been used for the determination of absolute wave-lengths in the spectrum of the Sun and for the same lines, as far as possible, in the vacuum-arc spectrum. The experimental procedure follows very closely that already described in Paper I (**1**).

The dispersion of the Oxford prism spectroscope has dropped to 0·5 mm A^{-1} at 6550 A, and moreover we should expect the slit pattern to be broadened relative to the dispersion compared with the instrumental performance at shorter wave-lengths (**6**). Both factors increase the range of wave-lengths presented to the etalon in the slit image. It is not practicable to work with a spectroscope slit width much less than 0·1 mm on account of exposure times and the narrowing of the heterochromatic channels in which the absorption lines must be measured. This means that a 2·5 mm spacer is the longest it is permissible to use in the interferometer without serious scatter from order to order (**20**); even shorter spacers are desirable from this point of view.

Work was also attempted with a 1·5 mm spacer, and a full discussion of these results, which proved to be unreliable, is given in Paper III (to follow). For the reasons there explained, errors in the absolute wave-lengths measured with a 2·5 mm spacer and longer are likely to be small, and errors in the red shifts only accidental. The measurements at 6580 A, the region of the resonance line, were repeated after the work described in Paper III was done. For the lines 6569·2, 6592·9 and 6593·9 A which are measurable with fair certainty, the differences in the red shifts obtained by the original and by the improved procedure were less than 0·001 A. The slight changes in the experimental arrangements from those described in Paper I (**1**) are discussed in Paper III.

The results now given were all obtained with a 2·5 mm spacer, with interferometer plates silvered to give just over 90 per cent reflection in the red. The plate silverings for the 6580 A region were slightly heavier than for the 6490 A region.

Solar plates.—The solar exposures were all obtained at the centre of the 180 mm image in focus at the spectroscope slit. With slit widths from 0·08 mm to 0·10 mm the exposure times at 6580 A were 8–12 minutes on Ilford Rapid Process Panchromatic plates. The sensitivity of these plates is falling off quite rapidly at this wave-length, but there is very little difference in sensitivity between the I.R.P.P. plates and Astra 7 or Astra 8, which were also tried. In the 6490 A region with a slit width of 0·09 mm the exposure times were 1½–2 minutes on the I.R.P.P. plates. Kodak Press Contrast developer was used throughout. The plates for the 6490 A region were obtained in 1952 August, and those used for the 6580 A region in 1954 April and August.

Vacuum-arc plates.—Whenever possible the lines given in Table I were measured also in the vacuum arc. The vacuum-arc wave-lengths measured at Allegheny Observatory for the lines of Table I are given in Table II, together with King's intensity estimates. The iron lines have been measured by Burns and Walters (**11**), the calcium measures are those of Wagman (**21**).

With our experimental arrangements an iron line of arc intensity 2 is on the limit of measurability. Some vacuum-arc measures have been made for the line 6575·045 A in Table I (this is a line of King's estimated intensity 2) but only a computed value is given by Burns and Walters. With the arc conditions we aim at, i.e. a pole separation of not less than 10 mm, currents not exceeding 8 amp. and pressures of a few cm of mercury, exposures of 4–5 hours are barely sufficient for such lines. For the faint arc lines in the 6580 A region the exposure

times were reduced for some plates by using the spectroscope undiaphragmed (17). In the 6490 A region only the strong iron line at 6494·981 A has been measured, the exposure time required being only 5 min; the fainter line at 6496·464 A was not visible on these plates.

The definitive calcium arc plates were obtained using graphite or carbon pole-pieces, the positive pole cored and filled with calcium chloride. The arc so produced would not always draw out to the full 10 mm, and for the calcium plates the pole separation was 6–10 mm. For the strong calcium lines at 6490 A the exposure times were less than 2 min, but at 6580 A, for the resonance line, with slightly heavier silvering on the interferometer plates, about one hour was required with the diaphragmed spectroscope and approximately 20 min with the diaphragm removed. Some of the earlier work was done with a rod of calcium metal in a copper holder as the positive pole-piece and a copper negative pole-piece. This was a much more convenient source to use than the calcium salt, but calcium metal in a form suitable for turning is not easy to procure, and at 6490 A there is a possibly overlapping copper line.

TABLE II

Vacuum-arc lines

(*Allegheny Observatory measured wave-lengths*)

Iron lines		Calcium lines	
Wave-length in A	Int.	Wave-length in A	Int.
6494·981	25	6493·780	80
6496·464	5	6499·649	30
6569·215	5		
6592·913	10	6572·781	8
6593·875	4		

A rotary vacuum oil pump was used to maintain the pressure in the arc at 5 cm of mercury or less, as read by a closed-arm U-type mercury gauge mounted on the arc. The readings of such a gauge are subject to uncertainty owing to the possible presence of condensable vapours in the closed limb. The gauge was therefore tested by means of an absolute aneroid type gauge; this showed that the pressures actually used had been about 8 cm of mercury when the arc was cold, rising to 14 cm when it became hot.

Ilford HP3 plates and Kodak Press Contrast developer were used for all the arc spectra. The arc plates at 6490 A were obtained in 1952 August and those at 6580 A in 1954 July and August.

1.3. *Plate measurement and reduction.*—The plates were measured on the Cambridge machine fitted with a rotary stage as already described (1). A modification of the rotating table has been made which considerably eases the subsequent reduction of the measures. It enables the cadmium pattern centre O (see Fig. 1) to be brought within a few thousandths of a mm over O′, the centre of rotation of the table. The plate is clamped to an upper stage which can be turned by means of a tangent screw over a lower stage to which it is pinned. The lower stage is itself pinned to the rotating table and can be turned over it by a tangent screw with a motion perpendicular to that of the upper stage. These motions

are used to secure that the four arcs of any one cadmium ring have very closely the same setting when they are turned into the line of travel of the microscope. In this way the distance $OO'(\rho)$ can easily be reduced to under 0·01 mm. This means that the difference between the micrometer settings of the two positions in which any one arc cuts the line of travel of the microscope is, very nearly, the true diameter of the interference ring, assuming no shift of pattern centre. A small correction depending on ρ and the distance of the spectrum line from O may be necessary, but the solution of a triangle for each measured arc is no longer required, and angular readings for the arcs are not necessary, except for identification purposes.

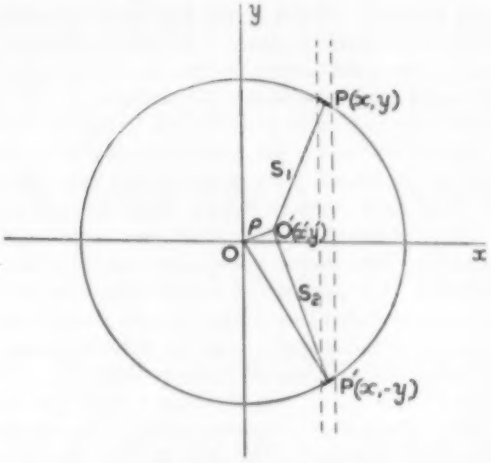

FIG. 1.—*Plate reduction.*

The reduction now proceeds as follows. Suppose we have a system of rectangular coordinates with origin at the cadmium pattern centre O, and x-axis along the arms of the cadmium cross which lie parallel to the spectroscopic dispersion. Any spectrum line then lies approximately parallel to the y-axis, and we suppose that two arcs of the line interference pattern lie at P and P′, (x, y) and $(x, -y)$. From the measures in the cadmium pattern we can determine O′, the centre from which the measures have been made. Let O′ have coordinates (x', y') and let the measured distances O′P, O′P′ be s_1 and s_2. Assuming that O is also the centre of the line pattern, as we may for this region so close to the cadmium red line, then the diameter D of the ring of which P and P′ are parts is given by

$$D^2 = 2 \cdot OP'^2 = 2s_1 \cdot 2s_2 + \tfrac{1}{2}(2s_1 - 2s_2)^2 - 4\rho^2 + 2x \cdot 4x'.$$

Because O′ is very close to O the second and third terms are negligible, and we get

$$D^2 = 2s_1 \cdot 2s_2 + 2x \cdot 4x'.$$

Our measures give $2s_1$ and $2s_2$ directly. In the very small correction term, $4x'$ comes immediately from the measures in the cadmium pattern arms lying along the x-axis ($4x'$ is $2\Delta r$ in Paper I, Section 2.1 (1)), and the x-coordinate of the spectrum line need only be known very approximately. We note further that the correction term is constant for all the rings of any one line, for a given O′.

The rest of the reduction follows exactly as described in Paper I with the considerable simplification that we have no corrections for the chromatic variation of phase change or camera focal length.

1.4. *Observed wave-lengths.*—The absolute wave-lengths obtained for the absorption lines are given in Table III. The solar lines have been corrected for diurnal rotation and the Earth's orbital motion. The wave-lengths are mean values for the 18 mm spectroscope slit height and refer to a line of points extending over 0·1 of the solar diameter at the centre of the disk. The measures have all been made with a 2·5 mm spacer (approximate order of interference 8100). At 6490 A the lines fall close together and in the 'normal' position they were all measured on the violet side of the pattern centre (the same side as the centre of the heterochromatic fringes). Plates A412, A413 were obtained with the lines shifted to the red side of the pattern centre. At 6580 A the lines in the 'normal' position fall on both sides of the pattern centre and the measured plates were all obtained with only slight variations about this position.

Wave-lengths are given to 0·001 A in Table III, though all the reductions have been carried through to 0·0001 A; the means in column 3 and the standard deviations of the mean in column 4 are based on the four-figure values for the individual plates. The faint lines at 6580 A were very difficult to measure; we note that the plates obtained in 1954 April give wave-lengths in the mean 0·002 A longer than those from the 1954 August plates (or 0·001 A longer for the better-determined lines). On the basis of the investigations described in Paper III, the April values are somewhat less reliable than the August values. The mean wave-length in column 3 is the straight mean for the nine plates.

The wave-lengths for the arc lines are given in Table IV. These again were all obtained with the 2·5 mm spacer. In the 6490 A region the first two columns of the individual plate values were measured in the 'normal' position, and the last three in the 'shifted' position. The lines at 6580 A were all measured in the normal position. The plate values in the first two columns at 6580 A were obtained with the diaphragmed spectroscope and those in the last four columns with the full aperture. It will be seen that there is no change in the measured wave-lengths on this account.

Comparing the mean values in Tables III and IV with those in Tables I and II, we see that the solar wave-lengths now obtained are on the average 0·001 A shorter than Babcock's values, and than the A.O.–B.S. values. The seven arc wave-lengths average 0·002 A shorter than the Allegheny Observatory values, though the differences are somewhat erratic. We should have expected the rather higher pressures now used in the vacuum arc to have resulted in longer wave-lengths rather than in shorter ones.

Section II

A general discussion of the solar red shift in different spectral regions

2.1. *An analysis of the results so far obtained.*—We have now measured absolute wave-lengths for solar lines and vacuum-arc lines over the wave-length range 5080 A–6580 A, and in this section we will consider the red shifts shown by the solar lines. The results from Paper I and those now given in Section I are collected together in Table V. Columns 1, 2 and 3 give the element, Rowland number and identifying wave-length for the line. The next two columns are from Miss Moore's 1945 Multiplet Table (**16**) and give the multiplet number of the line and the excitation potential in volts of the lower state involved in the transition.

TABLE III

Measured wave-lengths in the solar spectrum (individual plate values)

Date 1952 and plate No.				Aug. 21·39	Aug. 21·41	Aug. 23·45	Aug. 23·48	Aug. 23·54	Aug. 23·55			
El.	Row. Int.	Mean obs. wave-length in A	Standard deviation of mean	A399	A400	A412	A413	A414	A415			
w.v.	1	6490·790	± 0·0007	·791	·788	...	...	·791	·791			
Ca	6	6493·788	0·0006	·786	·786	·790	·787	·789	·789			
Fe	8	6494·992	0·0006	·994	·991	·994	·991	·992	·993			
Fe	2	6496·471	0·0005	·473	·471	·470	·472	·471	·473			
Ba+	4	6496·908	0·0005	·909	·907	·909	·907	·907	·909			
Fe	1	6498·944	0·0006	·942	·942	·943	·944	·944	·946			
Ca	4	6499·655	0·0007	·654	·652	·656	·653	·656	·656			
Date 1954 and plate No.				April 7·46	April 7·49	April 8·48	April 10·50	Aug. 14·52	Aug. 14·57	Aug. 16·38	Aug. 16·65	Aug. 16·68
El.	Row. Int.	Mean obs. wave-length in A	Standard deviation of mean	A705	A706	A716	A722	A777	A778	A780	A783	A784
Fe	5	6569·221	± 0·0004	·221	·223	·223	·222	·221	·220	·220	·220	·220
Ca	1	6572·783	0·0010	·788	·782	·785	·786	·781	·780	·782	·780	·780
Fe	1	6574·230	0·0007	·232	·230	·233	·233	·231	·228	·229	·227	·230
w.v.	1	6574·848	0·0004	·849	·849	·849	·851	·848	·847	·847	·847	·848
Fe	2	6575·023	0·0005	·024	·023	·024	·025	·023	·021	·024	·022	·022
Fe	6	6592·925	0·0007	·925	·924	·925	·925	·922	·922	·930	·925	·924
Fe	4	6593·884	0·0008	·883	·883	·886	·885	·882	·879	·884	·884	·886

TABLE IV

Measured wave-lengths in the vacuum arc (individual plate values)

Plate No. {Fe / Ca				A422a A395a	A422b A395b	A434a A432	A434b A433a	A435 A433b	
El.	Row. Int.	Mean obs. wave-length in A	Standard deviation of mean						
Ca	6	6493·777	± 0·0004	·777	·776	·777	·779	·777	
Fe	8	6494·980	0·0003	·980	·981	·980	·980	·981	
Ca	4	6499·645	0·0001	·645	·644	·645	·645	·645	
Plate No. {Fe / Ca				A750 A752	A753 A754	A760 A765	A767 A766	A772 A773	A775 A776
El.	Row. Int.	Mean obs. wave-length in A	Standard deviation of mean						
Fe	5	6569·216	± 0·0004	·218	·216	·216	·215	·216	·216
Ca	1	6572·778	0·0002	·778	·778	·778	·779	·777	·778
Fe	2	6575·017	0·0008	...	...	...	·015	·017	·018
Fe	6	6592·913	0·0004	·913	·913	·912	·911	·914	·913
Fe	4	6593·869	0·0003	·868	·868	·870	·868	·868	·870

Column 6 gives the fractional angstroms of the measured arc wave-length. As we saw in Section 1.2, the pressure estimated for the vacuum arc is of the order $\frac{1}{8}$ of an atmosphere, and this is applicable to the earlier as well as to the present measures. The line shift at such a pressure does not often exceed 0·001 A, but it is nevertheless desirable to correct the results for the small pressure shift as far as is possible. In order to estimate the correction we have used Babcock's systematic study of the shifts in iron lines between the vacuum-arc and the arc with pressures up to one atmosphere (**5**). Babcock found that the shifts were always to the red as the pressures increased, and he derived an empirical relation between the depression d (cm^{-1}) per atmosphere of a spectral term and the excitation potential V (volts) of the term. For triplet terms he deduced the relation $d = 1{\cdot}15V^2 - 1{\cdot}93V$, and for quintet and septet terms $d = 1{\cdot}15V^2 - 1{\cdot}27V$. The shift for any line is given by the difference between the depressions for the two terms involved in the transition. Such an observational relation is really necessary for each element individually, but for the small pressure correction now required we have used Babcock's results for the iron lines for the calcium and manganese lines as well. Some pressure shifts have been given by Monk (**14**) for a number of manganese lines: they are of the same order of magnitude as those now used. For the calcium lines no such measures appear to be available. Corrections ranging from zero to 0·0018 A have been applied to the measured arc wave-lengths to give the corrected vacuum-arc wave-lengths in column 7.

Column 8 of Table V gives the measured solar wave-length, and the difference between column 8 and column 7 gives the observed solar red shift in column 9. This quantity, expressed in milliangstroms, we will denote by Δ in the discussion following. The line equivalent width in column 10 is that given by Allen (**2**); it is his value in mA derived from r_b the central intensity of the line corrected for blending.

TABLE V

The solar red shift

El.	Row. Int.	Wave-length in A	Mult. No.	Ex. Pot. in volts (low)	Meas. arc wave-length	Vac.-arc wave-length	Meas. sol. wave-length	Red shift in mA Δ	Eq. width (Allen) mA	Factor for equiv. "ergs"	Equiv. "ergs"
Fe	5	5068·8	383	2·93	·7609	·7600	·7696	9·6	130	0·985	128
Fe	5	5074·7	1094	4·20	·7446	·7436	·7564	12·8	106	0·984	104
Fe	3	5078·97	1092	4·28	·9722	·9710	·9792	8·2	88	0·983	86
Fe	4	5079·2	66	2·19	·2202	·2195	·2291	9·6	106	0·983	104
Fe	4	5079·7	16	0·99	·7367	·7363	·7461	9·8	104	0·983	102
Fe	4	5083·3	16	0·95	·3340	·3336	·3440	10·4	111	0·982	109
Fe	6	6008·6	982	3·87	·5576	·5564	·5648	8·4	86	0·792	68
Mn	6	6013·5	27	3·06	·4880	·4870	·4946	7·6	76	0·791	60
Mn	6	6016·6	27	3·06	·6385	·6375	·6448	7·3	92	0·790	73
Mn	6	6021·8	27	3·06	·7949	·7939	·8000	6·1	92	0·789	73
Fe	7	6024·1	1178	4·53	·0574	·0558	·0657	9·9	106	0·789	84
Fe	4	6027·0	1018	4·06	·0503	·0491	·0558	6·7	61	0·789	48
Ca	6	6493·8	18	2·51	·7773	·7765	·7878	11·3	148	0·704	104
Fe	8	6494·98	168	2·39	·9804	·9794	·9923	12·9	176	0·704	124
Ca	4	6499·6	18	2·51	·6448	·6440	·6546	10·6	92	0·703	65
Fe	5	6569·2	1253	4·71	·2160	·2142	·2212	7·0	78	0·691	54
Ca	1	6572·8	1	0·00	·7781	·7781	·7827	4·6	33	0·690	23
Fe	2	6575·0	206	2·58	·0168	·0160	·0230	7·0	60	0·690	41
Fe	6	6592·9	268	2·72	·9127	·9118	·9247	12·9	112	0·686	77
Fe	4	6593·9	168	2·42	·8688	·8678	·8835	15·7	74	0·686	51

The first effect we look for in the results is a change in the red shift with wave-length such as is predicted on the relativity theory. An inspection of the table shows, however, that there is no correlation of the mean shift in each region with the wave-length of the region. The mean shifts for the wave-length groups are 10·1 mA at 5080 A, 7·7 mA at 6020 A, 11·6 mA at 6490 A and 9·4 mA at 6580 A. Nor is there any obvious dependence of the red shift on excitation potential. We note that the calcium resonance line $4^1S–4^1P^o$ at 6572·8 A, which from Spitzer's prediction should have the largest red shift as a result of the relativity shift and a red collisional shift, has in fact the smallest value of Δ measured. The dominant feature of the results is the change in red shift with line strength, and this shows to some extent within each wave-length group. The number of lines in any one group is too few, and the observational uncertainty of the red shift of a single line too great, to derive a relation between line strength and red shift at any one wave-length; we must therefore discuss the results obtained in the different spectral regions simultaneously.

The equivalent width of a line in milliangstroms (or in cm^{-1}) is a variable unit in which to express line strengths, because it refers to the continuous background intensity which changes with the wave-length region. If we express the strength of a line in absolute units of energy absorbed from the continuous spectrum, then we have a unit which has at least the same physical significance at all wave-lengths. We have therefore expressed line strengths in a unit which we will call equivalent "ergs", by allowing for the variation in the continuous background intensity. Column 11 in Table V gives the ratio of the continuous spectrum intensity $I_\lambda(0)$ at the line wave-length λ to that at 5000 A, using Minnaert's table (**13**) of the observed normal monochromatic intensity $I_\lambda(0)$ per $d\lambda = 1$ cm. The equivalent "ergs" in column 12 of Table V are obtained by multiplying the equivalent width in column 10 by the factor in column 11. The absolute magnitude of the line strength unit is for our purpose quite arbitrary; we have aimed at using a unit of the same order of magnitude as the familiar equivalent width in milliangstroms, and the two units are in fact equal at 5000 A.

Fig. 2 shows a plot of Δ, the red shift in mA, against the logarithm of the equivalent "ergs". We see that there is a reasonably well-defined increase of Δ with line strength, though the scatter of the points is quite considerable. Assuming a linear relation between the two quantities the computed correlation coefficient is +0·509. The corresponding significance level is very nearly 0·02 (**12**), that is, there is a probability of $\frac{1}{50}$ that a coefficient of this size would result purely from chance. The two regression lines for the distribution are shown in the figure.

A wave-length dependence of Δ would show in Fig. 2 by the systematic departures of the Δs in the different spectral regions from the mean curve, and there is some indication of such an effect. If Δ is proportional to wave-length λ (as on the relativity theory or for a Doppler shift) then we should expect to reduce the scatter of the points by plotting Δ/λ against line strength instead of Δ. Fig. 3 shows Δ/λ (λ also in milliangstroms) plotted against log equivalent "ergs". There is obviously some reduction in the scatter of the observed points. The computed regression lines shown in Fig. 3 are much closer together and the correlation coefficient is now +0·683, corresponding to a significance level better than 0·001. In Fig. 3 the relativity shift corresponds to $\Delta/\lambda = 21{\cdot}2 \times 10^{-7}$.

We conclude then that Δ is dependent upon wave-length as well as upon line strength, though in an empirical approach we can only guess at the form of the two dependences. If we next assume that Δ is proportional to λ^2 and plot Δ/λ^2 we are expressing the shift in units proportional to frequency; Fig. 4 shows Δ/λ^2(in cm^{-1}) plotted against log equivalent "ergs", with the computed regression lines. This again reduces the scatter in the observed points from that in Fig. 2, the correlation coefficient is +0·737, higher than for the Δ/λ plot.

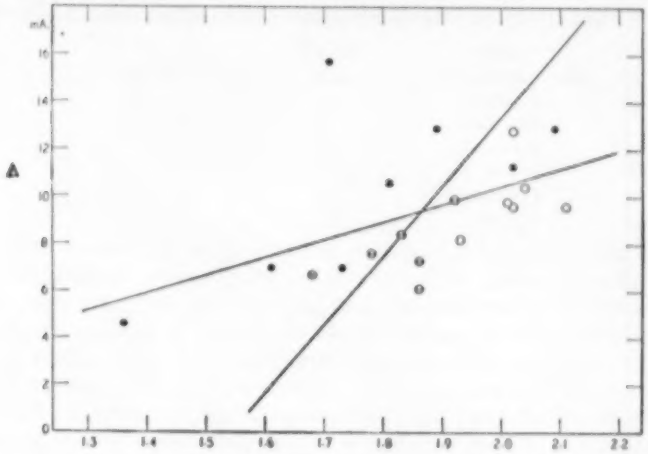

FIG. 2.—*Red shift Δ as a function of log equivalent "ergs". Open circles: lines of wave-length less than 5100 A. Barred circles: lines of wave-length between 5100 A and 6100 A. Filled circles: lines of wave-length greater than 6100 A.*

2.2. *Comparison with the A.O.–B.S. results.*—The existence of a relationship between red shift and Rowland number in individual spectral regions has been several times pointed out in the A.O.–B.S. papers (**7, 9, 10**). The use of Rowland numbers to express line strengths obscures the fact that there is a relationship common to all regions, since the strength of lines of the same Rowland number is now known to vary considerably in different regions of the spectrum. Burns regarded the intensity effect in the red shift as an insuperable obstacle to accepting the predicted relativity shift as established for the solar lines (**8**). The intensity effect is also to be found in the work of St John (**18**) who interpreted it as originating from motions in the different photospheric levels. What is new in the present discussion is that the relationship we have found is common to all wave-length regions, and within the observational scatter is a linear one between Δ/λ^2 and the logarithm of the absorbed energy. It is obviously important to see if this relationship is also to be found in the earlier results.

The A.O.–B.S. papers and the paper by St John both contain large numbers of measured red shifts with which the present results may be compared. St John's material is, however, more heterogeneous than that of the A.O.–B.S. workers; his solar wave-lengths are means of grating measures by himself and interferometric measurements by Babcock, and the vacuum-arc wave-lengths are obtained, some using a vacuum arc and some from the air arc with corrections to a vacuum

source. Burns, Meggers and Kiess give red shifts from wave-lengths interferometrically measured in the solar spectrum and in the vacuum-arc spectrum. The same experimental arrangement and procedure are used for all regions of the solar spectrum and the same technique for the vacuum-arc spectra. Their material should undoubtedly be homogeneous and for the purpose of this comparison we have accordingly used the A.O.–B.S. results. The solar spectrum in the A.O.–B.S. work is that of the integrated disk; there are possible small differences between integrated-disk wave-lengths and centre-of-disk values (**25**), so that we should not necessarily expect quantitative agreement with the Oxford results.

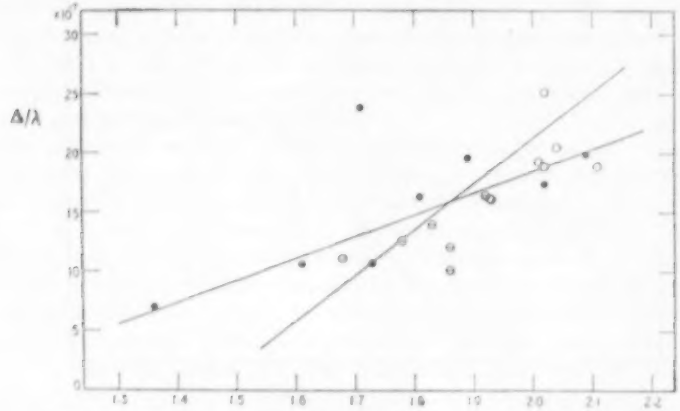

FIG. 3.—*Δ/λ as a function of log equivalent "ergs". Symbols as in Fig. 2.*

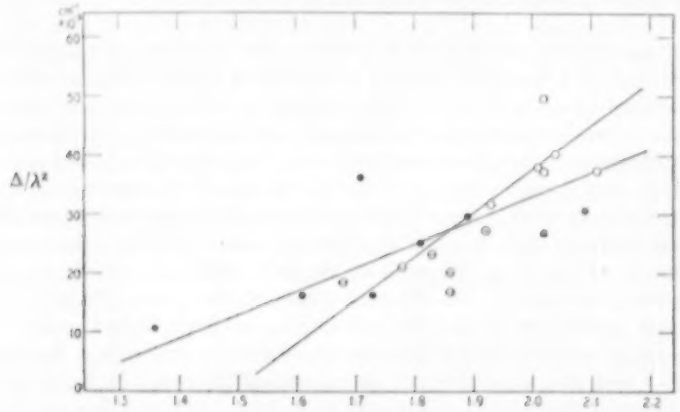

FIG. 4.—*Δ/λ^2 as a function of log equivalent "ergs". Symbols as in Fig. 2.*

From the tables on pp. 112, 130, 142 in *Publications of the Allegheny Observatory* VI, VII, VIII, all the unblended lines of neutral elements were listed for which a red shift is given in these tables and an equivalent width in Allen's tables. The A.O.–B.S. lines of weight *D* were omitted since the estimated uncertainty in the solar wave-lengths is more than 1 part in 3×10^6.

The equivalent widths were taken from Allen's tables as follows: 3978–4300 A (**4**), 4277–6600 A (**2**), and 6600–6768 A (**3**). This procedure gives 158 lines with measured red shifts and equivalent widths, namely 131 Fe, 12 Ca, 6 Ti, 5 Ni and 4 Mn. The distribution in wave-lengths and in equivalent widths is shown in Table VI. These results may be analysed in exactly the same way as the 20 entries in Table V. The equivalent widths given in milliangstroms were again expressed in equivalent "ergs".

TABLE VI

Lines providing measured red shifts from the A.O.–B.S. tables

Wave-length range in A	No. of lines	Range of equivalent widths
3977–4500	39	82–749 mA
4500–5000	21	68–166
5000–5500	19	76–132
5500–6000	14	26–137
6000–6500	59	21–245
6500–6768	6	74–130

Our first comparison is for identical lines in the A.O.–B.S. and the Oxford results. Red shifts are not given in the A.O.–B.S. tables above for the lines 5078·97, 5079·2, 6572·8 and 6575·0 A; our comparisons are therefore with the remaining sixteen lines of Table V which are common to both series of measures. For these sixteen lines correlation coefficients are shown in Table VII together with the corresponding Oxford results. The abscissae in each of the plots to which the coefficients refer are log equivalent "ergs", and the respective ordinates are given at the top of the columns. Fig. 5 shows the Δ/λ^2 scatter diagram for the 16 A.O.–B.S. observations, together with the regression lines. The significance level, for the correlation coefficient +0·643 for the 16 lines, is between 0·01 and 0·001.

TABLE VII

Correlation coefficients from the A.O.–B.S. and the Oxford observations

	Δ	Δ/λ	Δ/λ^2
A.O.–B.S. 16 lines	+0·560	+0·625	+0·643
Oxford 20 lines	+0·509	+0·683	+0·737

The A.O.–B.S. results thus confirm the observational relation deduced from the Oxford measures, with a rather larger scatter of the observed points.

It may be objected that the results we have obtained are due to the individual peculiarities of the lines we have selected, and the confirmation from 16 A.O.–B.S. results does not meet the point. In order to test the generality of the relation between Δ/λ^2 and line strength we have examined the whole of the A.O.–B.S. results, which multiplies the number of lines by nearly 10, and extends the wave-length range by 1000 A. Fig. 6 shows for the 158 points the relation between Δ/λ^2 and log equivalent "ergs". We see that 90 per cent of the lines fall in the range of line strengths we have already covered. In order that the few stronger lines, which greatly increase the range in log equivalent "ergs", should not influence the result we have calculated the correlation coefficient and regression lines for log equivalent "ergs" only up to 2·2, since the strongest line in Table VII falls in the interval 2·1–2·2. The calculated correlation

coefficient is +0·504, which for the 141 points used indicates for our empirical relation a significance level better than 0·001. The regression lines are shown in Fig. 6 (by a broken line beyond the range for which they were computed). The y on x regression line, which is based on the assumption of errors only in Δ/λ^2, is probably the significant one in this case; it will be seen that this line (the less steep one in Fig. 6), which has been computed for the weaker lines, also fits the strong lines very well. The smaller correlation coefficient for the 141 points indicates a larger scatter for them than for the 16 A.O.–B.S. points in Table VII, possibly a consequence of unsuspected blends in the solar lines.

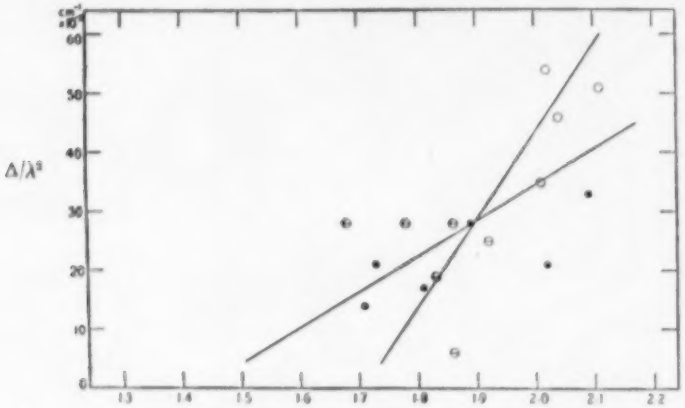

FIG. 5.—*Δ/λ^2 as a function of log equivalent "ergs". A.O.–B.S. measurements for identical lines. Symbols as in Fig. 2.*

The strongest lines in Fig. 6 nearly double the range over which we may examine the relation between Δ and line strength; they should moreover be less affected by blends than the weaker lines. In order to make use of them to the greatest advantage we have used the 9 strongest lines from Fig. 6 together with the 16 identical lines from Table VII which we believe to be reasonably free from blends. For these 25 lines (using all A.O.–B.S. results) the plot of Δ/λ against log equivalent "ergs" gives a correlation coefficient of +0·785, and the plot of Δ/λ^2 against log equivalent "ergs" a correlation coefficient of +0·882. Fig. 7 shows the latter plot with the computed regression lines; the dotted line is the regression line (y on x) for the Δ/λ^2 plot of the 20 Oxford lines.

2.3. *Conclusion.*—For the change of red shift with line intensity, we have found a well-defined functional form applicable at all wave-lengths. The differential shift between weak and strong lines is larger than the absolute shift we should expect either from the relativity theory or from collisional shifts. Observationally the intensity effect is the most important result and the one we should try to interpret first. The quantity Δ/λ^2 appears to be the most significant one in the increase of red shift with line strength, and this suggests that the solar red shift arises from the displacements of atomic energy levels which vary as the ratio of the line absorption coefficients. In so far as the abundances and excitation potentials of the different elements involved are comparable, the displacements vary as the ratio of the atomic absorption coefficients.

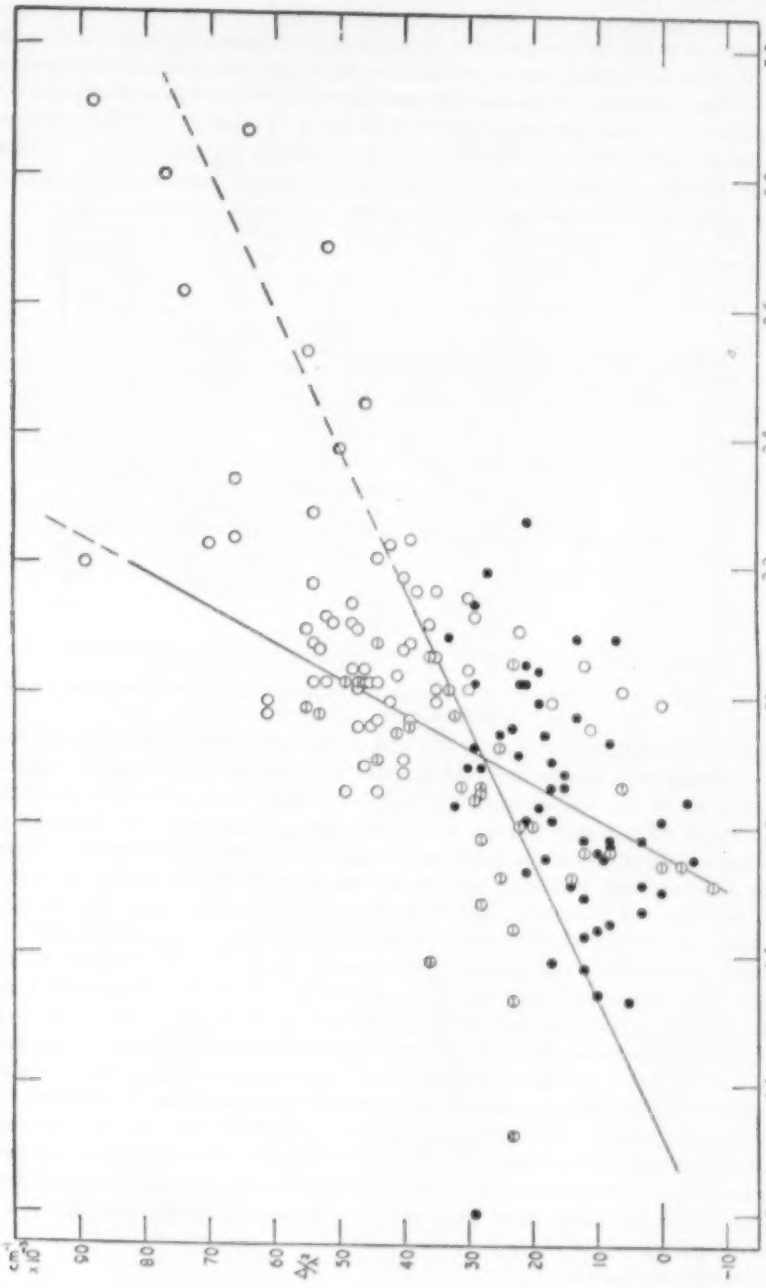

FIG. 6.—$\Delta\lambda/\lambda$ as a function of log equivalent "exp" for all the A.O.-B.S. measured red shifts. Symbols as in Fig. 2.

In view of the observational results we must conclude that our approach to the problem of the solar red shift should still be largely empirical. It is essential to determine as precisely as possible the intensity and wave-length variations in Δ. In particular we require more information about the red shifts of the stronger lines. The behaviour of the few stronger lines which have been included in our discussion is in good agreement with that of the weaker lines, but these stronger lines are all confined to the violet region of the spectrum and the strongest of them is only Rowland number 10. Observations of strong lines in other spectral

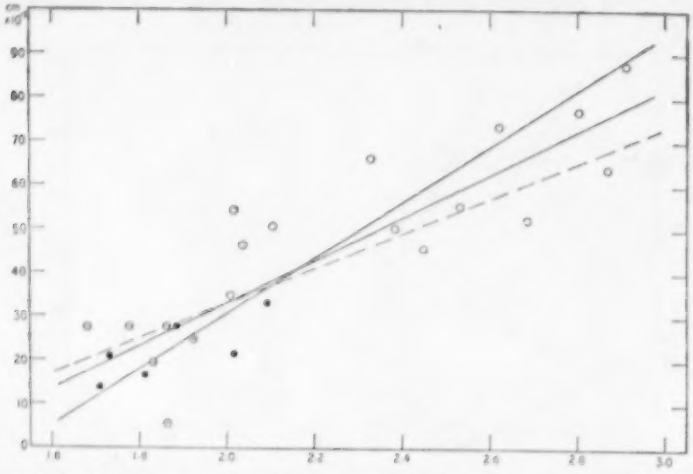

FIG. 7.—*A.O.–B.S. measurements. Δ/λ² as a function of log equivalent "ergs" for identical lines and stronger lines. Symbols as in Fig. 2.*

regions are needed, and moreover the red shifts measured by Miss Warga (**22**) for the strong magnesium lines are anomalous. For the wave-length variation we have not, in the visible region, a very large range from which to detect the rather small wave-length change in Δ. We can only improve the situation by reducing as far as possible the accidental errors in the measured red shifts. Some of the observational scatter in the results we have discussed arises, no doubt, from unsuspected blends in the solar spectrum, possibly from the peculiar behaviour of individual elements and factors other than wave-length and line strength which affect red shifts. The smaller scatter of the Oxford results (Table VII) suggests, however, that accidental errors of measurement are responsible for at least some of the large scatter of the A.O.–B.S. results in Fig. 6. The method of circular channels apparently gives increased accuracy of measurement, and the paper to follow suggests improvements in technique which should give wave-lengths with an accuracy as great as the nature of the lines allows.

Acknowledgments.—The observational and theoretical aspects of this work have been constantly discussed with Professor Plaskett and I gratefully acknowledge his help. I should also like to thank Miss B. Oliver for some computational assistance, and the Lady Anne Pery and Dr Hindmarsh for silvering the interferometer plates.

University Observatory,
Oxford:
1955 *April* 16.

References

(1) M. G. Adam, *M.N.*, **112**, 546, 1952; *Comm. Univ. Obs. Oxford*, No. 36.
(2) C. W. Allen, *Mem. Comm. Solar Obs.*, **5**, 1934.
(3) C. W. Allen, *M.N.*, **96**, 843, 1936.
(4) C. W. Allen, *Mem. Comm. Solar Obs.*, **6**, 1938.
(5) H. D. Babcock, *Ap. J.*, **67**, 240, 1928.
(6) R. J. Bray, *M.N.*, **114**, 540, 1954; *Comm. Univ. Obs. Oxford*, No. 45.
(7) K. Burns, *Publ. Alleg. Obs.*, VI, 141, 1927.
(8) K. Burns, *J.O.S.A.*, **20**, 216, 1930.
(9) K. Burns and C. C. Kiess, *Publ. Alleg. Obs.*, VI, 125, 1927.
(10) K. Burns and W. F. Meggers, *Publ. Alleg. Obs.*, VI, 105, 1927.
(11) K. Burns and F. M. Walters, *Publ. Alleg. Obs.*, VI, 159, 1929.
(12) R. A. Fisher and F. Yates, *Statistical Tables*, p. 42, London, 1943.
(13) M. Minnaert, *The Sun* (ed. G. P. Kuiper), p. 95, Chicago, 1953.
(14) G. S. Monk, *Ap. J.*, **57**, 222, 1923.
(15) C. E. Moore, *A Multiplet Table of Astrophysical Interest*, Princeton, 1933.
(16) C. E. Moore, *A Multiplet Table of Astrophysical Interest*, rev. ed., Princeton, 1945.
(17) H. H. Plaskett, *M.N.*, **112**, 177, 1952; *Comm. Univ. Obs. Oxford*, No. 33.
(18) C. E. St John, *Ap. J.*, **67**, 195, 1928.
(19) L. Spitzer, *M.N.*, **110**, 216, 1950.
(20) P. J. Treanor, *M.N.*, **109**, 389, 1949; *Comm. Univ. Obs. Oxford*, No. 28.
(21) N. E. Wagman, *Univ. Pittsburg Bull.*, **34**, 1, 1937.
(22) M. Warga, *Publ. Alleg. Obs.*, VI, 151, 1928.
(23) *Revision of Rowland's Preliminary Table*, Mount Wilson, 1928.
(24) *Trans. I.A.U.*, III, 93, 1928 (Table IV).
(25) *Trans. I.A.U.*, IV, 62, 1932.

INTERFEROMETRIC MEASUREMENTS OF WAVE-LENGTHS

III. A NOTE ON OBSERVATIONAL TECHNIQUE IN THE METHOD OF CIRCULAR CHANNELS

M. G. Adam

(Communicated by the Director of the University Observatory, Oxford)

(Received 1955 August 29*)

Summary

While the method of circular channels has unique advantages for wave-length measurements, it is more sensitive to errors due to irregularities in the interferometer plates, than is the usual method of parabolic channels. The experimental arrangement is examined from this point of view, and it is shown that by slight changes in the original set up errors in the absolute wave-lengths due to plate irregularities, can be reduced to less than 0·001 A.

To obtain interference fringes of absorption lines in a continuous spectrum relatively free from inter-order scatter, Treanor (**5**) has shown that the slit pattern of the auxiliary spectroscope should be considerably narrower than the range of the interferometer. The high spectroscopic resolution thus required is necessarily associated with high dispersion, and this in turn makes it impossible, in any conventional arrangement, to photograph simultaneously the fringes of the cadmium primary standard line and the fringes of absorption lines in a different spectral region, except by the use of an auxiliary camera. Treanor's interferometric method of circular channels may, however, be adapted (**1**) to overcome this serious limitation in measuring wave-lengths, and all the wave-lengths determined at Oxford since 1949 have been measured directly against the primary standard. In this sense the solar wave-lengths fulfil for the first time the most essential requirement of secondary standards.

Simultaneity of exposure of the standard and the unknown lines requires, however, photographic equality of the illumination from the two sources. In the experimental arrangement so far used, the equality has only been achieved at the cost of using a larger area of the interferometer plates for the cadmium light than for the solar (or arc) light. Fig. 1 (*a*) shows the optical trains for the cadmium and solar light as used since 1952 ; the arrangement differs very little from that already described in Paper I (**1**). A diaphragm D_2 in front of the cadmium lamp is imaged by the lens L, the field lens F_2 and the collimating lens C as a circle 13 mm diameter between the interferometer plates at P. Similarly the field lens F_1 and C image the spectroscope collimator (**2**) at I as a rectangle 3·8 mm wide by 0·77 mm high in a plane 5·4 cm behind the interferometer plates. Each point on any spectrum line uses a patch of this size on the interferometer plates, but the patch is shifted laterally and vertically depending on the point on the field lens from which the light comes. The shaded rectangles in

* Received in original form 1955 May 5.

Fig. 1 (*b*) show the total plate areas used by lines in positions 1 and 3 on the field lens, while the circle corresponds to the diaphragm D_1 (14 mm in diameter) in front of the interferometer and represents, closely enough, the plate area used by the cadmium light. We ignore the spread by multiple reflections at this stage. It is thus clear that not only is the plate area used by the cadmium standard larger than that used by the solar lines, but also different lines do not use identical areas on the plates. Any departures from plane parallelism in the plates will introduce errors in wave-lengths.

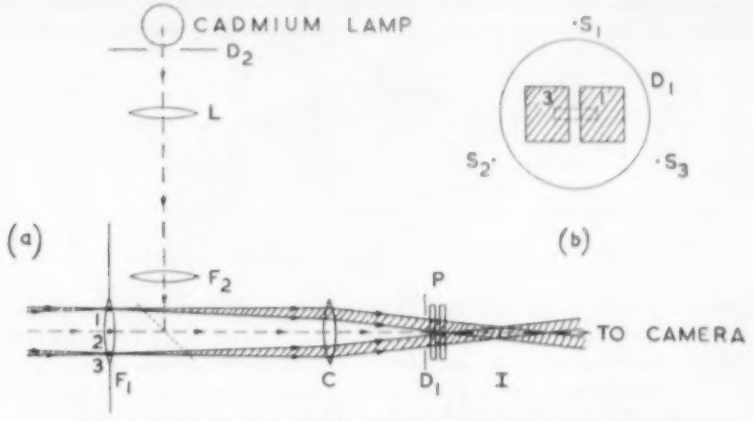

FIG. 1.—*Interferometer illumination for solar and cadmium light.*

Errors introduced by plate irregularities vary inversely as the length of spacer used. The general agreement between the wave-lengths measured with a 2·5 mm spacer and a 5 mm spacer in Paper I indicated that any such errors were within the uncertainty of the observations. When, however, a 1·5 mm spacer was brought into use at 6500 A with the experimental arrangement above, it was found that the wave-lengths measured with it were systematically shorter by approximately 0·004 A than those measured with the 2·5 mm spacer. The differences were shown equally by the arc and solar lines, they were not, apparently, dependent upon line strength and, for a region so close to the primary standard, cannot be ascribed to uncertainty in the chromatic variation of phase change, or camera focal length, or displacement of the pattern centre. We concluded that they arose from non plane-parallelism of the interferometer plates.

If our explanation is correct it indicates that, as the plates are normally set up, the air gap t between them is greater in the middle than at the edges. In determining wave-lengths we use $2t/(p+\epsilon)$, p and ϵ being the integral and fractional orders of interference. $2t$ is derived from the cadmium pattern and refers to the full circle in Fig. 1 (*b*), but ϵ refers only to that area of the plates used by the solar line. In order to get a quantitative measure of the plate irregularities it was decided to photograph the localized fringes formed between the plates when they are set at a small angle. The experimental arrangements necessary to secure sharp fringes which accurately contour the surfaces are pointed out by Rasmussen (**3**) and Tolansky (**4**), and Rasmussen has used this method to test interferometer plates. The plates were set up in the usual mount with three pieces of mica 0·012 mm–0·015 mm thick placed in the positions

usually occupied by the spacer studs. The wedge angle between the plates was adjusted by means of the interferometer springs to give approximately one fringe per mm in cadmium green light. By micrometer measures across the fringe photographs, values of $2t$ (with an arbitrary zero) were deduced at 642 points over the plate area and these have been used to draw the "contour map" of the air gap which is shown in Fig. 2. The figure shows the irregularities of the plates as a pair in one particular orientation when they are set out as parallel as possible, and $2t$ is arbitrarily set equal to zero on the contour line indicated. The interval between the contours is 1/100 of a wave-length of cadmium green light ; between the stronger lines it is $\lambda/20$ corresponding to $\lambda/40$ on each plate.

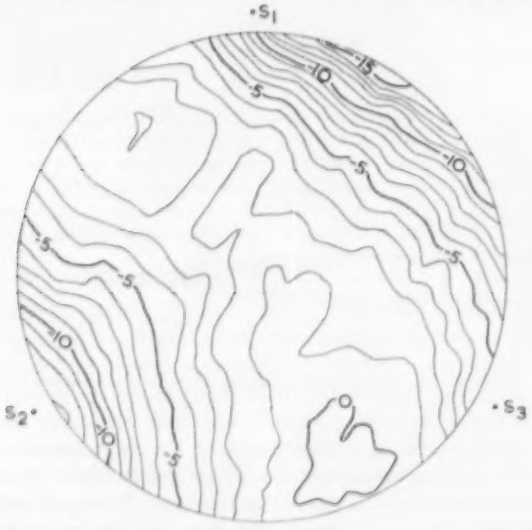

FIG. 2.—*Variations from planeness of the pair of interferometer plates.*

The plate curvature is of the form we have predicted and the variations in $2t$ are comparable with those to be expected from the tolerances given by the makers. The curvature is, however, rather more than sufficient to account for the wave-length anomalies we have found. It is possible that the curvature is accentuated in setting up the interferometer with the very thin mica separators and by the unequal spring pressure which is used to set the plates at a small angle (**3**). The stud positions at which the pressure is applied are indicated by S_1, S_2, S_3 in Fig. 2 and in Fig. 1 (*b*). If the curvature is in part introduced by spring pressure it may well vary with spacer length.

The elimination of errors due to plate irregularities.—In order to test the plates under normal conditions an Osira cadmium lamp was used as the light source for the spectroscope. The wave-length of its red line was measured exactly as for a solar or an arc line in terms of the cadmium red line produced in the side arm of our experimental arrangement. By changing the position of minimum deviation the spectroscope cadmium line can be placed in any position across the field lens F_1. We specify the position by the distance in mm on the photographic plate from the pattern centre, positive on the violet side and negative on the red side.

The results of three such sets of measures using the 1·5 mm spacer are shown in Table I below, the line positions correspond to the limiting ones normally used in measuring wave-lengths. $\Delta\lambda$ is the "error" in the wave-length of the spectroscope cadmium red line. For the first two sets of measures in Table I the experimental arrangements were those of Fig. 1 (*a*). If these differences $\Delta\lambda$ arise,

TABLE I

Differences in Cd red measured wave-lengths

Line position mm	$\Delta\lambda$ (i)	$\Delta\lambda$ (ii)	$\Delta\lambda$ Coinc : patches
+16	−0·0049	−0·0040	+0·0011
+6	−0·0044	−0·0039	−0·0004
−6	−0·0030	−0·0034	−0·0004
−16	+0·0001	−0·0046	+0·0007

as we suppose, from the different areas on the plates used by the two cadmium sources, then we should expect to remove them by making the areas coincident. By using a 33 cm lens for the field lens F_1, the spectroscope collimator is imaged between the interferometer plates. This focused patch (3·8 mm × 0·77 mm) is shown in Fig. 1 (*b*) by the dotted rectangle. The aperture in the diaphragm D_2 before the cadmium lamp, was also made rectangular 3·8 mm × 0·77 mm, and this is imaged as before between the plates (approx. 1 : 1) to coincide with the spectroscope collimator image. The last column of Table I shows the values of $\Delta\lambda$ obtained with the 1·5 mm spacer with these coincident patches. As we expect, the large fairly systematic differences in the wave-lengths have disappeared and the remaining small differences are probably within the uncertainty of their determination.

Using the same interferometer plates a similar test was also made of the errors to be expected with a 2·5 mm spacer and the experimental arrangement of Fig. 1. We should expect smaller differences than were shown by the 1·5 mm spacer, but the $\Delta\lambda$s obtained were in fact all under 0·001 A and probably not greater than their estimated uncertainty. These results certainly suggest that plate curvature is to some extent introduced in setting up the interferometer. The precise amount no doubt varies on different occasions and presumably depends also on the relative orientation of the plates.

With interferometer plates of the quality of the pair examined above (Table I) coincidence of the spectroscope and standard light patches is sufficient to secure absolute wave-lengths correct, as far as plate errors are concerned, to 0·001 A. But even with coincident patches, in the method of circular channels multiple reflections carry the spectroscopic and standard light into different regions on the interferometer plates, and with a less good pair of plates, which were also used, wave-length errors of 0·001–0·002 A could still be caused on outlying lines (2·5 mm spacer). We have taken care of this spreading-of-beams effect by modifying the diaphragm on the field lens F_2 ; side arms have been added to the simple cross which give on the photographic plate two cadmium red "lines" more remote in

the field than any solar or arc line being measured. The diaphragm on F_1 is correspondingly modified so that there is no overlap of the solar and cadmium light on the plate. From the "errors" in the cadmium lines the small corrections to the solar or arc wave-lengths can be deduced. With this procedure the absolute wave-lengths should be free (to less than 0·001 A) from errors introduced by plate irregularities. The reduction in the plate area used by the cadmium light gives a corresponding reduction in light flux; this may be compensated by increasing the red light reflectivity of the beam-splitting cube and, if necessary, the intensity of the solar light must be reduced by filters.

We must then point out that the absolute wave-lengths given in Papers I and II (**1**) may be slightly in error due to the effect of plate irregularities. On the basis of subsequent tests on the two pairs of plates used, we estimate the maximum value of such errors at 0·002–0·003 A. Other lines of evidence suggest, however, that it is unlikely that such a large effect is in fact present in the values given. In that the solar and vacuum arc wave-lengths have been determined with identical experimental procedures, their values will be affected by plate irregularities in exactly the same way. Consequently the red shifts, used for the discussion in Paper II, have no systematic errors due to plate irregularities, just as they have none due to the uncertainty in the chromatic variation of phase change, or camera focal length, or displacement of the pattern centre.

University Observatory,
Oxford:
1955 *August* 27.

References

(**1**) M. G. Adam, *M.N.*, **112**, 546, 1952; **115**, 405, 1955; *Comm. Univ. Obs. Oxford*, No. 36; No. 49.
(**2**) H. H. Plaskett, *M.N.*, **112**, 177, 1952; *Comm. Univ. Obs. Oxford*, 33.
(**3**) E. Rasmussen, *K. Danske Vidensk. Selsk. Mat.-Fys. Medd.*, **23**, 3, 1945.
(**4**) S. Tolansky, *Multiple Beam Interferometry*, p. 21, Oxford, 1948.
(**5**) P. J. Treanor, *M.N.*, **109**, 389, 1949; *Comm. Univ. Obs. Oxford*, 28.

ON THE FLEXURE OF MERIDIAN CIRCLES

R. d'E. Atkinson

(Communicated by the Astronomer Royal)

(Received 1955 March 25)

Summary

The methods which have been used or suggested for determining meridian-circle flexure are without exception unsatisfactory. Very few of them can detect a second harmonic, and many of the results actually obtained are unacceptable astronomically. The paper analyses in detail the effects of uncertainties in the flexure function, and also in the refraction, on the solar corrections, giving a more rigorous treatment than has so far been used; this rigour, and also an improvement in the methods of determining flexure observationally, both seem desirable if any further advance is to be made in the precision of the results. A new method of directly determining all harmonics of the flexure function is proposed, and the necessary equation of condition is set up for a particular case which seems the most suitable one.

Introduction.—It is universally recognized that the flexure of a meridian circle is one of the most difficult of instrumental errors to determine. As was first pointed out by Bessel (1), a value applicable to the horizontal position can be obtained immediately, by observing the two collimators after they have been set on one another; but the natural assumption that the flexure at other points on the circle will be this "horizontal flexure" multiplied by the sine of the zenith distance frequently proves irreconcilable with the astronomical results. Various methods of determining the true form of the flexure, as a function of zenith distance, have been suggested, and some have been tried very extensively, but none seems free from fairly serious objection; since any uncorrected error will enter directly into the declinations of every star catalogue based on the instrument in question, and will also affect the corrections to the Sun's elements, the position is definitely unsatisfactory. The present paper reviews the different attacks which have been made on this problem, discusses in detail the effects on the solar elements which different correction functions will produce, and proposes a new method of measurement which appears to be free from the objections that have been explicitly noticed.

In order to avoid misunderstanding, it is first desirable to clarify a point of terminology. Flexure is sometimes spoken of as positive if it "increases the zenith distances", whether these are north or south, and the increase is then meant in the numerical sense and not algebraically; it is, however, simpler in some ways to regard the flexure as an ordinary transcendental function of z, with z positive north of the zenith (say), and to agree that in all cases the observed Z.D. is to be increased *algebraically* by the amount of the flexure in order to get the true Z.D. Such flexure functions as $f = f_0 \sin z$ must then be called anti-symmetrical, not symmetrical, about the zenith, although they correspond to an

arithmetically (or even "geometrically") symmetrical effect; a flexure varying as $\cos z$ will similarly be spoken of as symmetrical about the zenith, although it deflects the zenith point, and although arithmetically it increases the Z.D.'s on one side of the zenith and decreases them on the other. In the present case, the algebraical approach seems definitely more convenient than the geometrical, and we shall follow this convention throughout.

The nature of "flexure".—It is well known that if the eye-end and objective-end of the telescope suffered identical flexures, their combined astronomical effect would be zero. The two tubes can be made nearly identical, especially if a draw-tube for focusing is dispensed with (**2**); if their lengths are exactly equal, and if the "length" (flange to second nodal point) of the lens cell is equal to the "length" (flange to focal plane) of the micrometer box, and if the instrument is also well balanced (as it normally is, with some delicacy) both with and without the eye-end and cell, interchanging the latter will eliminate the effect of any differential flexure of the bare tubes which may still exist, at least if this occurs only as a first harmonic (or as a sum of odd harmonics) in the circle readings; but the objective and micrometer themselves are of course quite dissimilar, and any internal movement in either will have the same astronomical effect as a flexure, with the added complication that it may possibly be non-elastic, and may even show discontinuities. For this reason, and also because it will not in any case eliminate any even harmonics, there seems little point in actually interchanging the two ends, and the practice has indeed been fairly generally abandoned, even in instruments which readily permit it. Personality errors should be eliminated by the systematic use of a reversing prism, but if this precaution is omitted they also will enter into the "flexure"; indeed, in at least one programme (**3**), a systematic difference in the zenith distances of near-zenith stars was found, depending on whether the observer lay head-north or head-south, even though a reversing prism was used, and it thus seems that this device cannot be relied on implicitly. Certainly there is no reason why such personality effects as are not eliminated should vary as $\sin z$, or should not have a discontinuity at the zenith.

The problem is (as it seems) further complicated by the possibility of flexure in the circle; the circle readings have to be combined with the Z.D. micrometer readings in most (but not all) flexure tests, and of course in all astronomical observations, and even if one assumes that circle flexure will vary as $\sin(z-\gamma)$ there may be no evident reason why γ should be small. If it is not, the combined flexure of telescope and circle will have terms in both $\sin z$ and $\cos z$; in the Washington 9-inch T.C., the "circle flexure" was found to be considerably larger than the other (**3**), and it seems that the resultant might have any phase.

It is however a little surprising that observable circle flexure should exist at all. The true flexure of an elastic but symmetrical circle, firmly attached to the main axis all round but free to droop under its own weight, would produce only the same effects as slight constant displacements of the various microscopes, and would thus be completely irrelevant even if only one microscope were used; the microscope displacements would not even be noticed, since the microscopes are initially adjusted on the basis of the circle divisions as actually read. If the circle is not equally stiff all round, or is not attached to the axis in a uniform and symmetrical way, detectable circle flexure may of course exist; but if local weaknesses are postulated, they seem in general more likely to affect the differences of the microscope-readings than the sum of all four (or six), and on the whole

one would then be inclined to expect observable circle-flexure to occur as a fairly high harmonic of z, not merely as the first, which is what has been found in practice. A single local excess of weight would be effective, but it seems somewhat improbable that any manufacturing flaw of this sort could be large enough. There is, however, one case where an apparent first harmonic would be found alone: a uniform circle which was effectively attached to the axis at only two points, with one of those attachments stiffer than the other, would suffer rotations about some virtual pivot (the resultant of these two partial constraints), and if the constraints were elastic these rotations would be proportional to the sine of that pivot's Z.D., and would be equivalent to translations plus similar rotations about the axis; the translations would disappear with two or more microscopes, and the rotations would be interpreted as first-order flexure. The importance of this lies in the fact that the normal method of determining circle flexure is to have the circle "movable" (i.e. with respect to the telescope), to rotate it every other year (say) to a new position, and to analyse the measurements of horizontal (and perhaps also vertical) flexure in terms of these circle positions; it may, however, be much harder to guarantee a fully adequate and symmetrical connection between circle and axis when this provision for rotation is made than when the circle is deliberately constructed as a "fixed" one. It would thus not be altogether surprising if first-order circle flexure were an error introduced mainly by the provision made for detecting and measuring it, and a well-designed "fixed" circle might in that case be preferable to any attainable excellence in a movable one.

Methods for determining flexure.—(*a*) *Bessel's method.* Since the combined flexure of circle and telescope is what is required astronomically, the ideal would be to determine this directly at a number of different zenith distances. In principle, as again Bessel first pointed out, it would be possible to set up a pair of collimators in some other position than the horizontal, or in a series of such positions, to determine the flexure for each position, and to express the results as a function of z. This method could not be employed, as it stands, in an ordinary pavilion, and does not appear to have been explored at all; but it would seem reasonably practicable if the lower of the two collimators were replaced by a plane mirror and the upper one were fitted with a Bohnenberger eyepiece. However, even if suitable arrangements could be made, the collimator method does not really give the true astronomical flexure in any case, but only the difference of two values 180° apart; thus however many collimator positions one uses it cannot detect any even harmonics in the flexure function, and in particular it cannot detect a second harmonic. (This weakness seems not to have been pointed out previously.) If it can be assumed that there are no harmonics above the first, there is no real need for a large number of collimator positions after all; a single pair of vertical collimators, in addition to the horizontal pair, is sufficient to determine the complete function, and the lower one of the vertical pair can then be replaced by the ordinary mercury-pool (**4**).

The "vertical flexure", i.e. the flexure (including that of the circle) evaluated by the use of vertical collimators or their equivalent, is not really material in a modern instrument, since it is eliminated by reversal. Indeed, if the flexure function is expressed as a Fourier series in z, this is true of all the cosine terms in the complete series. If there are no sine harmonics above the first, it must thus be sufficient to determine the horizontal flexure f_0 by means of the collimators, reverse the instrument regularly, and assume that $f = f_0 \sin z$; rotating the circle

in addition should be unnecessary, so far as this question goes, whether there is circle flexure or not. If the circle is never moved, many of the corrections discussed below can also be obtained with greater weight; and since the only information which is obtained by moving it is information that is not wanted, it would seem better to keep it in one position even if it is designed to be movable.

(*b*) *Loewy's method.* Methods of test of this kind, i.e. employing only collimators, mirrors, etc., but not stars, may be classed as "purely instrumental"; there may also be "purely astronomical" methods (or, at least, checks); and there are methods which we may call mixed "instrumental-astronomical" ones. Two other purely instrumental methods seem worthy of mention here. The first is due to Loewy (**5**); a meniscus lens, with its concave radius of curvature equal to half the length of the telescope and its focal length equal to half that radius, was very firmly mounted in the central cube, with the concave side towards the eyepiece. Using the concave side as a mirror, a real image of the Z.D. micrometer wire could be seen in the same focal plane, and the setting for coincidence noted; the variation of this setting, as the telescope was pointed to various zenith distances, gave the flexure of the eyepiece half of the telescope. Using the lens property, a mark on the telescope objective could also be imaged in the focal plane; and the variation of Z.D. micrometer settings on this, as the telescope was moved, gave the sum of the flexures of the two halves. The difference of the two then followed. The main difficulty, that of determining the flexure of the auxiliary lens and mounting itself, was solved (it was claimed) by adding weights to this mounting, repeating the observations, and "eliminating" the flexure due to the original weight. If the difficulty certainly can be got over in this way, the method appears sound; but in the case of the reflection observations it is tilts of the mounting, even more than bodily displacements, which are to be feared, and it might be difficult to be sure that the loads were always quite suitably applied, from this point of view. Even a small miscalculation here can have very serious effects indeed. The results actually obtained were claimed to be very consistent, and it is interesting to note that they did indicate the presence of an appreciable second harmonic; the flexure was found to be

$$F = +1''{\cdot}04 \sin z + 0''{\cdot}17 \cos z + 0''{\cdot}30 \sin 2z - 0''{\cdot}23 \cos 2z. \qquad (1)$$

The method evidently yields only the telescope flexure, without the circle flexure. However, it was argued that the latter would be expected to be zero; and the horizontal collimators, which, of course, measure the combined (horizontal) flexure, gave $+1''{\cdot}15$, in fairly good agreement with the $+1''{\cdot}04$, above, for the telescope only. This is perhaps the only case in the literature where an important second harmonic was directly determined; but the possibility that some flexure of the mounting was not fully accounted for by the process of varying the loading cannot be entirely ruled out. The method is inconvenient, since the meniscus prevents all astronomical observations while it is in place, and it does not seem to have been adopted elsewhere.

(*c*) *Bonsdorff's method.* The other purely instrumental method is due to Bonsdorff (**6**); a plane mirror was supported in front of the objective, by a mounting designed to guarantee that flexure of the mounting would move the mirror strictly parallel to itself, while flexure of the telescope would not affect it at all. Auto-collimation measurements were then made with this mirror, in a variety of telescope positions, so as to derive the complete flexure function of the

telescope. It was stated that adding extra weights to the mirror verified that it was functioning correctly, the reading at any one Z.D. being unaffected, as it should. It was also stated that the results indicated a variation purely with $\sin z$, but this appears to be incorrect; the treatment given to the individual readings would necessarily have removed any term in $\cos z$, and if these readings themselves are examined they indicate not only that there was such a term, but that it was actually about three times as large as that in $\sin z$. It is unfortunate that no comment was made on this; it seems rather improbable that so large a $\cos z$ term could be real, for in this case also the circle flexure evidently does not enter. The method is believed to have been tried at several other observatories, but to have been found difficult in most cases. It is clear that perfection of design, and high precision in manufacture, are essential if the mirror's movements are to be sufficiently parallel; a slight difference in stiffness as between two members that were nominally identical, or a slight difference in friction as between two joints that were both nominally free, would be enough to impair the action, and it would perhaps not be very surprising if two superficially indistinguishable mountings gave somewhat different results.

With both these methods, if the results did not agree with those obtained from the collimators, it would be difficult to know what to do with them. The difference might indeed be ascribed to circle flexure; but since the circle readings must be used in the astronomical work itself this would mean that the collimator results had to be relied on after all, and the others rejected (so far, at least, as the first harmonic is concerned), unless the form of the circle flexure could be discovered independently.

(*d*) *The "R. and D. method"*. By "mixed" instrumental-astronomical methods we understand those in which stars are observed, but nothing is assumed about their positions except the fact that for any one star the (mean) declination is constant; its absolute value does not enter. In addition, an instrumental arrangement is made which permits the same star to be observed in two or more different positions of the telescope, related to one another by some condition which is known with precision; and a comparison of the circle readings actually obtained, with those to be expected on the basis of the known condition, gives a condition which the flexure must satisfy. The best-known of these methods is that of observing the star both directly and by reflection in a mercury pool. The precisely-known condition in this case is that the sum of the two observed circle readings, together with the appropriate flexures, must be exactly 180°; moreover, half the difference of the two readings should give the star's altitude, without relying on the ordinary nadir pool at all. Since the nadir observation is of a different kind from all observations of stars (and is also made in a different position of the observer, and of the micrometer), this possibility of eliminating any systematic error that may affect it appears at first sight valuable.

The method was tried extensively at Greenwich (**7**), but the results were never very satisfactory. It seems probable that one reason for this lay in the unsuitable nature of the pavilion in this particular case (**8**). (The aperture of the Airy T.C. pavilion is only 3 ft. wide, and is 16 ft. above the axis of the instrument; and the instrument itself is also partly sunk in a pit, so that the mercury pool is in many cases below ground level, which may perhaps add to the refraction dangers inherent in the pavilion.) The method appears to have been found more successful at Washington (**9**), though a mercury pool can of course be used with a wide

pavilion-aperture on very still nights only. It has not been employed recently at all; and actually, even in ideal circumstances, it is defective in principle: it cannot detect or eliminate any component of flexure which is antisymmetrical about the horizon. This weakness does not appear to have been pointed out in the literature, at least in this precise form; it seems to deserve explicit consideration.

Let c be the circle reading, reckoned from the zenith, positive for Z.D. north, when the telescope is set on a star at zenith distance z (as refracted). (For convenience, we speak of the combination of Z.D. micrometer reading and circle reading as the "circle reading c".) Let $f(c)$ be the flexure at the circle reading c, positive if its effect is such that the true Z.D. is greater (algebraically) than c by the amount of the flexure; so that the zenith distance of a star (including refraction) is

$$z = c + f(c). \tag{2}$$

Let c_D be the reading for a given star if it is observed directly, and c_R the reading if it is observed by reflection in the mercury pool; c_R is supposed corrected for the necessary small change of latitude of the pool, though this precaution has perhaps not invariably been observed in practice.

Then we have

$$z = c_D + f(c_D) \tag{3}$$

and

$$z = \pi - c_R - f(c_R). \tag{4}$$

Let f now be divided into a portion, f_S, symmetrical about the horizon, and a portion, f_A, antisymmetrical about it; then $f_S(c_R) = f_S(c_D)$ and $f_A(c_R) = -f_A(c_D)$. Inserting these in (3) and (4), and adding and subtracting the results,

$$2z = c_D - c_R + \pi + 2f_A(c_D) \tag{5}$$

and

$$0 = c_D + c_R - \pi + 2f_S(c_D). \tag{6}$$

Equation (5) shows that any systematic error affecting the zenith (or the nadir) is indeed eliminated when the true Z.D. is inferred in this way (since it will enter equally into c_D and c_R); and equation (6) is an equation of condition for determining f_S; we may assume for example

$$f_S(c) = \Sigma\,[a_{2n}\cos 2nc + b_{2n+1}\sin(2n+1)c] \tag{7}$$

using as many terms as seem reasonable, and on taking a sufficient number of observations we shall be able to solve by least squares for the a's and b's and so determine f_S completely. But there is no similar equation of condition for f_A, and f_A is present in (5) and also, of course, in (3) and (4): thus one cannot say that "the combination of a direct observation with a reflected one eliminates the effect of flexure", nor can one infer a total flexure for use with single direct observations (which must be the majority), unless f_A is known on other grounds.

The terms which are antisymmetrical about the horizon are, of course, the odd cosines and the even sines of c (or, as we may equally well say, of z); neither odd nor even sines are cancelled out by reversing the instrument. Thus even if the instrument is reversible the mercury-pool method will leave undetected and operative any term in $\sin 2z$ (or in $\sin 4z$, etc.) which may exist; and in addition it will fail to detect or eliminate any term in $\cos z$ (or in $\cos 3z$, etc.) if the instrument is not reversible, as the Airy T.C. itself was not. Higher harmonics than the second are perhaps unimportant, at least unless they occur in the circle rather than in the telescope, or are used to describe discontinuities, but it seems a little dangerous to assume that even the second harmonics are absent. It is an unfortunate coincidence that neither the collimator method nor the mercury-pool method can

say anything about a term in sin $2z$, nor can such a term be eliminated by interchanging the lens and eye-end, or by reversing the instrument.

(*e*) *The "astronomical method" (flexure and refraction).* In practice, no matter what methods are used for determining flexure to begin with, they are fairly often discarded again at a later stage of the same programme, the final choice of a flexure function being then based exclusively on the astronomical criterion that the distance from the pole to the equator is 90°. This is, of course, sufficient to determine one parameter only, and the flexure is therefore assumed to be of the form $f = f_0 \sin z$, with f_0 so adjusted that the astronomical criterion is satisfied. All preliminary determinations of flexure, e.g., with the collimators, are thus reduced to the status of mere devices for keeping the arithmetic compact; an accurate determination is pointless, except perhaps as a check that no unexplained change has occurred, and any arbitrarily assumed value of f_0 near the final one would be sufficient. Occasionally, when the original determinations of horizontal flexure and of refraction led to positions of the pole and equator which, together, did not satisfy the astronomical criterion, the flexure determinations have been kept and the refraction ones amended instead; but in either case the situation so created is rather unsatisfactory. It is always undesirable to throw away apparently good observations without discovering why they are wrong, and particularly so if it is only done in order to preserve others which may themselves be erroneous. The Washington 6-inch results for 1925–41 (**10**) and 1941–9 (**11**), which can certainly be classed as among the best available, show this difficulty very plainly; at the latitude of Washington, flexure and refraction are definitely hard to separate, on the basis of above-pole and below-pole declination comparisons, and when the distance from pole to equator proved to need correction it was necessary to sacrifice either the preliminary determinations of flexure or those of refraction with little to go on. In the former series, the refraction coefficient was changed by about 0″·16 although the probable errors of the rejected values (slightly different at different dates) had been ±0″·016; in the latter series, the flexure coefficient was changed by 0″·04 while the probable errors of the rejected determinations (**12**) were ±0″·03. The conflict in the second case is superficially less, but only because the equator-point error which had to be corrected was much less; if it had been as large as the other, the flexure coefficient would have had to be changed by 0″·23.

In both cases, of course, everything that was known about possible systematic uncertainties, as opposed to the visible probable errors, was considered before making the decision; but it does now appear at least formally possible that the provisional determination of refraction and the provisional determination of first-order flexure may both have been substantially correct, and that the error of the equator-point may have been due to a second harmonic in the flexure, which could not have been detected by the methods used. And at least it is clear that a considerable advance in the reliability of the final results might be hoped for, if the different possibilities could be more surely separated. It is the case, unfortunately, that even though two alternative correction functions may not be clearly distinguishable over a moderate range of near-polar stars, they may have appreciably different runs over the 47 degrees of declination, centred on the equator, which are involved in solar observations; planetary observations necessarily involve a somewhat larger range still, and the range of declinations observed in preparing a star catalogue may be larger again. It seems worth while now to investigate just how serious these effects may be; we shall see that they can in fact appreciably exceed the probable errors claimed for some of the solar corrections.

Analysis of the solar corrections.—It is well known that if the residuals (Obs.-Tab.) of the Sun's declination are analysed, they yield corrections to the Sun's mean longitude L, to the obliquity ϵ, and to the two quantities h and k from which the eccentricity and the longitude of perigee can be inferred; in addition, there usually remains a constant term, $-\Delta\delta_0$ (**13**), which is commonly regarded as "the error of the equator-point". $\Delta\delta_0$ would be zero if the instrumental errors, and the refraction, were correctly known and allowed for; if it is not zero, and is to be removed, this must be done by applying some specifically assumed correction-function, such as

$$\Delta_c\delta = p + q\sin z \tag{8}$$

(if the first harmonic of the flexure is held to be responsible) or

$$\Delta_c\delta = p + q\tan z \tag{9}$$

(if the refraction is); as we have now seen, it may be desirable to consider also

$$\Delta_c\delta = p + q\sin 2z. \tag{10}$$

In each case, if the latitude has already been so adjusted that declinations above and below pole are consistent, the constants p and q are to be so chosen that the function vanishes at the pole, i.e. we must have

$$\Delta_c\delta = K(\cos\phi - \sin z) \tag{11}$$

or

$$\Delta_c\delta = K(\cot\phi - \tan z) \tag{12}$$

or

$$\Delta_c\delta = K(\sin 2\phi - \sin 2z), \tag{13}$$

where ϕ is the latitude; and in current practice K is then determined so as to make

$$\Delta_c\delta(E) = \Delta\delta_0 \tag{14}$$

if $\Delta_c\delta(E)$ is the "equatorial" value of $\Delta_c\delta$, i.e. its value when $\delta = 0$. Whichever of the functions (11), (12), or (13) is selected, it will act as a systematic correction to the $D\delta_0$ which characterize a star catalogue obtained with this instrument (as compared with others), and this has indeed been the principal purpose of deriving it; in addition, as was remarked by Hough (**14**), it will in general affect the solar corrections too.

The equation of condition in its usual form is

$$-\Delta\delta_0 + \sin\epsilon\cos\alpha\,\Delta L + \sin\alpha\Delta\epsilon + 2\cos\alpha\sin\delta\Delta h - 2\sin\epsilon\cos^2\alpha\cos\delta\Delta k = \Delta\delta \tag{15}$$

where $\Delta\delta$ are the declination residuals; and since the coefficient of Δk never changes sign it is clear that $-\Delta\delta_0$ is not strictly the mean value of these residuals; it is also not the value of the left-hand side of (15) when $\delta = \alpha = 0$; and neither of these values is strictly the one to which (11), (12), or (13) ought to be adjusted. Although, as we shall see, the practical error is not as yet really serious, it might easily become so if experimental accuracy improved a little further; we will therefore now establish what the rigorous condition for $\Delta_c\delta$ is.

We may eliminate δ from (15) by means of the relation

$$\tan\delta = \tan\epsilon\sin\alpha; \tag{16}$$

if we also insert the numerical value of ϵ, we obtain

$$\begin{aligned} &-\Delta\delta_0 + 0{\cdot}398\cos\alpha\Delta L + \sin\alpha\Delta\epsilon + (0{\cdot}413\sin 2\alpha - 0{\cdot}010\sin 4\alpha)\Delta h \\ &-(0{\cdot}389 + 0{\cdot}398\cos 2\alpha + 0{\cdot}009\cos 4\alpha)\Delta k = \Delta\delta \end{aligned} \tag{17}$$

(neglecting higher harmonics); and this form shows explicitly that the coefficients are for the most part very conveniently orthogonal if we can assume equal weights

at equally-spaced values of α (**15**). We shall make this assumption for the present; the question of weighting will be further considered at a later stage. An additional simplification, so far as $\Delta_c\delta$ is concerned, follows from the fact that any function depending only on z is the same in the autumn as in the spring, at the same values of δ; since (for the Sun) α and δ are connected by (16), we may express $\Delta_c\delta$ by a Fourier series in α, and it must therefore be by one that is symmetrical about $\alpha = \pi/2$ and $-\pi/2$. It can thus only involve the even cosines and odd sines of α, and these are all orthogonal to the coefficients of both ΔL and Δh, so that it is only the quantities $\Delta\delta_0$, $\Delta\epsilon$, and Δk which can be affected by the kind of correction we have to consider.

If we difference two least-squares solutions, both having identical coefficients on the left, and employing "observational" quantities on the right which differ by the correction function $\Delta_c\delta$, the resulting equations are exactly what we would get if we solved the equation

$$-\Delta_c\delta_0 + \sin\alpha\Delta_c\epsilon - (0{\cdot}389 + 0{\cdot}398\cos 2\alpha + 0{\cdot}009\cos 4\alpha)\Delta_c k = \Delta_c\delta \qquad (18)$$

as if it were an equation of condition, to obtain the three additional corrections $\Delta_c\delta_0$, $\Delta_c\epsilon$, and $\Delta_c k$ by the regular least-squares process. In the "corrected" solution, these will be added to the original $\Delta\delta_0$, $\Delta\epsilon$, and Δk, which have already been obtained by solving the "uncorrected" equation (17); and the rigorous criterion for the choice of the magnitude (but not, of course, the form) of the correction function $\Delta_c\delta$ is that there shall then be no absolute term left, i.e.

$$\Delta_c\delta_0 + \Delta\delta_0 = 0. \qquad (19)$$

Writing $\Delta_c\delta$ as a Fourier series in α (with the restriction already noted), i.e. putting

$$\Delta_c\delta = c_0 + c_2\cos 2\alpha + c_4\cos 4\alpha + \ldots + d_1\sin\alpha + d_3\sin 3\alpha + \ldots \qquad (20)$$

in (18), we may readily derive the normal equations

$$\Delta_c\delta_0 + 0{\cdot}389\Delta_c k = -c_0 \qquad (21)$$

$$\tfrac{1}{2}\Delta_c\epsilon = \tfrac{1}{2}d_1 \qquad (22)$$

$$0{\cdot}389\Delta_c\delta_0 + (0{\cdot}389^2 + 0{\cdot}0792)\Delta_c k = -0{\cdot}389c_0 - 0{\cdot}199c_2 - 0{\cdot}0045c_4; \qquad (23)$$

and separating (21) and (23)

$$\Delta_c k = -2{\cdot}51c_2 - 0{\cdot}057c_4 \qquad (24)$$

$$\Delta_c\delta_0 = -c_0 + 0{\cdot}977c_2 + 0{\cdot}022c_4. \qquad (25)$$

Equation (19) thus leads to

$$c_0 - 0{\cdot}977c_2 - 0{\cdot}022c_4 = \Delta\delta_0 \qquad (26)$$

as the rigorous condition for adjusting the "amplitude" of the selected $\Delta_c\delta$.

The "equatorial" value of $\Delta_c\delta$ is given by

$$\Delta_c\delta(E) = c_0 + c_2 + c_4, \qquad (27)$$

and it is, of course, $-\Delta_c\delta(E)$ which is strictly "the error of the equator-point". The traditional criterion for adjusting $\Delta_c\delta$, namely (14), is clearly not identical with (26).

We may replace (26) by an approximation which eliminates the need for explicitly deriving the Fourier series (20). The summer-solstice value of $\Delta_c\delta$, $\Delta_c\delta(S)$ say, is

$$\Delta_c\delta(S) = c_0 - c_2 + c_4 + d_1 - d_3 \qquad (28)$$

while the winter-solstice value is

$$\Delta_c\delta(W) = c_0 - c_2 + c_4 - d_1 + d_3; \tag{29}$$

we thus have

$$\tfrac{1}{2}[\Delta_c\delta(S) + \Delta_c\delta(W)] = c_0 - c_2 + c_4, \tag{30}$$

and the right-hand side of this is very similar to that of (26); indeed, if c_2 and c_4 happen to be in the same ratio as the coefficients of $\cos 2\alpha$ and $\cos 4\alpha$ in (17), i.e. if $c_4 = +0{\cdot}023c_2$, (30) becomes

$$\tfrac{1}{2}[\Delta_c\delta(S) + \Delta_c\delta(W)] = c_0 - 0{\cdot}977c_2$$

while (26) becomes

$$\Delta\delta_0 = c_0 - 0{\cdot}977c_2,$$

so that the correct adjustment of $\Delta_c\delta$ is obtained when

$$\tfrac{1}{2}[\Delta_c\delta(S) + \Delta_c\delta(W)] = \Delta\delta_0. \tag{31}$$

This equation may be regarded as a "rule of thumb" condition for adjusting $\Delta_c\delta$, and it will always be a fairly good one, since c_4 and 2·3 per cent of c_2 will both be small even if they are not equal; thus, so long as we rely on declination measurements only, we may say that the correct adjustment of $\Delta_c\delta$ is obtained by making *the mean of its two "tropical" values*, and not its equatorial value, equal to $\Delta\delta_0$. To take a particular case, if we wish to remove a $\Delta\delta_0$ of $+0''{\cdot}40$ (say) by means of a $\Delta_c\delta$ of the form (12), in latitude 40°, use of the equatorial value will lead to

$$\Delta_c\delta = 0''{\cdot}235 - 0''{\cdot}197\tan z \tag{32}$$

while the tropical mean leads to

$$\Delta_c\delta = 0''{\cdot}204 - 0''{\cdot}171\tan z; \tag{33}$$

the difference amounts to $0''{\cdot}03$ at the zenith, to $0''{\cdot}05$ at the equator, and to $0''{\cdot}10$ at $\delta = -30°$, and the two resulting star catalogues would differ systematically by a $D\delta_0$ of this magnitude. Actually, as we shall see below, these differences should normally be reduced by anything up to 50 per cent; but the traditional use of (14) still appears a little undesirable, more especially since the amount of labour which it saves is trivial.

It may be useful to tabulate the results of applying the harmonic analysis (20) to the three functions (11), (12), and (13), for three representative ϕ-values. The five coefficients of (20), all normalized to $c_0 - 0{\cdot}977c_2 - 0{\cdot}022c_4 = +1$, i.e. adjusted to cancel a $\Delta\delta_0 = +1''{\cdot}00$, and the corresponding values of K to insert in (11), (12), and (13), are shown in Table I, and values for other latitudes may be interpolated graphically.

TABLE I

	Correction (11) (sin z)			Correction (12) (tan z)			Correction (13) (sin $2z$)		
	$\phi = 30°$	40°	50°	30°	40°	50°	30°	40°	50°
c_0	1·015	1·019	1·023	0·969	0·933	0·868	1·092	1·092	1·092
c_2	+ ·016	+ ·020	+ ·023	− ·032	− ·066	− ·135	+ ·094	+ ·094	+ ·094
c_4	+ ·001	+ ·001	+ ·001	+ ·000	+ ·003	+ ·011	+ ·004	+ ·004	+ ·004
d_1	− ·266	− ·231	− ·194	− ·247	− ·352	− ·484	− ·262	− ·080	+ ·080
d_3	− ·006	− ·005	− ·004	+ ·004	+ ·013	+ ·038	− ·011	− ·003	+ ·003
K	+ ·755	+ ·738	+ ·743	+ ·406	+ ·428	+ ·366	+ ·687	+ ·604	+ ·604

We may use these figures to study the effect of removing any particular $\Delta\delta_0$ by any one of the three assumed correction functions. If, for example, observations in latitude 50° have yielded a $\Delta\delta_0$ of $+0''\cdot30$ (after correcting the pole), and it is decided that an erroneous first harmonic in the flexure is responsible, then since $0''\cdot30K = 0''\cdot223$ in this case, the correction function is

$$\Delta_c\delta = +0''\cdot223(\cos\phi - \sin z) \tag{34}$$

and we see from (22) and (24) that the solar corrections previously obtained will be modified by the subsidiary corrections

$$\Delta_c\epsilon = 0''\cdot30\, d_1 = -0''\cdot06 \tag{35}$$

and

$$\Delta_c k = -0''\cdot30(2\cdot51c_2 + 0\cdot06c_4) = -0''\cdot02. \tag{36}$$

If we decided to correct the same $\Delta\delta_0$ by means of a second harmonic in the flexure, we should have similarly

$$\Delta_c\delta = +0''\cdot181(\sin 2\phi - \sin 2z) \tag{37}$$

$$\Delta_c\epsilon = +0''\cdot02 \tag{38}$$

$$\Delta_c k = -0''\cdot07, \tag{39}$$

while the decision to correct it by modifying the refraction instead (**16**) would result in

$$\Delta_c\delta = +0''\cdot110(\cot\phi - \tan z) \tag{40}$$

$$\Delta_c\epsilon = -0''\cdot15 \tag{41}$$

$$\Delta_c k = +0''\cdot10. \tag{42}$$

The differences between these solutions appear appreciable, in view of the fact that the internal probable errors claimed for $\Delta\epsilon$ and Δk may be of the order $\pm 0''\cdot03$ or less, and it is somewhat embarrassing if one has to choose between them arbitrarily.

Table I also allows us to put the effects of an inability to decide between different correction functions in another way. For any given latitude, we may difference the figures for two different correction formulae (or may make any linear combination of all three such that the sum of the three amplitudes is zero), and the result will be an expression which will leave the separation between pole and equator unchanged. For lat. 40°, for example, subtracting the "$\sin z$" figures from the "$\tan z$" ones and multiplying by $\Delta\delta_0 = +1''\cdot000$, we get

$$\begin{aligned}\Delta_c\delta &= +0''\cdot428(\cot\phi - \tan z) - 0''\cdot738(\cos\phi - \sin z)\\ &= -0''\cdot055 - 0''\cdot428\tan z + 0''\cdot738\sin z,\end{aligned} \tag{43}$$

and this expression can of course be multiplied by any other amplitude-constant instead without altering its property of leaving the pole-equator separation unchanged. (It vanishes at the pole, of course, but it does not and should not vanish at the equator; for this reason it might be a little difficult to construct it without using the above harmonic analysis.) By direct trial, one can see how large an amplitude it may be given without seriously affecting the below-pole minus above-pole declination differences, $\delta' - \delta$, on which the adjustment of the pole itself depended; if the original choice, as between a flexure adjustment and a refraction adjustment, was demonstrably wrong, the application of (43), with a suitable (perhaps negative) amplitude, will result in an improved run of these $\delta' - \delta$, but even when this does not happen, the run will not be made worse over an appreciable range of amplitudes. This is, of course, merely a quantitative

version of the qualitative statement that flexure and refraction are not clearly separable. (In general, applying (43) will also slightly change the pole itself, owing to the fact that a finite range of circumpolar declinations is involved; this effect can be dealt with by a further approximation if necessary.)

The harmonic analysis of (43), taken directly from the appropriate coefficient-differences in Table I, is

$$\Delta_c\delta = -0''\cdot086 - 0''\cdot086\cos 2\alpha + 0''\cdot002\cos 4\alpha - 0''\cdot121\sin\alpha + 0''\cdot018\sin 3\alpha, \quad (44)$$

and the corresponding solar corrections, from (22), (24), and (25), are (for this amplitude, i.e. $1''\cdot00$)

$$\Delta_c\epsilon = -0''\cdot12, \quad \Delta_c k = +0''\cdot22, \quad \text{and (necessarily)} \quad \Delta_c\delta_0 = 0;$$

even though the largest amplitude likely to be permissible (so far as the circumpolars go) is probably not over $0''\cdot3$ or $0''\cdot4$, the uncertainty thus introduced is somewhat unwelcome.

Actually, the above analysis is an over-simplification. In general, corrections to the solar elements are derived from residuals in α as well as from those in δ, and it is usual to form combined normal equations and treat both sets of residuals together. The equation of condition for the right ascensions, if (as is usually done) we give equal weights to all $\Delta\alpha$ rather than to all $\Delta\alpha\cos\delta$, is

$$\begin{aligned} &-E + \cos\epsilon\sec^2\delta\Delta L - \cos\alpha\tan\delta\Delta\epsilon + 2\sin\alpha\sec\delta\Delta h \\ &\qquad - 2\cos\alpha\sec\delta\cos\epsilon\Delta k = \Delta\alpha, \end{aligned} \quad (45)$$

and if we eliminate δ as before this becomes

$$\begin{aligned} &-E + (1\cdot004 - 0\cdot086\cos 2\alpha)\Delta L - 0\cdot217\sin 2\alpha\Delta\epsilon \\ &+ (2\cdot136\sin\alpha - 0\cdot044\sin 3\alpha + \ldots)\Delta h \\ &- (1\cdot877\cos\alpha + 0\cdot042\cos 3\alpha + \ldots)\Delta k = \Delta\alpha. \end{aligned} \quad (46)$$

This equation shows much the same kind of orthogonality as (17); and when they are combined, with equal weights for equal intervals of α as before, almost all the non-diagonal terms in the normal equations still vanish. If we add (17) and (18) and solve them together with (46) in this way, remembering that (17) and (46) themselves have already been solved together, and giving equal weights to an observation in R.A. and to one in Dec. (as is usual), we find that equations (21), (22) and (23) reappear with their right-hand sides and the terms in $\Delta_c\delta_0$ unchanged; the coefficient of $\Delta_c\epsilon$ in (22) is increased from 0·500 to 0·524, and the coefficient of $\Delta_c k$ in (23) is increased from 0·231 to 1·994. Equations (25), (22) and (24) are thus replaced by

$$-\Delta_c\delta_0 = c_0 - 0\cdot042c_2 - 0\cdot001c_4 = +\Delta\delta_0 \quad (47)$$

$$\Delta_c\epsilon = 0\cdot954\,d_1 \quad (48)$$

$$\Delta_c k = -0\cdot108c_2 - 0\cdot002c_4. \quad (49)$$

Table I can readily be re-normalized by dividing each column by the value of $c_0 - 0\cdot042c_2 - 0\cdot001c_4$ appropriate to that column. The "c_0" which result are now all very close to 1·0, while the new "c_2" (and "c_4") are not substantially altered; thus the rigorous criterion (47), for adjusting $\Delta_c\delta$, which replaces (26), is now only slightly different from

$$c_0 = \Delta\delta_0, \quad (50)$$

and falls almost half-way between (14) and (31). $\Delta_c k$ is in all cases now very small, while $\Delta_c\epsilon$ is changed less than 15 per cent from its previous value; these last two statements reflect the fact, well known qualitatively, that in a "combined"

solution Δk is determined mainly by the α-residuals and $\Delta\epsilon$ by those in δ. Except where the original c_0 (Table I) differ markedly from unity, such difference-equations as (43) and (44) reappear without any major modification, and the star corrections are also little affected.

The above conclusions have been obtained on the basis of equal weights for normal points, both in α and δ, which are evaluated for equally-spaced α-values. Weights are sometimes assigned in proportion to the numbers of observations made in these ranges, and this will in general involve reduced weights for the winter months, and will somewhat upset the orthogonality and separability which have much facilitated the present analysis. For any moderately uniform distribution of observations, the results will not be very greatly altered; but there are additional weighting considerations, some of them difficult, and the total amount of uncertainty which these import may be appreciable.

In the first place, there is some evidence that residuals in α (seconds of arc) should be replaced by residuals in $\alpha\cos\delta$; this would reduce the weights near both solstices systematically, but not by very large amounts. Secondly, the usual assumption that observations in α and δ have equal weights is probably based on little more than the difficulty of coming to any decision at all on really objective grounds. The systematic errors of the two methods are certainly quite different; but they are very hard to assess. The question how far (22), (24), and (25) should or should not be replaced by (47), (48), and (49) depends entirely on this relative weighting, and it is difficult to feel much confidence about any particular choice. The resulting uncertainty is not great except for Δk, but is clearly not reflected in the probable errors. In the third place, it would seem at first sight logical to underweight all low-altitude declination measurements, and this includes all those made on the Sun in winter, and not only those made on sub-pole stars; at Greenwich, the winter Sun is only a few degrees higher than the limit at which sub-pole declinations are rejected altogether. The temptation to give full weight to every measurement of the Sun's declination which can be obtained in the winter months, even though the altitude is low, is a strong one, since for several months on end no observations except low-altitude ones can be obtained at all; but if the full weight is not really there it would be better to accept the fact. The weights at low altitudes can be adequately assessed for night-time observations, both in the north and in the south, and it is improbable that the weight at noon could be better. Against this must be set, however, the possibility that noon observations in summer may be so much worse than those on high-altitude stars as to be no better than the winter ones; it is the scatter in the solar residuals themselves which should really decide their formal weights. The same arguments apply in R.A. too, in principle, though the actual variation of weight may be less here. Whenever it seems even reasonably correct, taking everything into account, to assign equal weights to normal points that are equally spaced in α, the resulting simplification of the analysis is so great that it should probably be done, but in some cases it might clearly be improper.

However this may be, there can be little question that so long as the real form of the flexure function is unknown it will be impossible to eliminate most of the uncertainties discussed above, either in the solar corrections Δk and $\Delta\epsilon$, or in the systematic declination corrections of the star places which may be obtained with the instrument in question; a detailed and reliable determination of the complete flexure function would clearly still be worth a considerable effort, if it could be achieved.

The "pentag" method of determining flexure.—It seems possible that this might be done, more completely than it has in the past, by making use of an optical square, or "pentag". This consists in principle of two plane mirrors very rigidly mounted together so as to enclose an angle of 45°; it has the property that a ray of light incident on one mirror, in the plane perpendicular to the line joining them, and then reflected in the other mirror also, is deviated through 90° whatever its angle of incidence. If the angle between the mirrors is $45°+v$, the ray is deviated by $90°-2v$. For our present purpose, the exact value of v is quite unimportant (so long as it does not exceed 1′ or so), but its constancy must be guaranteed within a small fraction of a second. Small "squares", as used in range-finders etc., are commonly made as solid prisms, and the most economical form is then pentagonal. When larger ones are required, fabrication from plates is more suitable; there are obviously several ways of constructing a "hollow pentag" out of fused quartz only, and it should be quite practicable to achieve the necessary permanence even with a fairly large effective aperture.

If such a pentag is mounted in front of the objective of a transit circle, by a counterpoised system supported only on the east–west axis, or on the ball-races through which the main counterpoise system acts, the circle reading for any star will always be $90°-2v$ greater, or less, than that for a direct observation of the same star, except for the difference of the two flexures. If c_1 is the reading with the pentag, and c the reading without, and if the upper sign refers throughout to the arrangement in which $c_1 \sim c+\pi/2$, we have

$$z = c + f(c) \tag{51}$$

$$z = c_1 \mp \pi/2 \pm 2v + f(c_1) \tag{52}$$

and so

$$0 = c_1 - c \mp \pi/2 \pm 2v + f(c \pm \pi/2) - f(c). \tag{53}$$

Writing $f(c) = \Sigma(a_n \cos nc + b_n \sin nc)$, we obtain the equation of condition as

$$\begin{aligned} f(c) - f(c \pm \pi/2) \mp 2v \equiv \pm 2\Sigma[\sin n\pi/4\{a_n \sin n(c \pm \pi/4) \\ - b_n \cos n(c \pm \pi/4)\}] \mp 2v = c_1 - c \mp \pi/2; \end{aligned} \tag{54}$$

or, putting in successive values of n and transforming so as to remove half the double signs

$$\begin{aligned} &\sqrt{2}a_1 \cos(c \mp \pi/4) + 2a_2 \cos 2c + \sqrt{2}a_3 \cos(3c \pm \pi/4) + \ldots \\ &\quad + \sqrt{2}b_1 \sin(c \mp \pi/4) + 2b_2 \sin 2c + \sqrt{2}b_3 \sin(3c \pm \pi/4) + \ldots \mp 2v \\ &\quad = c_1 - c \mp \pi/2. \end{aligned} \tag{55}$$

The coefficients vanish identically for harmonics of order $n = 4m$, so that terms of these orders in the flexure function cannot be determined by this method. Although one may not feel entirely certain that a fourth harmonic will be negligible merely because the third and fifth ones may be found to be so, it appears somewhat improbable that any harmonic (of c) as high as the fourth can really be appreciable, unless it is used to describe a discontinuity. The only likely discontinuity would seem to be in the zenith, and a discontinuity there is readily discoverable and can with advantage be explicitly removed before proceeding to any Fourier analysis; the indeterminacy of the fourth harmonic should then be unimportant. We must, however, consider the case $n = 0$.

A zero harmonic in the "flexure" is the same thing as a constant error in all the circle readings used in flexure work or on stars; it may be put down as a

systematic error in taking the nadir, or as a "wrong" division error of the nadir division. As is well known, this is eliminated by reversal, if it really is a wrong division error; if it is a systematic error in taking the nadir which is not reversed by reversing the instrument, it is in effect a wrong co-latitude. In either case, it seems substantially irrelevant, so far as the astronomical results are concerned.

As there is no absolute term in the trigonometrical series in (55), the quantity v, the intrinsic error of manufacture in the pentag, can be obtained as one of the unknowns. Formally, it might always be convenient to do this; but it seems improbable that its value could be obtained in this way with as much accuracy as should be attainable in a pure laboratory determination. If not, and if the least-squares value always agreed with the laboratory one within their probable errors, one would of course gain by substituting the laboratory value, and transferring the term $2v$ in (55) to the right-hand side.

The unknowns in (55) would evidently all separate completely if observations of stars could be made all round the circle. The total range of c_1-values is much greater than the range of z-values of observable stars, since the pentag allows stars to be observed when the telescope is pointing very considerably below the horizon; but the total range of c-values is of course only the same as the range of observable z, say from $-80°$ to $+80°$, and the range over which three different telescope positions are possible for the same star is appreciably more restricted again, since when the telescope is too far below the horizontal the incoming beam will foul a collimator. There is, however, no star which cannot be observed in at least two positions, and the separation of the unknowns should be quite adequate, for a moderate number of terms.

There seems no need to construct a pentag large enough to cover the entire aperture of the instrument. A four-inch beam will allow observations on a large enough number of stars for a flexure programme, and one would then presumably stop the beam down to this figure whether or not the pentag was in. The various coefficients in (55) can be evaluated for each star in the programme once for all.

If the indeterminacy of the fourth harmonic is considered undesirable, a "pentag" giving some other deflection than 90° could be constructed. The modifications in the analysis are straightforward, but the laboratory determination of the exact angle might be difficult and the astronomical one might have to be accepted; there are also some other disadvantages.

Although errors in positioning the pentag which affect the angle of incidence are completely immaterial, errors which tilt the plane of incidence are not. A small rotation from the correct position, either about the direction of the incoming beam or about the axis of the telescope, will mean that the star is observed somewhat before or after transit, and therefore not quite at culmination. The error should however be easy to allow for, since the error in transit time (which will be known) is of the first order while that in zenith distance is of the second.

It thus appears that use of a pentag should permit a better determination of the flexure than has as yet been possible by any method. It is superior to the mercury pool in permitting a second harmonic to be detected; in permitting observations over a much greater range of z-values, including all values near the zenith itself; and also in being far less liable to be interfered with by a breeze. (Since the mercury pool demands extreme steadiness in the air surrounding it, it introduces a strong temptation to reduce the pavilion aperture dangerously at all times.) The pentag is superior to all "pure" instrumental devices (even

if these were, in their own field, free from objection) in using stellar observations exclusively, so that no systematic error due to the rather different nature of a collimation, or auto-collimation, observation can enter; in addition, of course, it is superior in that it includes the effects of any circle flexure (which no pure instrumental method except the collimator one has yet succeeded in doing), and especially in being almost independent of the precision with which the auxiliary apparatus itself is mounted.

Royal Observatory,
Greenwich:

1955 *March* 17.

References and Notes

(1) F. W. Bessel, *A.N.*, **3**, 209, 1825.
(2) This has been done in the new Washington 7-inch, and it seems to have much to recommend it.
(3) *Pub. U.S. Nav. Obs.*, XV, Part V, 150, 1948.
(4) *Pub. U.S. Nav. Obs.*, IX, Part I, p. A CII, 1920.
(5) M. Loewy, *C.R.*, **87**, 889, 1878; **91**, 6, 1880.
(6) I. Bonsdorff, *Pulk. Obs. Bull.*, VI, **105**, 1915.
(7) *Greenwich Observations*, 1865, etc.; F. W. Dyson and R. T. Cullen, *M.N.*, **84**, 470, 1924.
(8) G. B. Airy, *Mem. R.A.S.*, **32**, 9, 1864.
(9) *Pub. U.S. Nav. Obs.*, IX, Part I, p. A CXVI, 1920.
(10) *Pub. U.S. Nav. Obs.*, XVI, Part I, 1949.
(11) *Pub. U.S. Nav. Obs.*, XVI, Part III, 1952.
(12) This p.e. is taken from the previous series, as none is stated in the later work, but it should presumably hold fairly well for both.
(13) In some cases, e.g. in *Cape Annals*, this term is written as $+\Delta\delta_0$; $\Delta\delta_0$ then has the same sign as the mean of the residuals. However, the quantities ΔL, $\Delta\epsilon$, etc., are corrections, not errors, and it seems more consistent to use the same convention for all.
(14) *Ann. Cape Obs.*, VIII, Part IV, p. 39D, 1915.
(15) The separability of the corrections, if the weights are equal, was noted by Gill (*Ann. Cape Obs.*, II, Part V, p. 9D, 1907), but he did not put the equation in this form.
(16) It is improbable that the circumpolar declinations would tolerate so large a change as this, in lat. 50°; but it has sometimes been found advisable to assume that the refraction south of the zenith is different from that to the north. If one first adds $-0''{\cdot}110\cot\phi$, i.e. $-0''{\cdot}092$, and then adds $0''{\cdot}110(\cot\phi - \tan z)$ to all the solar residuals $\Delta\delta$, one has corrected the south residuals only; equations (40), (41), and (42) are in that case adjusted for a $\Delta\delta_0$ of $+0''{\cdot}30 - 0''{\cdot}09 = +0''{\cdot}21$ and not for $\Delta\delta_0 = +0''{\cdot}30$.

THE ANALYSIS OF THE OBSERVATIONS OF THE VARIATION OF LATITUDE

A. M. Walker and Andrew Young

(Received 1955 April 2*)

Summary

A statistical model of the variation of latitude is formulated and a detailed analysis of its properties is made. Difficulties arising from the necessity to account for observational errors are discussed.

A computational procedure is obtained and applied to a 35-year series of observations in which the z-term has not been taken into account. It is found that the damping factor is

$$\kappa = 0{\cdot}322 \pm 0{\cdot}103 \text{ year}^{-1},$$

giving a relaxation time of about 3·1 years; and the free period is

$$2\pi/\gamma = 1{\cdot}267 \pm 0{\cdot}039 \text{ years}$$
$$= 462{\cdot}8 \pm 14{\cdot}2 \text{ mean solar days.}$$

The value of κ is several times that of the only previous determination, and the free period is longer than has hitherto been determined.

These results are provisional pending the completion of a full numerical analysis.

Part I. *Introduction*

1. If l, m are direction cosines of the instantaneous axis of rotation of the Earth with respect to right-handed axes fixed in the Earth, the dynamical equations of motion may be written

$$\left.\begin{aligned} \dot{l} + \gamma m &= -\omega_0 F/A, \\ \dot{m} - \gamma l &= \omega_0 G/A, \end{aligned}\right\} \tag{1}$$

the solution of which, if l_0, m_0 are the initial values of l and m, is

$$\left.\begin{aligned} l &= l_0 \cos\gamma t - m_0 \sin\gamma t + l_1, \\ m &= l_0 \sin\gamma t + m_0 \cos\gamma t + m_1. \end{aligned}\right\} \tag{2}$$

Here, $2\pi/\gamma$ is the so-called Chandler period of the (circular) free component of the motion, ω_0 is the mean angular velocity of the Earth, (A, A, C) are the moments of inertia and F and G are the products of inertia of the Earth. Assuming that the products of inertia are periodic with periodicities of a year and sub-multiples of a year, the forced motion, l_1, m_1, will have elliptical components corresponding to each period in F and G.

This dynamical theory suggests that harmonic analysis of values of l and m, which are observed as the variation of latitude, should yield the value of the Chandler period and the various periods of the forced motion. However, very many investigations over different intervals have been made by a number of workers and have all yielded different values of the Chandler period. As early as 1917, Kimura gave an empirical formula for $2\pi/\gamma$ containing components with periods of 22, 26·67, 50 and 80 years from which Melchior (1) has calculated a table of values of the Chandler period during the interval 1900–1960. The maximum value

* Received in original form 1954 October 18.

is 1·2066 years in 1914 and the minimum is 1·1123 years in 1929. Different authors have found, by harmonic analysis of different intervals, Chandler periods within this range of values. Melchior has developed a theory relating variations of the Chandler period to changes in the axes of the elliptic forced motion.

In 1940, Harold Jeffreys (**2**) rejected the validity of harmonic analysis as a means of determining the Chandler period on the ground that undamped free vibrations in the sense of elementary dynamics probably have no physical existence. Irregular disturbances of the motion may well repeatedly change the phase of the motion; despite this there exists a natural free period.

The appearance of the series of observations suggests that statistical fluctuations are not negligible, and harmonic analysis cannot take such fluctuations adequately into account. Jeffreys's paper, in fact, contains the only example so far published of an analysis which is based on a proper statistical model. Jeffreys's treatment is re-examined in this paper in the light of recent developments in the theory of time series analysis. The problems of estimation and statistical inference associated with his model are discussed in detail, account being taken of the fact that the effect of observational errors may not be negligible. The theory of the statistical analysis is given below in Part II. The principal steps of the computational procedure based on the statistical analysis are outlined at the beginning of Part III, which contains the results of carrying out this analysis on a certain series of observations.

An analysis of the residual motion is given in Part IV.

Part II. *The Statistical Model*

2. *Specification of the statistical model.*—The equations of motion (1), including a damping term, may be written

$$\left.\begin{aligned} \dot{l}+\kappa l+\gamma m &= -F_1, \\ \dot{m}+\kappa m-\gamma l &= \ \ G_1, \end{aligned}\right\} \tag{3}$$

where $F_1=\omega_0 F/A$, $G_1=\omega_0 G/A$ and κ is the coefficient of damping.

Now let

$$\left.\begin{aligned} F_1(t) &= F_S(t)+f_1(t), \\ G_1(t) &= G_S(t)+g_1(t), \end{aligned}\right\} \tag{4}$$

where F_S, G_S are the systematic parts of F_1 and G_1 respectively and $f_1(t)$, $g_1(t)$ are the fluctuation terms, $\{f_1(t), g_1(t)\}$ being in fact a stochastic process in two variables with zero means. We make the usual assumption that F_S and G_S have a yearly period, and can be represented to a sufficiently good approximation by the first few terms of their Fourier series, e.g.

$$F_S(t)=c_f+\sum_{r=1}^{p}(a_{fr}\cos \nu r t+b_{fr}\sin \nu r t),$$

where p is a small integer and $2\pi/\nu=1$ year.

The simplest statistical assumption as regards the fluctuation terms is that $\{f_1(t)\}$ and $\{g_1(t)\}$ are independent stationary impulse processes. This means that only the integrals $I(t)=\int^t f_1(u)du$ and $J(t)=\int^t g_1(u)du$ strictly exist, $\{I(t)\}$ and $\{J(t)\}$ being statistically independent homogeneous additive processes, characterized by the property that the change of I (or J) in any time interval depends only on the length of the interval, and changes in non-overlapping

time intervals are statistically independent of one another (see e.g. Bartlett (3), Chapter III, Section 6, and Moyal (4), page 165). If the impulses are discrete, the changes in I or J are discontinuous.

From (3), F_S and G_S give rise to forced components $l_s(t)$ and $m_s(t)$ of the same form (the damped components may be ignored since the motion may be assumed to have started a very long time ago); and for the fluctuation terms we have

$$x(t)+iy(t)=\int^t e^{(i\gamma-\kappa)(t-u)}(i\,dJ(u)-dI(u)), \tag{5}$$

where

$$\left.\begin{aligned} x(t)&=l(t)-l_s(t),\\ y(t)&=m(t)-m_s(t). \end{aligned}\right\} \tag{6}$$

Thus x, y are the contributions to the motion of the statistical fluctuations in the products of inertia of the Earth.

If we now consider observations at times separated by a constant interval h, and write

$$\begin{aligned} l_n&=l(t_0+nh)=l_{sn}+x_n,\\ m_n&=m(t_0+nh)=m_{sn}+y_n, \end{aligned}$$

we find that

$$\left.\begin{aligned} x_{n+1}-\alpha x_n+\beta y_n&=\epsilon_{n+1},\\ y_{n+1}-\beta x_n-\alpha y_n&=\eta_{n+1}, \end{aligned}\right\} \tag{7}$$

where

$$\left.\begin{aligned} \alpha&=e^{-\kappa h}\cos\gamma h,\\ \beta&=e^{-\kappa h}\sin\gamma h,\\ \epsilon_{n+1}&=-\int_0^h e^{-\kappa u}\{\cos\gamma u\,dI(\overline{n+1}h-u)+\sin\gamma u\,dJ(\overline{n+1}h-u)\},\\ \eta_{n+1}&=\int_0^h e^{-\kappa u}\{\cos\gamma u\,dJ(\overline{n+1}h-u)-\sin\gamma u\,dI(\overline{n+1}h-u)\}. \end{aligned}\right\} \tag{8}$$

The residuals $\{\epsilon_n, \eta_n\}$ form an independent stationary process, i.e. its properties are invariant under translation of the time axis, and $\{\epsilon_{n+r}, \eta_{n+r}\}$, $(r=0, 1, 2\ldots)$ are all statistically independent. If we make the further natural assumption that the rates of increase of variance per unit time for I and J are equal, we have also

$$\left.\begin{aligned} \operatorname{var}\epsilon_n&=\operatorname{var}\eta_n=\sigma^2 \text{ say},\\ \text{and}\qquad \operatorname{cov}(\epsilon_n,\eta_n)&=0. \end{aligned}\right\} \tag{9}$$

Thus we have arrived at a model identical with that postulated by Jeffreys (2, page 143) apart from his additional assumption that the residuals follow a normal distribution.

Our assumptions for the fluctuation terms can of course give only a very approximate representation of the actual mechanism, but an analysis based on them may nevertheless still be sufficiently accurate to be useful. That Jeffreys's model follows from our statistical treatment may be regarded as an argument for using this as a working hypothesis. In (2) the model is introduced by analogy with Yule's treatment of the problem of a pendulum bombarded by randomly arriving particles, but this has since been shown to be incorrect (see e.g. Bartlett (5), page 35).

The assumption of normality of the residuals is more difficult to justify. This is approximately true only provided that the mean number of impulses during the interval of observation, h, is large, a condition which is perhaps not very realistic for values of h which are usually considered in practice (of the order of a month). Jeffreys even claims (**2**, page 148) to have identified a period of more than 12 years during which the effects of fluctuations were negligible. Hence it is advisable to dispense with the normality assumption if at all possible. It is not difficult to show that we can do so provided that the effect of observational error can be ignored, so that equations (7) can be used as they stand. However, as Jeffreys points out, observational errors are not necessarily small compared with x_n and y_n, so that they should be allowed for in the model. Unfortunately when this is done an important part of the analysis becomes very complicated unless the residuals are normally distributed, and indeed is tractable only when both the residuals and observational errors are normally distributed.

We therefore re-define (x_n, y_n) to include the effect of errors of observation and assume that

$$\left.\begin{aligned} x_n &= x'_n + u_n, \\ y_n &= y'_n + v_n, \end{aligned}\right\} \tag{10}$$

where both $\{x_n', y_n'\}$, which satisfies (7), and the errors of observation, $\{u_n, v_n\}$, are normal. It seems reasonable to assume that

$$\left.\begin{aligned} \operatorname{var} u_n &= \operatorname{var} v_n = \sigma'^2, \text{ say}, \\ \operatorname{cov}(u_n, v_n) &= 0, \end{aligned}\right\} \tag{11}$$

and $\{u_{n+r}, v_{n+r}\}$, $(r = 0, 1, 2, \ldots)$, are all statistically independent and also that $\{u_n, v_n\}$ is statistically independent of the series $\{x'_n, y'_n\}$.

These properties, together with

$$\left.\begin{aligned} l_{sn} &= c_l + \sum_{r=1}^{p} (a_{lr} \cos vrnh + b_{lr} \sin vrnh), \\ m_{sn} &= c_m + \sum_{r=1}^{p} (a_{mr} \cos vrnh + b_{mr} \sin vrnh), \end{aligned}\right\} \tag{12}$$

and

$$\left.\begin{aligned} x_{n+1} - \alpha x_n + \beta y_n &= \epsilon_{n+1} + u_{n+1} - \alpha u_n + \beta v_n = \epsilon'_{n+1}, \text{ say}, \\ y_{n+1} - \beta x_n - \alpha y_n &= \eta_{n+1} + v_{n+1} - \beta u_n - \alpha v_n = \eta'_{n+1}, \text{ say}, \end{aligned}\right\} \tag{13}$$

completely specify the model. Equation (12) specifies the true dynamical contributions to the motion as opposed to the statistical fluctuations; equation (13) results from inserting (10) in (7).

3. *Correlational and spectral properties of the model.*—It is not difficult to show from (13) that the autocovariance matrix for lag s, defined by

$$V(s) = \begin{bmatrix} \overline{x_n x_{n+s}} & \overline{x_n y_{n+s}} \\ \overline{y_n x_{n+s}} & \overline{y_n y_{n+s}} \end{bmatrix},$$

is given by

$$\left.\begin{aligned} V(s) &= \left\{\frac{\sigma^2 e^{-\alpha s h}}{1 - e^{-2\alpha h}}\right\} \begin{bmatrix} \cos s\gamma h & \sin s\gamma h \\ -\sin s\gamma h & \cos s\gamma h \end{bmatrix}, \qquad (s > 0), \\ V(0) &= \left\{\sigma'^2 + \frac{\sigma^2}{1 - e^{-2\alpha h}}\right\} \begin{bmatrix} 1 & 0 \\ 0 & 1 \end{bmatrix}. \end{aligned}\right\} \tag{14}$$

The autocorrelation matrix for lag s, ($s>0$), obtained by replacing x_n, y_n in $V(s)$ by $x_n/\sigma(x)$, $y_n/\sigma(y)$, where $\sigma^2(x)=\text{var}\,x$, $\sigma^2(y)=\text{var}\,y$, is therefore

$$R(s)=\lambda e^{-\kappa sh}\begin{bmatrix}\cos s\gamma h & \sin s\gamma h\\ -\sin s\gamma h & \cos s\gamma h\end{bmatrix}, \tag{15}$$

where

$$\lambda=\sigma^2/\{\sigma^2+\sigma'^2(1-e^{-2\kappa h})\}. \tag{16}$$

Equation (15) summarizes the main correlational properties of the model and was in effect given by Jeffreys. The theoretical correlograms for the autocorrelations of the $\{x\}$ and $\{y\}$ series are identical, consisting of an exponentially damped simple harmonic oscillation, and a phase shift of 90° yields the theoretical correlogram for the cross-correlations.

This result expresses the physical fact that, apart from the damping, the expected motion is given by a simple rotation of the pole about its mean position through the angle $s\gamma h$ in time sh. The effect of the observational errors is seen in the reduction of all the lag correlations by the factor λ.

We also note that the spectral density matrix $F(\omega)=(1/2\pi)\sum_{s=-\infty}^{\infty}V(s)e^{-is\omega}$, i.e. the Fourier transform of the autocorrelation matrix, is given by

$$2\pi F(\omega)=\sigma'^2\begin{bmatrix}1 & 0\\ 0 & 1\end{bmatrix}+\sigma^2\{(1+\alpha^2+\beta^2-2\alpha\cos\omega)^2-4\beta^2\sin^2\omega\}^{-1}$$
$$\times\begin{bmatrix}1+\alpha^2+\beta^2-2\alpha\cos\omega & -2i\beta\sin\omega\\ 2i\beta\sin\omega & 1+\alpha^2+\beta^2-2\alpha\cos\omega\end{bmatrix}. \tag{17}$$

4. *Analysis of the systematic components of the variation.*—We now have to consider methods of estimating the unknown parameters in the model, and of calculating the precision of our estimates, given an actual series of observations $\{l_r, m_r\}$ $(r=1, 2, \ldots N)$. There is also the associated problem of testing whether the model is consistent with the observations. The parameters fall naturally into two groups, the first consisting of those which occur in the equations (12), i.e. c_l, a_{lr}, b_{lr}, c_m, a_{mr}, b_{mr}, defining the systematic components of the variation, and the second of those associated with the equations (8) and (13), i.e. α, β (or κ and γ), σ^2 and σ'^2, which define the behaviour of the fluctuations. The two groups can be dealt with to a large extent independently of each other; we must however begin by considering estimates of the parameters in the first group, since these are required before we can calculate the estimates for the second group. We shall assume from now on that N is sufficiently large for an asymptotic theory to be used; this may not necessarily be true in practice (see Section 6 below), but no exact theory has yet been developed.

It can be shown by using an approach due to Whittle (**6, 7**) that the maximum likelihood estimates are asymptotically the same as those obtained by standard harmonic analysis i.e.

$$\left.\begin{aligned} c^*_l&=\frac{1}{N}\sum_{i=1}^{N}l_i, \qquad a^*_{lr}=\frac{2}{N}\sum_{i=1}^{N}l_i\cos vrih, \qquad b^*_{lr}=\frac{2}{N}\sum_{i=1}^{N}l_i\sin vrih,\\ c^*_m&=\frac{1}{N}\sum_{i=1}^{N}m_i, \quad a^*_{mr}=\frac{2}{N}\sum_{i=1}^{N}m_i\cos vrih, \quad b^*_{mr}=\frac{2}{N}\sum_{i=1}^{N}m_i\sin vrih.\end{aligned}\right\} \tag{18}$$

They are asymptotically unbiased (and are in fact exactly unbiased if the observations cover a number of complete years). Their asymptotic variances

and covariances are given by the inverse of the information matrix as in classical maximum likelihood theory, but are easily obtained directly. We find that the estimates fall into asymptotically uncorrelated groups (c^*_{l1}, c^*_{m}), $(a^*_{l1}, a^*_{m1}, b^*_{l1}, b^*_{m1})$, $(a^*_{l2}, a^*_{m2}, b^*_{l2}, b^*_{m2})$, etc., and that if we write $\mathbf{c}^{*\prime}=(c^*_{l1}, c^*_{m})$, $\mathbf{a}^*_1{}'=(a^*_{l1}, a^*_{m1})$, $\mathbf{b}^*_1{}'=(b^*_{l1}, b^*_{m1})$, etc., these being row vectors and $\mathbf{c}^*$, $\mathbf{a}^*_1$, $\mathbf{b}^*_1$, etc. the corresponding column vectors,

$$\left.\begin{aligned} &\operatorname{cov}(\mathbf{c}^*, \quad \mathbf{c}^{*\prime}) \sim 2\pi F(0)/N, \\ &\operatorname{cov}(\mathbf{a}^*_r, \mathbf{a}^*_r{}') \sim \operatorname{cov}(\mathbf{b}^*_r, \mathbf{b}^*_r{}') \sim 2\mathscr{R}\{2\pi F(vrh)\}/N, \\ &\operatorname{cov}(\mathbf{a}^*_r, \mathbf{b}^*_r{}') \sim -2\mathscr{I}\{2\pi F(vrh)\}/N, \end{aligned}\right\} \tag{19}$$

where $F(\omega)$ is the spectral density matrix given by (17), and the symbols $\mathscr{R}$ and $\mathscr{I}$ denote real and imaginary parts. Thus c^*_l, c^*_m are asymptotically uncorrelated and have variance

$$\left\{\sigma'^2 + \frac{\sigma^2}{1+\alpha^2+\beta^2-2\alpha}\right\}\Big/N$$

and the asymptotic covariance matrix for the group $(a^*_{lr}, a^*_{mr}, b^*_{lr}, b^*_{mr})$ is

$$\begin{array}{c} \\ a^*_{lr} \\ a^*_{mr} \\ b^*_{\ r} \\ b^*_{mr} \end{array}\!\!\begin{array}{c} \begin{array}{cccc} a^*_{lr} & a^*_{mr} & b^*_{lr} & b^*_{mr} \end{array} \\ \begin{bmatrix} P_r & 0 & 0 & -Q_r \\ 0 & P_r & Q_r & 0 \\ 0 & Q_r & P_r & 0 \\ -Q_r & 0 & 0 & P_r \end{bmatrix} \end{array} \tag{20}$$

where

$$P_r = \frac{2}{N}\left\{\sigma'^2 + \frac{\sigma^2(1+\alpha^2+\beta^2-2\alpha\cos vrh)}{(1+\alpha^2+\beta^2-2\alpha\cos vrh)^2-4\beta^2\sin^2 vrh}\right\},$$

and

$$Q_r = \frac{4}{N}\left\{\frac{-\sigma^2\beta\sin vrh}{(1+\alpha^2+\beta^2-2\alpha\cos vrh)^2-4\beta^2\sin^2 vrh}\right\}. \tag{21}$$

All these estimates are also distributed asymptotically in the multivariate normal form, so that we can not only calculate their estimated standard errors, once estimates of α, β, σ^2, σ'^2, with standard errors which tend to zero as $N\to\infty$, have been obtained (estimates which have standard errors proportional to $1/\sqrt{N}$ are given in Section 5), but can also derive approximate tests of significance and confidence intervals for the true values of the parameters. For example, a^*_{lr} would be regarded as differing from zero at a level of probability approximately equal to 0·95 if it was greater in magnitude than $1{\cdot}96\sqrt{P^*_r}$, where P^*_r denotes the estimated value of P_r. Again the significance of the whole set of estimates $(a^*_{lr}, a^*_{mr}, b^*_{lr}, b^*_{mr})$ of the $(r-1)$th harmonic components could be judged by referring the expression

$$\{P^*_r(a^*_{lr}{}^2+a^*_{mr}{}^2+b^*_{lr}{}^2+b^*_{mr}{}^2)+2Q^*_r(a^*_{lr}b^*_{mr}-a^*_{mr}b^*_{lr})\}/(P^*_r{}^2-Q^*_r{}^2)$$

to a χ^2 distribution with four degrees of freedom; this follows from the fact that the inverse of the matrix (20) is

$$\frac{1}{(P_r^2-Q_r^2)}\begin{bmatrix} P_r & 0 & 0 & Q_r \\ 0 & P_r & -Q_r & 0 \\ 0 & -Q_r & P_r & 0 \\ Q_r & 0 & 0 & P_r \end{bmatrix}.$$

The latter test is useful in the problem of deciding on the appropriate value of p, i.e. on the order of the highest harmonics which should be included in the systematic variation. This cannot be specified exactly theoretically although it may be assumed that the amplitudes of the harmonic terms will, on the whole,

decrease as their order increases. Thus one might proceed by first allowing for fundamental terms only, i.e. taking $p=1$, and testing whether their amplitudes differ significantly from zero; then if they do so (which should certainly be the case here) taking $p=2$ and testing whether the amplitudes of the first harmonic terms differ significantly from zero, and so on, the value of p finally adopted corresponding to the order of the last harmonic terms whose amplitudes were significant. This method is somewhat laborious, since at each stage the estimates α^*, β^*, σ^{*2}, $\sigma^{*\prime 2}$ occurring in P^*_r and Q^*_r have to be recalculated, and will of course be misleading if some high-order harmonic has a fairly large amplitude; but it becomes more satisfactory if we increase the value of p by more than unity at each stage, and also continue as a check for at least one stage beyond that which first yields no significant harmonic terms. However, if the interval between consecutive observations is a rational fraction of the period (i.e. a year), there will be a maximum number of distinguishable harmonic terms irrespective of the number of observations, and if this number is not too large, it will be best to include them all in the specification (12) and carry out a complete harmonic analysis, even though some terms are found subsequently not to be significantly different from zero (see Section 9).

It may be noted that the above analysis can be shown to be asymptotically valid even when the residual fluctuations $\{\epsilon_n, \eta_n\}$ and the observational errors $\{u_n, v_n\}$ are not normally distributed. It is sufficient that the statistical independence properties stated in Section 2 should hold. The estimates (18) are of course then no longer maximum likelihood estimates.

There remains the question as to whether equations of the type (12) give a satisfactory representation of the systematic variation. Here, however, there is the difficulty that to test whether the observations are consistent with the model we must in general postulate some alternative hypothesis for the form of the systematic variation: for example, that we require additional terms $d_l n$ and $d_m n$ in l_{sn} and m_{sn} respectively to take account of a linear trend (corresponding perhaps to variation with a very long period). The only practicable way of avoiding this difficulty seems to be to divide the series into several consecutive sub-series, from each of which estimates of the form (18) are obtained. Then if the sub-series are sufficiently long for the asymptotic formulae (19) to apply, and for the correlations between the estimates for the different sub-series to be neglected, it is fairly easy to test whether corresponding estimates differ significantly. It is of course useful to examine the graphs of the estimated l and m residuals

$$\left.\begin{aligned} l_n^* &= l_n - c^*_l - \sum_{r=1}^{p} \{a^*_{lr} \cos vrnh + b^*_{lr} \sin vrnh\}, \\ m_n^* &= m_n - c^*_m - \sum_{r=1}^{p} \{a^*_{mr} \cos vrnh + b^*_{mr} \sin vrnh\}, \end{aligned}\right\} \tag{22}$$

plotted against n, in case these reveal any unusual features (but see Section 12).

5. *Analysis of the fluctuation components.*—Estimates of the second group of parameters α, β, σ^2 and σ'^2 are obtained from the auto-covariances and cross-covariances of the series $\{l_n^*, m_n^*\}$, which are defined by

$$\left.\begin{aligned} c_{11}(r) &= \frac{1}{N-r} \sum_{n=1}^{N-r} l_n^* l_{n+r}^*, \quad c_{22}(r) = \frac{1}{N-r} \sum_{n=1}^{N-r} m_n^* m_{n+r}^*, \\ c_{12}(r) &= \frac{1}{N-r} \sum_{n=1}^{N-r} l_n^* m_{n+r}^*, \quad c_{21}(r) = \frac{1}{N-r} \sum_{n=1}^{N-r} m_n^* l_{n+r}^*. \end{aligned}\right\} \tag{23}$$

The effect of the differences between l_n^* and x_n, and between m_n^* and y_n will become negligible for sufficiently large N, so that we can regard $c_{11}(r)$ as equivalent to

$$\frac{1}{N-r}\sum_{n=1}^{N-r} x_n x_{n+r}, \text{ and so on.}$$

If we do not take account of observational error, i.e. assume that $\sigma'^2=0$, the procedure is straightforward. Maximum likelihood estimates of α and β are asymptotically equivalent to those obtained by the method of least squares, i.e. by minimizing

$$\sum_n [(l_{n+1}^* - \alpha l_n^* + \beta m_n^*)^2 + (m_{n+1}^* - \beta l_n^* - \alpha m_n^*)^2],$$

which gives

$$\left.\begin{aligned} \alpha^* &= \{c_{11}(1)+c_{22}(1)\}/\{c_{11}(0)+c_{22}(0)\}, \\ \beta^* &= \{c_{12}(1)-c_{21}(1)\}/\{c_{11}(0)+c_{22}(0)\}. \end{aligned}\right\} \tag{24}$$

Also σ^{*2} is obtained as the mean square residual, equivalent to

$$\sigma^{*2} = \tfrac{1}{2}\{c_{11}(0)+c_{22}(0)\}\{1-\alpha^{*2}-\beta^{*2}\}. \tag{25}$$

It is easily shown that α^* and β^* are asymptotically unbiased and that

$$\operatorname{var}\alpha^* \sim \operatorname{var}\beta^* \sim \{1-\alpha^2-\beta^2\}/2N = (1-e^{-2\kappa h})/2N \tag{26}$$

$\operatorname{cov}(\alpha^*, \beta^*)\sim 0$, whence with estimates of κ and γ obtained from

$$e^{-2\kappa^* h} = \alpha^{*2}+\beta^{*2}, \qquad \cot\gamma^* h = \alpha^*/\beta^*, \tag{27}$$

these being also asymptotically unbiased, we find that

$$\operatorname{var}(\kappa^* h) \sim \operatorname{var}(\gamma^* h) \sim \{e^{2\kappa h}-1\}/2N. \tag{28}$$

These formulae remain valid when the ϵ_n and η_n are not normally distributed, although the estimates are not then equivalent to those obtained by the method of maximum likelihood.

In the general case, however, the maximum likelihood approach becomes very complicated. It is possible to proceed by the method of Whittle (**7**) but this involves very lengthy algebraic calculations, and yields a set of equations which are difficult to solve. A more practical method consists of using covariances for lags h and rh, as suggested by Jeffreys. The above estimate of γ, given by

$$\cot\gamma^* h = \{c_{11}(1)+c_{22}(1)\}/\{c_{12}(1)-c_{21}(1)\} = p(1)/q(1), \text{ say,} \tag{29}$$

where

$$p(r) = c_{11}(r)+c_{22}(r), \qquad q(r) = c_{12}(r)-c_{21}(r), \tag{30}$$

is easily seen (remembering equation (15)) to be consistent, i.e. to differ from γ by not more than any pre-assigned quantity ϵ, however small, with probability arbitrarily near unity, if N is taken to be sufficiently large. Similarly $\{p(r)\}^2+\{q(r)\}^2$ is found to be a consistent estimate of $4\sigma^4 e^{-2r\kappa h}/(1-e^{-2\kappa h})^2$, and so a consistent estimate of κ is given by

$$e^{2\kappa^* h(r-1)} = [\{p(1)\}^2+\{q(1)\}^2]/[\{p(r)\}^2+\{q(r)\}^2]. \tag{31}$$

The best value of r to take is not obvious. Clearly for large r the precision of κ^* will be low since the expected value of the denominator in (31) tends to zero exponentially with r, but there is also the effect of the final division by $r-1$. Jeffreys states that r should be chosen so that $e^{-r\kappa h}$ is about 0·45, but does not explain how he arrives at this result, and it is incorrect at least in the case of small κh, for which it can be shown that when $\lambda \simeq 1$, i.e. the observational error variance

is small, r should be as small as possible (see Section 6). In view of this, and the fact that the precision of κ^* can be calculated most accurately for small r, it seems best in general to use (31) with $r=2$.

It is easy to see that γ^* and κ^* are asymptotically unbiased, and that their asymptotic standard errors are proportional to $1/\sqrt{N}$. Formulae for these may be obtained by expressing $\gamma^*-\gamma, \kappa^*-\kappa$ as asymptotic linear functions of the quantities $\delta p(1)$, $\delta q(1)$, $\delta p(r)$, $\delta q(r)$ (where $\delta p(1)=p(1)-\overline{p(1)}$ and $\overline{p(1)}$ is the mathematical expectation of $p(1)$, etc.), and then using the expressions for the asymptotic variances and covariances of the p's and q's. The latter follow from formulae of the type

$$\operatorname{cov}\{c_{12}(r),\, c_{34}(r+s)\}=\left\{\frac{1}{(N-r)(N-r-s)}\right\}\sum_{i,\,j}\operatorname{cov}\{X_1(i)X_2(i+r),\, X_3(j)X_4(j+r+s)\}$$

$$\sim\left\{\frac{\sigma_1\sigma_2\sigma_3\sigma_4}{N-r}\right\}\sum_{v=-\infty}^{\infty}\{\rho_{13}(v)\rho_{24}(v+s)+\rho_{23}(v)\rho_{14}(v+2r+s)\}, \tag{32}$$

where e.g.

$$\operatorname{cov}\{X_1(i),\, X_3(i+v)\}=\sigma_1\sigma_3\rho_{13}(v). \tag{33}$$

(In this paper the sign $\sim$ means " is asymptotically equal to ".)
For instance we find that

$$(N-r)\operatorname{var}p(r)\sim 2\{\sigma'^2+\sigma^2/(1-e^{-2\kappa h})\}^2$$
$$\times\left[\frac{\lambda^2}{1-e^{-2\kappa h}}\left(1+e^{-2\kappa h}+e^{-2r\kappa h}\cos 2r\gamma h\{2r+1-(2r-1)e^{-2\kappa h}\}\right)\right.$$
$$\left.+(1-\lambda)\{1+\lambda(1+2e^{-2r\kappa h}\cos 2r\gamma h)\}\right].$$

After some rather heavy algebra, we arrive at the results

$$\operatorname{var}\gamma^* h\sim\left(\frac{e^{2\kappa h}}{2N}\right)\left[1-e^{-2\kappa h}+\frac{1-\lambda}{\lambda^2}\left(1+\lambda\{1+2e^{-2\kappa h}\}\right)\right], \tag{34}$$

$$\operatorname{var}\{\kappa^* h(r-1)\}\sim\frac{1}{2N}\left[\frac{e^{2r\kappa h}+e^{2(r-1)\kappa h}-2+(2r-1)(1-e^{2\kappa h})}{1-e^{-2\kappa h}}\right.$$
$$\left.+\frac{(1-\lambda^2)e^{2r\kappa h}+(1-\lambda)(1-3\lambda)e^{2\kappa h}}{\lambda^2}\right]. \tag{35}$$

In particular for $r=2$, (35) gives

$$\operatorname{var}\kappa^* h=\frac{e^{2\kappa h}}{2N\lambda^2}\{e^{2\kappa h}-1+2(1-\lambda)^2\}. \tag{36}$$

To estimate λ, we may use the equation

$$\lambda^{*2}e^{-2\kappa^* h}=[\{p(1)\}^2+\{q(1)\}^2]/[\{p(0)\}^2+\{q(0)\}^2]. \tag{37}$$

From (34) and (35) we obtain estimated standard errors of κ^* and γ^* on substituting κ^* and λ^* for κ and λ, and hence approximate confidence limits for κ and γ, since κ^* and γ^* can be shown to be asymptotically normally distributed. λ^* is also asymptotically normally distributed, with mean λ and variance

$$\operatorname{var}\lambda^*\sim[\lambda^2(e^{2\kappa h}-1)^2+2\lambda(1-\lambda)(e^{4\kappa h}-1)+(1-\lambda)^2(e^{4\kappa h}+4e^{2\kappa h}+2)]/2N. \tag{38}$$

We can therefore assess approximately the significance of the difference of λ^* from unity. If λ^* was considered not to be significantly lower than unity at an appropriate probability level, we should regard the observations as consistent with the

hypothesis that observational errors can be neglected. Finally a consistent estimate of σ^2, which is required in the estimation of the variances and covariances (19) of the harmonic components, may be obtained from the equation

$$\tfrac{1}{2}\{c_{11}(0)+c_{22}(0)\}=\sigma^{*\prime 2}+\sigma^{*2}/(1-e^{-2\kappa^* h})=\sigma^{*2}/\{\lambda^*(1-e^{-2\kappa^* h})\}. \qquad (39)$$

It should be noted that the normality assumptions of Section 2 are really used only in the derivation of equations (34), (35) and (38). Without these assumptions it is in general very troublesome to derive expressions for the asymptotic variances of γ^*, κ^* and λ^*, and the estimation of the variances is no longer straightforward.

The validity of the correlational structure given by the model (13) may be examined by comparing the sample covariances $c_{ij}(r)$ with the theoretical covariances $V_{ij}(r)$ defined by (14), or the sample correlations (obtained by dividing the corresponding covariances by $\sqrt{\{c_{ii}(0)c_{jj}(0)\}}$) with the theoretical correlations $R_{ij}(r)$ defined by (15). We can, for example, use the goodness-of-fit test associated with the "*G*-operators" introduced by Bartlett and Rajalakshman (**8**); this can be shown to be applicable here although the model is more general than those considered in their paper. In addition we can test whether $c_{11}(0)/c_{22}(0)$ and $c_{12}(0)$, which are asymptotically uncorrelated with the "*G*-forms" and with each other, differ significantly from 1 and 0 respectively, using the expressions for their asymptotic standard errors obtained by means of the general formula (32). It seems, however, difficult to construct a suitable test of the assumption that the residuals are normally distributed. Some indication of the appropriateness of the assumption may be obtained by constructing frequency distributions of $l_{n+1}^*-\alpha^* l_n^*+\beta^* m_n^*$ and $m_{n+1}^*-\beta^* l_n^*-\alpha^* m_n^*$, but it is not known how the significance of deviations of these from the normal form should be assessed; the standard χ^2 distribution certainly cannot be used.

6. *The effect of a small damping factor.*—Difficulties may occur in the above analysis if κh, the product of the damping factor and the interval between consecutive observations, is small. We then have from (35), provided that $r\kappa h$ is also small,

$$\operatorname{var}\{\kappa^* h(r-1)\}\simeq\frac{1}{N\lambda^2}\,[\lambda^2(r-1)^2\kappa h+(1-\lambda)^2+(1-\lambda)\kappa h\{2\lambda(r-1)+(1-\lambda)(r+1)\}], \qquad (40)$$

so that if $V(\kappa^*)$ denotes the coefficient of variation of κ^*,

$$\{V(\kappa^*)\}^2\simeq\frac{1}{N\kappa h}+\frac{(1-\lambda)^2+(1-\lambda)\kappa h\{2\lambda(r-1)+(1-\lambda)(r+1)\}}{N\lambda^2\kappa^2 h^2(r-1)^2}. \qquad (41)$$

If $r\kappa h$ is not necessarily small, the first term on the right-hand side of (41) is replaced by $(e^{2y}-1-2y)/2N\kappa h y^2$, where $y=(r-1)\kappa h$. Since this increases with y, $V(\kappa^*)$ will be approximately minimized by taking r to be as small as possible, i.e. $r=2$, when $1-\lambda$ is sufficiently small for the remaining terms to be neglected. If the latter are taken into account, the choice of y to minimize $V(\kappa^*)$ depends on κ and λ in a rather complicated way; however, as was indicated in Section 5, the accuracy of the approximation (35) tends to decrease as r increases, and the value $r=2$ seems suitable in general.

Since, to a good approximation, $V(\kappa^*)\geqslant(N\kappa h)^{-1/2}$ it is desirable that $N\kappa h$ should be appreciably greater than unity. Indeed, when this is not so, the approximate lower confidence limit for κ, given e.g. by $\kappa^*\{1-1{\cdot}96V^*(\kappa^*)\}$ for a confidence probability of 0·95, where $V^*(\kappa^*)$ is the estimated coefficient of variation, is likely to be negative, no matter how small the observational errors

may be. Thus, since negative values of κ are inadmissible, we can only consider the upper confidence limit; the precision of κ^*, or the estimate $1/\kappa^*$ of the "relaxation time", which has to a good approximation the same coefficient of variation $V(\kappa^*)$, cannot then be regarded as satisfactory.

There is, however, a more serious difficulty when the condition $N\kappa h \gg 1$ is not satisfied. This is that the asymptotic formulae for var $(\kappa^* h)$ and var $(\gamma^* h)$, the latter being approximately $(1/2N\lambda^2)[2\kappa h+(1-\lambda)(1+3\lambda)]$ for small κh, may no longer be good approximations. For the representation of $\gamma^*-\gamma$ and $\kappa^*-\kappa$ as linear functions of the $\delta p(r)$ and $\delta q(r)$, used in their derivation, is valid only on the assumption that the coefficients of variation of $p(r)$ and $q(r)$ are small, and it can be shown that (provided λ is not small) these coefficients of variation are both approximately equal to $(N\kappa h)^{-1/2}$. (This assumes that the asymptotic formulae for var $p(r)$ and var $q(r)$ are still applicable; it is difficult to estimate the relative error of these, but a rough argument suggests that they are of the same order of magnitude as that caused by replacing $\sum_{v=0}^{N} e^{-2v\kappa h}$ by $\sum_{v=0}^{\infty} e^{-2v\kappa h}$, i.e. as $e^{-2(N+1)\kappa h}$, which is e.g. less than 0·05 when $N\kappa h > 1{\cdot}5$.) The same difficulty arises in connection with the formula (38) for var λ^*. A further point is that the distributions of $\kappa^* h$, $\gamma^* h$ and λ^* may then no longer be approximately normal.

These difficulties are really due to the fact that when κh is sufficiently small the elements of the autocorrelation matrix decrease very slowly as the lag increases. In particular, when the effect of observational errors is small, so that we have $\lambda \simeq 1$, this can be shown to imply that the observations are equivalent to a very small number of independent observations, and hence we should not expect the asymptotic theory to apply.

A more refined method of statistical analysis which avoids these difficulties does not seem to be available at present; in any case it is conjectured that when $N\kappa^* h$ is of order unity, i.e. the time Nh covered by the observations is comparable with the estimated "relaxation time", it is not possible to obtain much information about the true values of the parameters in the model.

Jeffreys (**2**) estimated κ to be about 0·06, the unit of time being a year. Part of the evidence for this estimate is provided by a statistical analysis of a series of 154 observations at intervals of 0·3 year. However, with $N=154$, $h=0{\cdot}3$, $\kappa=0{\cdot}06$, $N\kappa h$ is only 2·8, so that the above difficulties certainly arise. In fact if we substitute these values of N, κ, h together with the value $\lambda=0{\cdot}933$ given by Jeffreys (**2**, p. 145) in (41) we obtain $V(\kappa^*)=0{\cdot}72$, which is sufficiently large to indicate that the analysis is not satisfactory If Jeffreys's estimate were accurate we should have the same situation arising in the analysis of the series of observations used in Part III below, for which $N=420$, $h=\frac{1}{12}$. However, our estimate of κ turns out to be much larger, i.e. $\kappa^*=0{\cdot}322$, giving $N\kappa^* h=11{\cdot}3$, and an estimated coefficient of variation $V^*(\kappa^*)=0{\cdot}31$. This value of $N\kappa^* h$ is not particularly large, and some doubt may therefore be felt as to the accuracy of the asymptotic formulae for standard errors and confidence limits. Despite this, however, the full analysis, the results of which are summarized, was thought to be justified.

Part III. *Computational Procedure and Preliminary Results*

7. *Computational procedure.*—Estimates c^*_l, c^*_{ml}, a^*_{l1}, a^*_{m1}, etc., defined by (18), are first obtained, it being supposed that the question of the order of the highest harmonic to be included has been settled.

These estimates are used to calculate the estimated residual series $\{l_n^*\}$ and $\{m_n^*\}$ from (22). From these series, auto-covariances and cross-covariances for lags $s = 0$, 1 and 2 are calculated and substituted in formulae (29), (31), (37) and (39) of Section 5 to give estimates of κ, γ, σ^2 and σ'^2. Further auto-covariances and cross-variances for higher lags are computed at this stage if the goodness-of-fit test mentioned at the end of Section 5 is to be applied to the results.

The estimated standard errors of κ^*, γ^* and λ^* are then calculated from (34), (35) and (38), and finally the estimated standard errors of c^*_l, c^*_m, etc. from (19), which also gives the covariances required for carrying out the approximate test of the significance of a set of harmonic coefficients of given order described in Section 4.

8. *Data used in the analysis.*—As yet we have only applied the results of this analysis to a series of 420 "monthly" values of l and m covering the 35 years 1900–1935 taken from the various publications of the International Variation of Latitude Service. In some cases data have been readjusted after original publication; the latest available values have always been taken in such cases.

For the reason discussed in Section 6 the longest possible series of results are needed. Unfortunately the data available have not been obtained in a uniform manner since 1900. Firstly, the number of stations at which observations have been made declined throughout the period. From the inception of the programme, at the beginning of 1900, to 1915 January, six stations (Carloforte, Tschardjui or Kitab, Mizusawa, Ukiah, Cincinnati and Gaithersburg) were in operation. In 1915 January, Gaithersburg ceased to operate, as did Cincinnati in 1916 January and Kitab in 1919 May. From 1919 May onwards only three stations were used in the determinations, this being the minimum number necessary for determining l, m and the so-called z-term. Secondly, the method of reducing the observations was changed at 1922·7.

Observations are made on twelve star fields, consecutive pairs of which overlap by about a month, and the values of l and m pertain to the mean date of each group-combination. For example, in the early years, star Group I was used for observation from September 23 to December 6, Group II from November 2 to January 4 and the published values of l and m for the group combination I–II refer to the mean date of the overlapping period November 2 to December 6. This gives 12 irregular intervals per year. After 1922·7 the group combinations were altered to make the intervals equal. A good account of the actual procedures and programmes is given by Melchior (**10**, Chapter 1). The irregularities in the intervals may be regarded as leading to slight, irregular phase changes in the motion and their effect will be to increase the uncertainty of the results. We feel that these series of results are better than the $\frac{1}{10}$ yearly series which are usually quoted and which Jeffreys used in his analysis. The reason for this preference is that the most essential requirement of the series examined is that successive terms should be in no way correlated except by the physical processes underlying the motion. This is true of the $\frac{1}{12}$ yearly series but the $\frac{1}{10}$ yearly series are derived from the former by graphical interpolation and in the process of drawing smooth curves through the rather irregular looking curves of the $\frac{1}{12}$ yearly series, correlations between successive runs of 3 or even 4 values must be introduced. Comparison of the graphs of the $\frac{1}{12}$ and $\frac{1}{10}$ yearly series do in fact indicate a high degree of smoothing. There must therefore be bias introduced into the auto-covariances for small lags. In the fuller analysis which we hope

to make later this will be examined more closely, particularly as it has a bearing also on a point raised by Professor Jeffreys (private communication) regarding the effect of errors introduced by changes in the star fields occasioned by their proper motions, and the effects of precession.

We have used the results from which the so-called z-term has *not* been removed, as the results so obtained appear to be possibly more homogeneous than those obtained when the z-term is taken into account. They are certainly unsmoothed. This point will require examination in our fuller analysis, as will also the effect of the important change in the method of reduction made in 1922·7.

9. *Preliminary results.*—For ease of computing, the 35-year means for each month have been calculated and analysed by the usual simple method of numerical Fourier analysis. This yields all terms up to the cosine term for the fifth harmonic. The results are given in Table I. As expected, the fundamental is the dominant term.

TABLE I

Results of harmonic analysis
(Unit 0″·01)

	c^*	a^*_1	b^*_1	a^*_2	b^*_2
l	+11·062	−55·105	−70·286	−2·138	+6·914
m	−10·057	+74·790	−45·276	−5·548	−3·105
Estimated standard error	±3·05	±10·77		±2·40	

	a^*_3	b^*_3	a^*_4	b^*_4	a^*_5	b^*_5	a^*_6
l	+2·348	−4·014	−1·757	+1·114	−0·905	+2·086	−0·771
m	+2·238	+3·943	+1·024	+1·219	−1·000	+1·257	−1·562
Estimated standard error	±1·70		±1·48		±1·39		±0·97

The series $\{l_n^*\}$ and $\{m_n^*\}$ were easily obtained by deducting from each value of l and m the 35-year mean for the appropriate month. This of course implies that all the components given in Table I have been removed whether or not they later turn out to be significant.

The auto-covariances and cross-covariances, $c_{ij}(r)$, $r = 0, 1, 2$, calculated from the series $\{l_n^*\}$ and $\{m_n^*\}$ are given in Table II (taking 0″·01 as the unit of measurement).

TABLE II

Covariances of $\{l_n^*\}$ *and* $\{m_n^*\}$

Auto-covariances		Cross-covariances	
$c_{11}(0)$	11 289·114 3	$c_{12}(1)$	4 583·685 0
$c_{11}(1)$	9 972·436 8	$c_{12}(2)$	8 192·782 3
$c_{11}(2)$	7 080·925 8		
$c_{22}(0)$	12 377·847 6	$c_{21}(1)$	−4 480·670 6
$c_{22}(1)$	10 716·248 2	$c_{21}(2)$	−8 071·636 4
$c_{22}(2)$	7 718·382 8		

From these were obtained the estimates and standard errors given in Table III.

Finally we calculated the estimated errors of the harmonic coefficients. These are given in the bottom line of Table I. The first and second harmonic terms, though relatively small, clearly differ significantly from zero, but it appears that the higher-order terms could be omitted. This is confirmed by applying

the χ^2 test described in Section 4, the results of which are given in Table IV. Ideally, the numerical analysis should now be repeated omitting the insignificant harmonics, but as their contributions to $\{l^*\}$ and $\{m^*\}$ are trivial this has not been considered necessary.

TABLE III

Constants for free motion

	Estimated standard error
$\kappa^* = 0{\cdot}322$	$\pm 0{\cdot}103$
$\gamma^* h = 23^\circ\ 40'$	$\pm 44'$
$\lambda^* = 0{\cdot}9803$	$\pm 0{\cdot}00347$
$\sigma^* = 24{\cdot}6$	...
$\sigma^{*\prime} = 15{\cdot}3$	...

TABLE IV

Significance of harmonic constants: χ^2 test

Order of harmonic	1	2	3	4	5
Value of χ^2	10·95	12·30	3·54	3·94	3·22
Degrees of freedom	4	4	4	4	2
$P(\chi^2)$	$<0{\cdot}05$	$<0{\cdot}02$	$>0{\cdot}30$	$>0{\cdot}30$	$>0{\cdot}20$

10. *Free period and damping coefficient.*—From Table III it is seen that

(i) the estimated damping coefficient is

$$\kappa^* = 0{\cdot}322 \pm 0{\cdot}103 \text{ year}^{-1}$$

giving a relaxation time of 3·1 years;

(ii) the estimated free period is

$$2\pi/\gamma^* = 1{\cdot}267 \pm 0{\cdot}039 \text{ year}$$

$$= 462{\cdot}8 \pm 14{\cdot}2 \text{ mean solar days.}$$

The period is better described as a 15-monthly rather than 14-monthly period.

11. *Discussion of the results.*—We have already remarked in Section 6 that the estimate of the damping coefficient κ is much larger than that given by Jeffreys.

The estimated free period is greater than those obtained by previous analyses, although it is in fact still compatible with the traditional value $2\pi/\gamma = 1{\cdot}2$ year. From the analysis of data for the years 1892–1933 Jeffreys obtained $2\pi/\gamma = 1{\cdot}223 \pm 0{\cdot}019$ years, which is in quite good agreement with the present result. He preferred a result, however, based on the analysis of data for the much shorter period 1908·3–1921·5 from which he obtained $2\pi/\gamma = 1{\cdot}202 \pm 0{\cdot}016$ year.

The need to take account of observational error in the model is clearly shown by the value of $1 - \lambda^*$, 0·0197, which is more than 5·6 times its estimated standard error and certainly differs significantly from zero. When the analysis of Section 5 ignoring observational error is carried out, we obtain the value $\kappa^* = 0{\cdot}560$ for the damping.

There appears to be only one other occasion on which so long a period has been suggested. Jeffreys (**9**, pp. 213–4) has made a solution, using Takeuchi's theory of the shell and an approximate treatment of the core of the Earth. It predicts a period of 460 days for the free motion—in close agreement with our present determination. We understand, however, that this theory gives an unsatisfactory value for the nutation and that further work is still in progress.

The standard deviation of the observational errors seems to be quite large, our estimate, 15·3 units, being more than four times that suggested by Jeffreys.

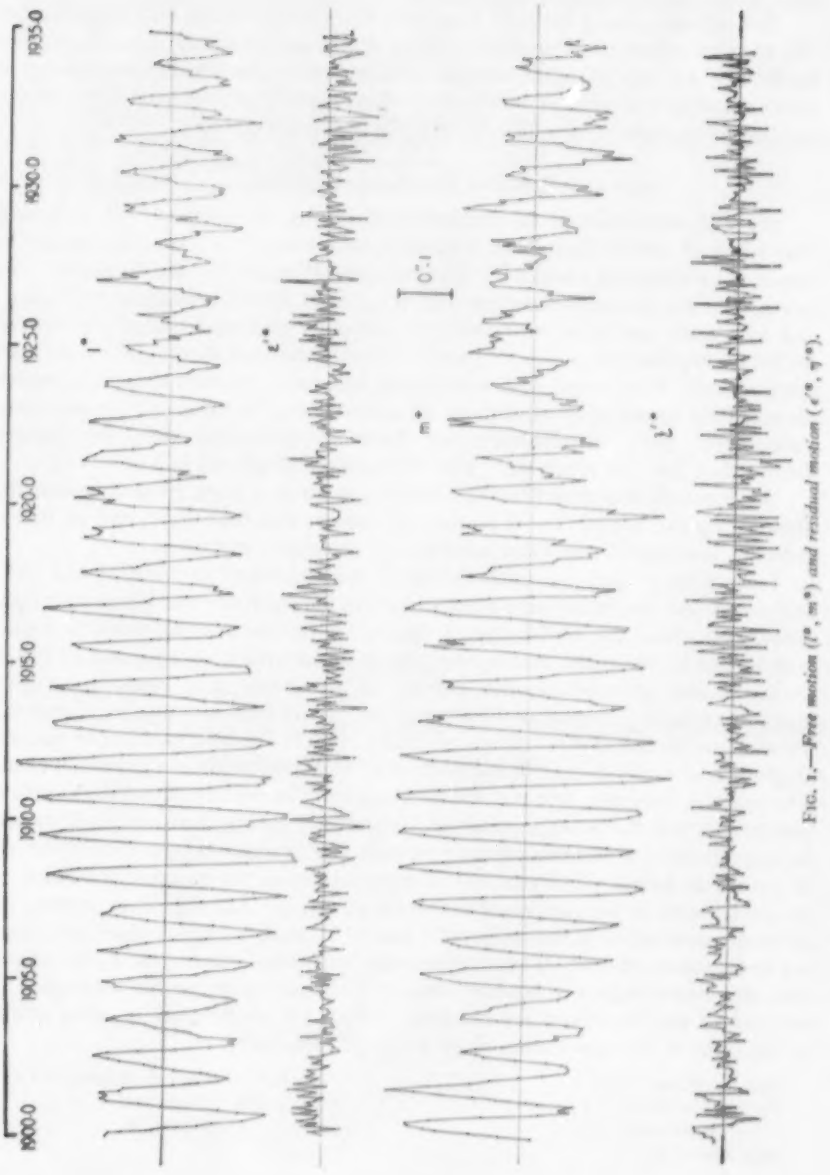

FIG. 1.—*Free motion* (l'', m'') *and residual motion* (ϵ'', η'').

This may be due in part to the uncertainties being increased by the slight irregularities of the intervals as suggested in Section 8. The increased uncertainty may be due however to the non-removal of the z-term.

In Sections 4 and 5 we have suggested other points which bear examination. We hope to report on these later. They deal mainly with the adequacy of the model but we may mention that the application of the Bartlett–Rajalakshman goodness-of-fit test requires a very much larger amount of numerical computation than has even been involved in the analysis so far completed!

Part IV. *The Residual Motion*

12. ***The distribution of the residuals.***—Reverting to equation (13), it is seen that when α° and β° have been evaluated, estimates ϵ'^*, η'^* of ϵ' and η' can be obtained by replacing x and y by their estimates l^* and m^*. We do not see how to separate the fluctuation components (ϵ, η) from the observational error (u, v) and so cannot test them separately for normality and randomness. However, we have computed the series $\{\epsilon'^*\}$ and $\{\eta'^*\}$ and examined them. They are both symmetrically distributed with zero means and have standard deviations which do not differ appreciably from those calculated from the values of the estimated parameters. Both distributions are flattened compared with the normal distribution, but not much so. The residuals are displayed in Fig. 1.

We conclude therefore that the evidence, as far as it goes, gives no reason for disbelieving the hypotheses of Section 2, namely, that both $\{\epsilon, \eta\}$ and $\{u, v\}$ are normally distributed and form independent stationary processes.

Jeffreys (**2**, p. 147) inspected the series corresponding to our $\{l^*\}$ and $\{m^*\}$ and concluded that there were abrupt changes in amplitude and phase at certain times. He chose the period 1908·3–1921·5 for further analysis since he found it to be one in which the motion was almost undisturbed. Inspection of Fig. 1 shows similar phenomena, the period up to about 1915 being apparently disturbance free. Thereafter the $\{l^*\}$ and $\{m^*\}$ series seem increasingly disturbed. To what extent this is due to physical causes, or to the smaller number of stations employed, or to the change in the method of reduction made in 1922 is not clear. The point is, however, not that the $\{l^*\}$ and $\{m^*\}$ series should follow a certain pattern but that the mean number of "impulses" during the intervals h should be large (Section 2) and this cannot be decided by a rather subjective examination of the actual series. The real test of departure from the assumptions made in the model rests in the analysis of the residuals $\{\epsilon, \eta\}$. Although these cannot be isolated, examination of the series $\{\epsilon'^*\}$ and $\{\eta'^*\}$, as stated above, does not reveal any non-random effects. There are nowhere any systematic runs of values longer than one would expect in random series. For this reason we do not regard as satisfactory any procedure for isolating periods for preferential analysis solely on the basis of the appearance of the series $\{l^*\}$ and $\{m^*\}$.

Dept. of Mathematics,
The University,
Manchester, 13:

Dept. of Applied Mathematics,
The University,
Liverpool, 3.

1955 *March* 25.

References

(1) P. Melchior, *Bull. Acad. Roy. Belg., Cl. Sci.*, ser. 5, **37**, 158–183, 1951.
(2) H. Jeffreys, *M.N.*, **100**, 139–155, 1940.
(3) M. S. Bartlett, *Stochastic Processes*, Mimeographed North Carolina lecture notes, 1946.
(4) J. E. Moyal, *J. Roy. Statist. Soc.* B, **11**, 150–210, 1949.
(5) M. S. Bartlett, *J. Roy. Statist. Soc.* B, **8**, 27–41, 1946.
(6) P. Whittle, *Trabajos de Estadistica*, **3**, 43–57, 1952.
(7) P. Whittle, *J. Roy. Statist. Soc.* B, **15**, 125–139, 1953.
(8) M. S. Bartlett and D. V. Rajalakshman, *J. Roy. Statist. Soc.* B, **15**, 107–124, 1953.
(9) H. Jeffreys, *The Earth*, 3rd edn., Cambridge, 1952.
(10) P. Melchior, *Observatoire Royal de Belgique, Monographie*, **3**, 1954.

ERRATUM

M.N., **115**, No. 1, 1955:

D. G. Ewart, *On the relation between the stream and the ellipsoid constants.*

P. 50, line 3 from bottom, for $y = \tau_1 t$ read $y = \alpha\tau_1 t$.

CONTENTS

PAGE

Meeting of 1955 May 13 :

Fellows elected 339

Presents announced 339

T. Gold, The symmetry of the corona of 1954 June 30 340

A. H. Jarrett and H. von Klüber, Interferometric measurements of the green corona line during the total solar eclipse of 1954 June 30 343

D. W. N. Stibbs, Radial velocities of cepheid variable stars in the southern hemisphere 363

Sergei Gaposchkin, The bright double-lined eclipsing variable CV VEL ... 391

A. E. Roy, Note on a set of models for unmixed stars 396

H. W. Newton and A. S. Milsom, Note on the observed differences in spottedness of the Sun's northern and southern hemispheres 398

M. G. Adam, Interferometric measurements of wave-lengths. II. Measurements at 6500 A and a general discussion of the solar red shift 405

M. G. Adam, Interferometric measurements of wave-lengths. III. A note on observational technique in the method of circular channels 422

R. d'E. Atkinson, On the flexure of meridian circles 427

A. M. Walker and Andrew Young, The analysis of the observations of the variation of latitude 443

Printed in London by Taylor & Francis, Ltd., 1956 May